Disruption of The Light/Dark Cycle and Outcome After Experimental Stroke

Dr Ku Mastura Ku Mohd Noor

MBBS, MMedSc (Anatomy)

Submitted in fulfilment of the requirements for the degree of Doctor of Philosophy to the Institute of Neuroscience and Psychology, College of Medical, Veterinary and Life Sciences, University of Glasgow

March, 2017

Abstract

Circadian rhythms optimise health by ensuring that the internal rhythms of metabolism and cardiovascular physiology are synchronised to daily variations in the light/dark cycle and other recurrent environmental challenges. Disruption in in the light/dark cycle (photoperiod disruption; PD) which occurs during shift work has been associated with changes in metabolism or physiology, (e.g. hypertension, hyperglycaemia) that may influence outcome after stroke. Evidence from pre-clinical studies indicates that hyperglycaemia and hypertension are associated with increased lesion growth and final infarct after focal cerebral ischaemia. Therefore, it was hypothesised that PD would impact on physiological parameters and increase sensitivity to focal cerebral ischaemia.

Investigating the effect of chronic photoperiod disruption on outcome following permanent focal cerebral ischaemia

For this purpose, a PD protocol was employed to simulate shift work patterns of light/dark (LD) exposure. Male Wistar rats were exposed to either a 12:12 LD cycle or a 6-hour phase advance protocol for 9 weeks. This was done by switching the lights on 6 hours earlier than the previous photoperiod every 3 days. T_2-weighted MRI was performed at 48 hours after permanent middle cerebral artery occlusion. Chronic PD for 9 weeks did not significantly affect food intake, body weight and key physiological parameters such as blood glucose and blood pressure and did not increase sensitivity to ischaemic damage in young, normotensive rats. This suggests that light alone is not a single factor to induce circadian disruption. The potentially adverse impact of shift work on stroke outcome may require additional factors such as high fat/high sugar diet or pre-existing co-morbidities.

Characterisation and optimisation of animal model for transient focal cerebral ischaemia

Results from the previous study of permanent ischaemia raised the question as to on how PD impacts on stroke outcome in the presence of reperfusion. In addition, since the majority of stroke patients present with co-morbid factors,

subsequent studies aimed to determine the impact of PD in the presence of pre-existing hypertension following transient focal ischaemia. Prior to this a pilot study was conducted to optimise the time of middle cerebral artery (MCA) occlusion and to characterise the associated neurological and functional outcomes. The following information was used to inform the subsequent studies; 1) the optimal MCA occlusion time in spontaneously hypertensive rats (SHR) was 30 min and 2) transient MCA occlusion resulted in reproducible functional impairments in both neurological score and the adhesive label test assessed at 7-days.

Impact of photoperiod disruption on sensitivity to focal cerebral ischaemia and microglia activation in spontaneously hypertensive rats

Adult male SHR underwent 30 min transient MCAO following the 9-week PD protocol. Reperfusion resulted in significant tissue salvage. However, PD in the presence of pre-existing hypertension did not exacerbate ischaemic lesion evolution assessed by diffusion-weighted MRI, and by measuring the final infarct volume. Furthermore, PD alone did not induce significant changes in microglia activation in the brains of SHR that were not subjected to ischaemia. Poor collaterals and pre-existing hypertension in SHR may explained to lesser effect of PD on lesion evolution, as there may have been less penumbral tissue available for PD to exert its detrimental effect.

Conclusion

The studies presented in this thesis demonstrated that PD did not increase sensitivity to focal cerebral ischaemia in normotensive rats. Similarly, PD in the context of major stroke co-morbidity/risk factor did not exacerbate ischaemic damage. This suggest that the primary mechanism of cardiometabolic disturbances among shift workers may not primarily mediated by shifting in the light/dark cycle.

Table of Contents

Table of Figures

Chapter 3

Chapter 4

Chapter 5

List of Tables

Acknowledgements

Firstly, I would like to thank my supervisors, Dr Chris McCabe and Dr Deborah Dewar for their invaluable input, guidance and continued support over the past 4 years. Thanks for all the opportunities you have offered me. It has been a period of intense learning, not only in the scientific arena but also on a personal level. I would also like to thank Ministry of Higher Education Malaysia for funding this research.

I would also like to thank all staff within the Wellcome Surgical Institute; Professor Mhairi Macrae, Dr Lisa Roy, Dr Emma Reid, Lindsay Gallagher, Linda Carberry, Ann Marie Colquhoun, and Jim Mullin for their guidance and technical assistance over the past 4 years. I would particularly like to thanks Lindsay Gallagher and Dr Lisa Roy for their surgical expertise in performing an MCAO surgery for studies in Chapter 3 and 4.

Massive thanks to Dr Cathy Wyse and Professor Stephany Biello for sharing their expertise and provided me with valuable resources for the circadian studies. I would also like to thank Mr Nosrat Mirzai from the Bio-Electronics Unit, College of Medical, Veterinary & Life Sciences for building the light box and sensors.

A big thank you to all my fellow students at the Wellcome Surgical Institute for keeping the spirits high and making this PhD a wonderful experience; Mariana, Biav, Rob, and Joachim. Thank you to MSc student Danial Agriva Tamba and a medical student Michael Clark who did the Iba-1 staining and ROI analysis for the study in Chapter 5.

Finally, thanks to my parents Ku Mohd Noor and Khalijah Abd Rahman, my wonderful husband Azmi Hashim and my amazing children; Tasneem Nasuha, Mawaddah and Umar Fawwaz for being with me through my ups and down and provided me through moral and emotional support in my life. I dedicate this thesis to them.

Author's Declaration

I declare that this thesis comprises my own work, unless otherwise acknowledged and has not been submitted for any other degree at the University of Glasgow or any other institution.

Ku Mastura Ku Mohd Noor

March, 2017

Published Manuscripts

Noor, K.M.K.M., Wyse, C., Roy, L.A., Biello, S.M., McCabe, C. and Dewar, D., 2016. Chronic photoperiod disruption does not increase vulnerability to focal cerebral ischemia in young normotensive rats. Journal of Cerebral Blood Flow & Metabolism, p.0271678X16671316.

Abstracts

Noor, K.M.K.M., Roy, L.A., Wyse, C., McCabe, C. and Dewar, D., 2015. No effect of chronic photoperiod disruption on vulnerability to focal cerebral ischemia in rats. 27th International Symposium on Cerebral Blood Flow, Metabolism and Function. Vancouver, Canada.

Noor, K.M.K.M., Wyse, C., Agriva, D., Biello, S., Dewar, D. and McCabe, C., 2017. Chronic photoperiod disruption does not increase sensitivity to transient focal cerebral ischaemia in spontaneously hypertensive rats. 28th Symposium on Cerebral Blood Flow, Metabolism and Function. Berlin, Germany.

List of Abbreviations

ADC	apparent diffusion coefficient
AMPA	α-amino-3-hydroxy-5-methyl-4-isoxazolepropionic acid
ANOVA	analysis of variance
ARRIVE	Animal Research Reporting In Vivo Experiments
ATP	adenosine triphosphate
BBB	blood brain barrier
BMAL1	Brain and Muscle Aryl hydrocarbon receptor nuclear translocator- Like 1
BP	blood pressure
Ca^{2+}	calcium ion
CBF	cerebral blood flow
CCA	common carotid artery
CLOCK	Circadian Locomotor Output Cycles Kaput
CPP	cerebral perfusion pressure
CRP	C-reactive protein
Cry	Cryptochrome
DAB	3, 3 -diaminobenzidine
DWI	diffusion-weighted imaging
ECA	external carotid artery
EDTA	ethylene diamine tetra acetic acid
ELISA	enzyme-linked immunosorbent assay
H2O2	hydrogen peroxide
HDL	high density lipoprotein
Iba-1	ionized calcium binding adaptor molecule-1
ICA	internal carotid artery
ICP	intra cranial pressure
ICV	inferior cerebral vein
IgG	immunoglobulin G
IL-1	interleukin-1
IL-16	Interleukin-16
IL-1b	interleukin-1 beta
IL-6	interleukin 6
ipRGCs	intrinsic photosensitive retinal ganglion cells
IS	inter-daily stability
IV	intra-daily variability
K^{+}	potassium ion
LD	light/dark
MABP	mean arterial blood pressure

MAP	mean arterial pressure
MCA	middle cerebral artery
MCAO	middle cerebral artery occlusion
MRI	magnetic resonance imaging
Na^+	sodium ion
NC3R's	National Centre for the Replacement, Refinement and Reduction of Animals in Research
NMDA	N-methyl-D-aspartate receptor
NOS	nitric oxide synthase
NADPH	nicotinamide adenine dinucleotide phosphate
NOX	nicotinamide adenine dinucleotide phosphate oxidase
NRF2	nuclear factor erythroid 2-related factor
NTS	nucleus tractus solitarius
$PaCO_2$	arterial carbon dioxide pressure
PaO_2	arterial oxygen pressure
PD	photoperiod disruption
Per	period
Per2	period 2
PET	positron emission tomography
PID	peri-infarct depolarisation
RARE	rapid acquisition with refocused echoes
ROI	region of interest
ROS	reactive oxygen species
rTPA	recombinant tissue plasminogen activator
SCN	suprachiasmatic nucleus
SE-EPI	Spin Echo-Echo Planar Imaging
SHR	spontaneously hypertensive rats
SHRSP	spontaneously hypertensive stroke-prone rats
TB	Tris-buffer
TIA	transient ischaemic attack
TNF-α	tumour necrosis factor-α
TPA	tissue-type plasminogen activator
TTC	triphenyltetrazolium Chloride
VMSC	vascular smooth muscles cells
WHO	World Health Organization
WKY	wistar Kyoto rats

Chapter 1-Introduction

1.1 Stroke

1.1.1 Stroke Facts and Figures

The World Health Organization (WHO) defines stroke as "rapidly developing clinical signs of focal (or global) disturbance of cerebral function, with symptoms lasting 24 hours or longer or leading to death, with no apparent cause other than of vascular origin". Therefore, transient ischaemic attack (TIA), which conventionally denotes complete resolution of all symptoms within 24 hours and patients presenting with stroke symptoms caused by head injury, subdural haemorrhage, tumours, and poisoning are excluded (Truelsen *et al.*, 2001). Stroke is the second leading cause of death worldwide after cancer, heart disease and respiratory disease. There are approximately 150,000 stroke incidents annually in the UK leading to nearly 40,000 deaths with approximately 1.1 million stroke survivors living in the UK (Stroke.org.uk, 2016). More than half of all stroke survivors are left dependent on others for everyday activities making stroke the most common disabling neurological disorder (Muir, 2013). Among survivors, 69% of 25-59 year olds were unable to return to work (Stroke.org.uk, 2016). Hence, the disease burden is great. The estimated economic costs of stroke in the UK from a societal perspective totals around £9 billion a year (Saka *et al.,* 2009). Despite the huge economic burden, research resources have been disproportionately allocated to stroke research, compared to cancer and cardiovascular diseases. In total, the combined research funding into stroke, cancer, coronary heart disease and dementia by governmental and charity organisations was £856 million. Of this total, only 7% was devoted to stroke (Stroke Association, 2014).

Stroke incidence as analysed within the UK General Practice Research Database has decreased between 1999 to 2008 (Lee *et al.*, 2011). Advancement in acute stroke therapy either with reperfusion by means of thrombolysis or mechanical recanalization, as well as rigorous measures of stroke prevention has accounted for the improved survival and functional outcome among stroke victims (Hachinski *et al.*, 2010). However, the efficacy and safety of current therapy (intravenous thrombolysis with recombinant tissue plasminogen activator; rTPA) is limited to a narrow therapeutic window (up to 4.5 hours) and

unfavourable side effects such as intra cerebral haemorrhage (Moskowitz *et al.*, 2010) (Hacke *et al.*, 2008). Stroke incidence has been estimated to escalate by the year 2030 especially in the developed countries due to expansion in population size and increase in ageing population (Truelsen *et al.*, 2006). There is no single method for preventing stroke. Reduction in stroke mortality and morbidity requires a multi-disciplinary approach that combines preventive measures, better control of stroke risk factors as well as safe thrombolytic and neuroprotective therapies to limit damage and promote repair to the injured brain.

1.1.2 Classification of Stroke

There are two major forms of stroke: ischaemic and haemorrhagic; the former being the most common. It is estimated that 85 to 90% of strokes are ischaemic. Most ischaemic strokes result from thromboembolism originating in extracranial vessels or the heart (Muir, 2013). Atherosclerosis which refers to the stiffening or hardening of the artery is characterised by an atheromatous plaque formation in the vessel wall. Plaque formation is a chronic process which is triggered by injury to the endothelial lining by disease conditions such as diabetes, hypertension and hypercholesterolemia. Complicated atherosclerotic plaques may rupture, leading to thrombus formation and occlusion of the artery (Hossmann and Heiss, 2014).

Embolic stroke accounts for 14-30% of all cerebral infarction and occurs following breakage of atherosclerotic plaque (Murtagh and Smalling, 2006)(Dirnagl *et al.*, 1999). Major sources of cardiac emboli are from atrial fibrillation (Figure 1.1) but they can also arise in many other conditions including; dilated cardiomyopathy, mechanical prosthetic valve and endocarditis (Arboix and Alió, 2010). The site of the cerebral arterial occlusion is often at bifurcation points of the arterial system due to a combination of turbulent flow and weakened vessel walls at these regions. Another small percentage of ischaemic strokes can be caused by lacunar or small vessel occlusion involving occlusion in one of the small deep penetrating arteries by microatheroma. Lacunar infarcts are commonly observed in diabetic and hypertensive patients, with the latter being the most important risk predisposing factor. The small

diameter (≤ 400μm) makes the vessel susceptible to occlusion and pathological changes induced by hypertension (Ogata, *et al.*, 2011). Depending on the brain region affected, ischaemic stroke patients typically present with contralateral weakness of the face, arm and leg (i.e. with the involvement of internal capsule and corticospinal tract) and slurred speech (Muir, 2013). Patients with previous episode of TIA are at increased risk for stroke with 30-day stroke risk is around 10%, mainly within the first 7 days (Muir, 2013).

Haemorrhagic strokes are primarily caused by hypertension. Due to sudden rupture of the blood vessel, the majority of patients presented with more acute and severe symptoms such as loss of consciousness, and seizure (Andersen *et al.*, 2009). About 10 to 15% of haemorrhagic strokes result from vessel ruptures either within the brain (intracerebral haemorrhage) or on the surface of the brain (subarachnoid haemorrhage) (Muir 2013).

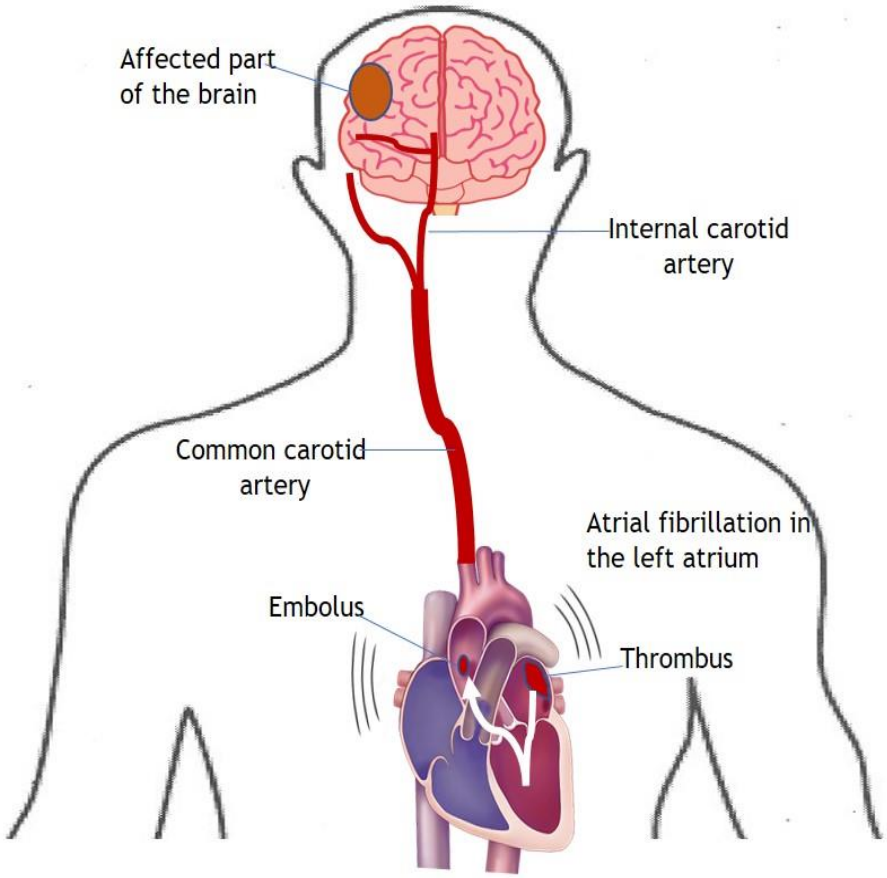

Figure 1.1 Mechanism of ischaemic stroke arising from a cardiac embolus. The embolus ascends from the heart to the cerebral circulation via the aorta and the common carotid artery. Adapted from (Go, 2009).

1.1.3 Stroke Risk Factors

A stroke risk factor as defined by Hankey is a characteristic of an individual that increases the risk for stroke compared to someone without that characteristic (Hankey, 2006). Some risk factors are potentially modifiable (i.e. high blood pressure, diabetes and obesity) which means intervention and treatment can reduce the chances of having a stroke. These risk factors, which often co-exist with the non-modifiable risk factors of age, sex, and ethnicity, contribute significantly to stroke incidence (Hankey, 2006). Primary stroke prevention includes identification of patient at risk of stroke, that may benefit from early intervention and treatment of modifiable risk factors (Goldstein *et al.*, 2006). A summary of both non-modifiable and modifiable risk factors for stroke is presented in Table 1.

1.1.3.1 Non-Modifiable Risk Factors

Age is the single most important non-modifiable risk factor, and the risk of having a stroke doubles every decade after the age of 55. By the age of 75, 1 in 5 women and 1 in 6 men will have a stroke (Stroke.org.uk, 2016). The number of people having strokes aged 20 to 64 increased by 25% from 1990 to 2010 worldwide (Feigin *et al.*, 2015). Together with diabetes, aging has been reported to enhance the intrinsic susceptibility of brain cells to injury, thereby increasing tissue damage produced by ischaemia (Biessels, Van der Heide, *et al.*, 2002).

Sex has also been identified as an unmodifiable risk factor for stroke. Incidence and prevalence of stroke among women of childbearing age are low compared to men (Go *et al.*, 2014). The prevalence however, increased substantially after the age of 50 due to decline in oestrogen levels associated with menopause, leading to increase susceptibility to cardiovascular risk factors (Go *et al.*, 2014).

Non-Modifiable Risk Factors	Modifiable Risk Factors
Age	Hypertension
Sex	Coronary heart disease
Race	Peripheral arterial disease
	Cigarette smoking
	Diabetes
	Atrial fibrillation
	Dyslipidaemia
	Obesity
	Physical inactivity
	Post-menopausal

Table 1.1 Non-modifiable and modifiable risk factors for stroke. Adapted from (Goldstein *et al.*, 2006).

1.1.3.2 Modifiable Risk Factors

Hypertension is defined as systolic/diastolic blood pressures (BP) consistently greater than 140/90mmHg and is the leading modifiable risk factor for stroke. A specific cause for hypertension only presented in a minority of patients (2%-5%) with underlying adrenal and renal diseases. In the remainder, no identifiable cause is found hence the term "essential hypertension" (Beevers *et al.*, 2001). Hypertension is responsible for 54% of strokes in the UK compared to diabetes (20%) (Stroke.org.uk, 2016). There is a linear relationship between blood pressure and stroke mortality in patients with treated hypertension; a 1 mmHg increase in systolic blood pressure increases stroke deaths by 2% (Palmer *et al.*, 1992). In the brain, the major deleterious effects induced by hypertension include structural changes in the cerebral vasculature and disruption in vascular regulatory mechanisms. Such alterations compromise tissue perfusion in the event of cerebral ischaemia and therefore increase the susceptibility to ischaemic injury (Iadecola and Davisson, 2008).

Diabetes is a complex metabolic syndrome with significant effects on systemic and cerebral vasculature (Baird *et al.*, 2002). It is characterised by

persistently high blood sugar (hyperglycaemia) that results from defective insulin secretion, or resistance to insulin action (Gavin *et al.*, 1997). Type 1 diabetes is the consequence of an autoimmune-mediated destruction of pancreatic Beta cells, leading to insulin deficiency. In this case, patients require lifelong insulin treatment. On the other hand, Type 2 diabetes occurs when the body is ineffective at using the insulin rather than absolute insulin deficiency (Biessels, van der Heide, *et al.*, 2002). Increased stroke risk is predominantly associated in Type 2 diabetes as stroke incidence often overlaps within the same age group in which Type 2 diabetes commonly occurs (Luitse *et al.*, 2012).

Chronic hyperglycaemia is associated with microvascular changes to the blood vessels in the eyes causing retinopathy, affecting functions of peripheral nerves (neuropathy) and kidneys (nephropathy). Macrovascular consequences lead to atherosclerotic plaque formation in larger arteries (Vithian and Hurel, 2010). More importantly, the relationship between disturbed glucose metabolism and ischaemic stroke is often bidirectional. People with diabetes have more than double the risk of stroke (Sarwar *et al.*, 2010). Conversely, acute stroke can give rise to abnormalities in glucose metabolism, and hyperglycaemia has been reported in 30–40% of patients with acute ischaemic stroke, and this was associated with poor functional outcome (Luitse *et al.*, 2012).

Patients with atrial fibrillation (AF) is associated with 4 to 5 folds of increased risk of cardioembolic stroke (Saposnik *et al.*, 2013). Recent study has shown that patterns of atrial fibrillation, especially of the persistent and permanent subtypes double the risk for cardio-embolic stroke (Vanassche *et al.*, 2015). Identification of patient with AF and treatment with anticoagulant is highly effective in ischaemic stroke prevention (Saposnik *et al.*, 2013). Meanwhile, obesity is particularly important as a risk factor for young onset ischemic stroke (Obesity increases risk of ischemic stroke in young adults). Mitchell and colleagues proposed that this association is partly explained by co-existing stroke risk factors such as diabetes and hypertension in the same age group. (Mitchell *et al.*, 2015).

1.2 Rodent Models of Focal Cerebral Ischaemia

The experimental stroke research aims to develop greater understanding of stroke pathophysiology, identify potential neuroprotective mechanisms and test new therapeutic strategies. It can also aid in elucidating factors which influence stroke risk and susceptibility. Various *in vivo* stroke models have been developed over the past 30 years in small (mice, rats, rabbits) and larger animals. Rodents are the species of choice in the majority of experimental stroke research due to clear advantages such as low maintenance costs and being ethically more acceptable compared to larger animals. Rodents are widely used as stroke models and their relevance to human stroke is supported by similarities in the anatomy of the cranial circulation between rats and humans, with both species possessing a circle of Willis (Yamori *et al.*, 1976)(Figure 1.2). Middle cerebral artery (MCA) occlusion model has been widely used in experimental stroke studies addressing pathophysiological processes or neuroprotective mechanism (Howells *et al.*, 2010). The availability of rat strains with stroke co-morbidities (i.e. hypertension and diabetes) allow better understanding of how these co-morbid factors impact on ischaemic damage.

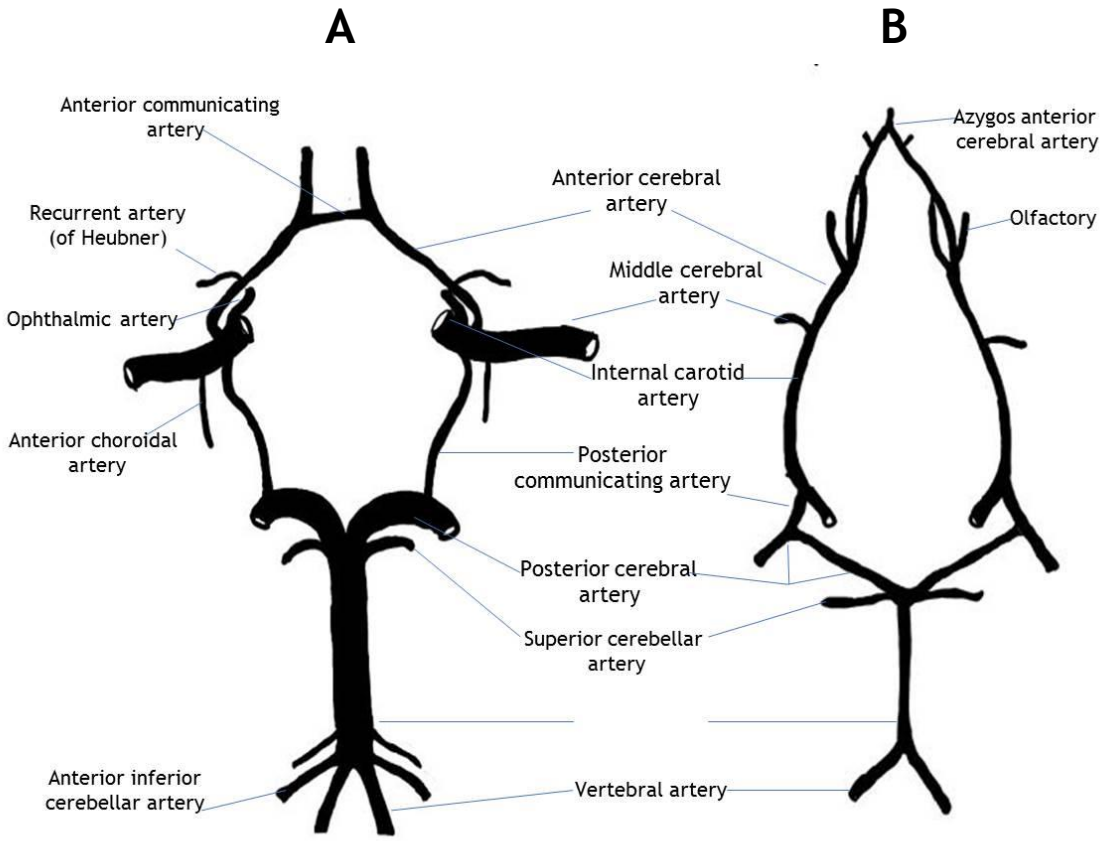

Figure 1.2 Circle of Willis in human and rats. Diagram showing the organization of the major cerebral arteries in Circle of Willis of a human (A) and a rat (B). Adapted from (Lee 1995).

1.2.1 Distal Diathermy Method

The distal diathermy method of inducing stroke involves removing the skull overlying the MCA which is then permanently occluded by diathermy of the artery (Figure 1.3A) (Tamura *et al.*, 1981). Complete occlusion is visually confirmed by cutting the portion of the artery. The extent of ischaemic damage is dependent on the site of vessel occlusion in which occlusion distal to lenticulostriate arteries produces a smaller lesion confined to the cortex (Figure 1.3B). Whereas proximal occlusion of the MCA produces bigger infarct encompasses both cortical and subcortical regions. The main advantages of this model are good reproducibility in infarct size and neurological deficits. Additionally, it has low post-surgical mortality as craniectomy reduces the deleterious effect of brain swelling, as well as visual confirmation of successful MCA occlusion. The main disadvantage is, with the craniectomy technique, it can cause injury to the underlying cortex or rupture of a vessel due to drilling or electrocoagulation. Therefore, this method demands a significant surgical skill in order to minimize surgical-induced tissue damage.

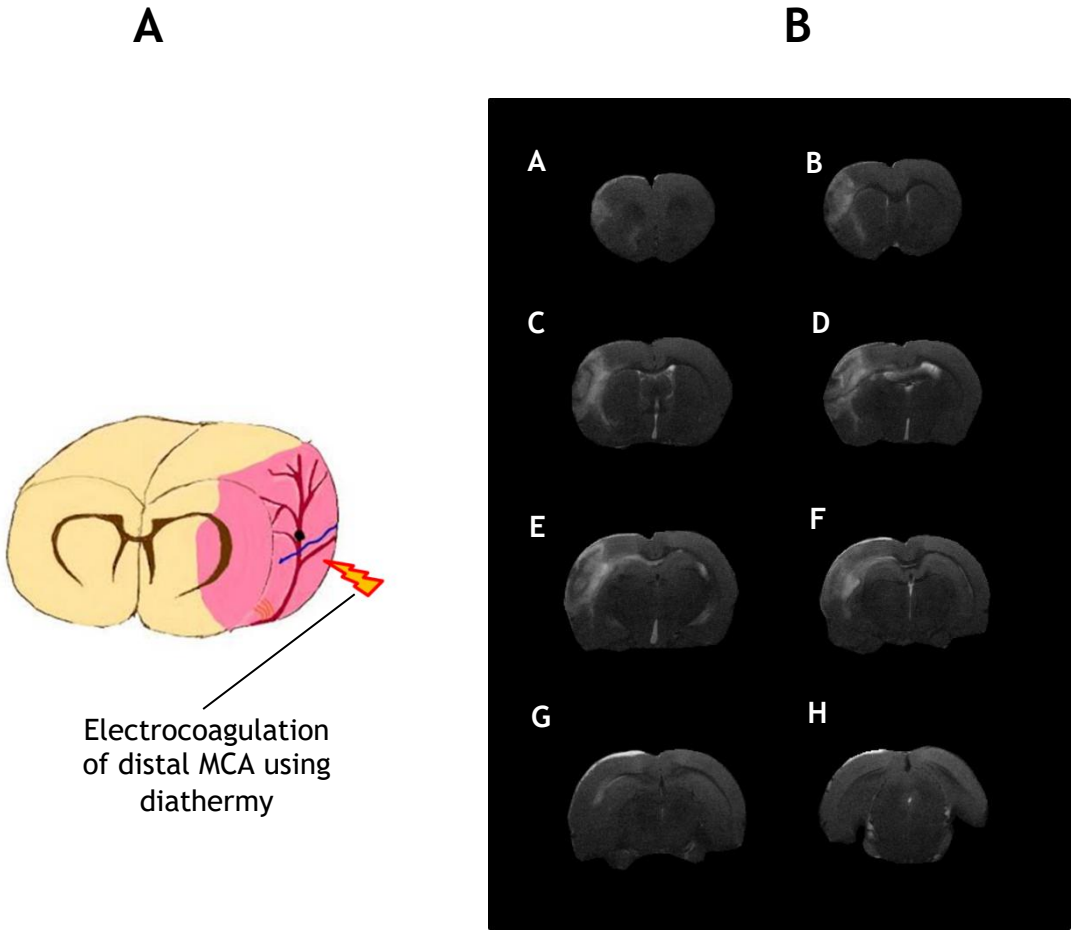

Figure 1.3 (A) Distal diathermy method of MCAO induced by electrocoagulation of the distal MCA (black spot). Pink shading denotes areas supplied by the distal branches of the MCA. Adapted from (Macrae, 2011). (B) T_2-weighted MRI coronal brain images showing rostral (A) to caudal (B) distribution of ischaemic damage 72 hours after permanent MCAO induced by distal diathermy method in adult, male Wistar rats. Ischaemic damage appears hyperintense and is primarily restricted to the cortex.

1.2.2 Intraluminal Filament Method

Middle cerebral artery and its branches are the most commonly affected cerebral vessels in human ischaemic stroke accounting for 70% of cases *(Bogousslavsky et al.,*1988). Therefore, the intraluminal methods for occluding this vessel are widely used. It was first described by (Koizumi *et al.*, 1986) and later modified by (Longa *et al.*, 1989). Technically, this method is less invasive and easier to master than craniectomy model (Macrae, 2011). The main advantages are the ability to precisely control the duration of ischaemia and avoids damage to the cranial structures. The access to MCA requires an exposure of the external and internal carotid artery via a midline incision in the neck. Suture is directly introduced into the internal carotid artery (ICA) and advances until it lodges at the proximal end of the anterior cerebral artery (ACA) and blocking the origin of the MCA (Figure 1.4A). Depending on the duration, blocking the origin of the MCA disrupts blood flow to its entire vascular territory and results in larger ischaemic lesions involving cortical and subcortical regions (Figure 1.4B). Since the lenticulostriate branches of the MCA are end arteries, the basal ganglia are exposed to severe ischemia. This technique may lead to inadequate MCA occlusion with highly variable lesion size. However, these can be solved by using a laser Doppler flowmetry to guide the placement of the suture. Vessel rupture and subsequent subarachnoid haemorrhage are also associated with this method, which can be minimised by using a silicone-coated suture (Schmid-Elsaesser *et al.*, 1998).

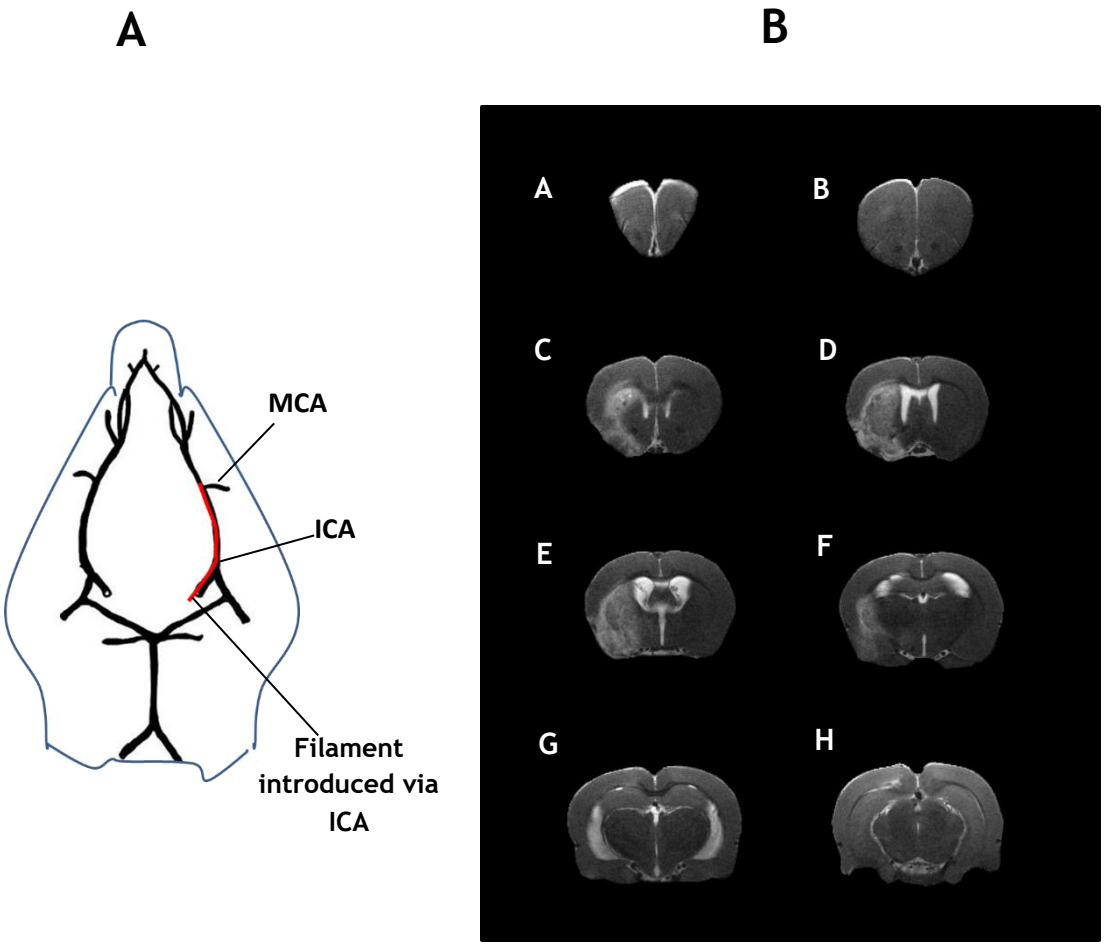

Figure 1.4 (A) Intraluminal filament model in a rat where a filament (shown in red) is introduced into the internal carotid artery and progressed until it blocks the origin of the MCA. (B) T_2-weighted MRI coronal brain images demonstrating rostral (A) to caudal (H) distribution of ischaemic damage 72 hours after a 90 min transient MCAO adult, male Sprague-Dawley rats. Ischaemic damage on T_2 images appears hyperintense involving both cortical and subcortical region. MCA: middle cerebral artery, ICA: internal carotid artery.

1.2.3 The Ischaemic Cascades: From Ischaemia to Infarction

Experimental stroke models have provided most of our knowledge on pathophysiological mechanisms involved in focal cerebral ischaemia. Recent developments suggest that stroke is not a purely vascular disorder. The pathophysiology of stroke involves complex interactions between components of the neurovascular unit namely; cerebral vasculatures, neurones, glia, and matrix components. Ischaemic brain injury involves a broad spectrum of pathophysiology and occurs as the manifestation of injury that evolves over space and time (Dirnagl *et al.*,1999). The major pathological mechanisms following cerebral ischaemia include excitotoxicity, peri-infarct spreading depolarisations, inflammation, necrosis and apoptosis (Figure 1.5). The primary injury in acute stroke is due to the early structural and biomechanical changes to the vasculature, neurones and their supporting cells, followed by secondary injury which is composed of more gradual cellular damage, that occurs in response to the primary injury (Dirnagl *et al.*,1999).

The brain is highly susceptible to ischaemic insult due to its limited capacity to store energy and its reliance on a continuous blood supply to maintain normal function. Following focal ischaemia delivery of oxygen and glucose is restricted and this leads to the rapid failure of adenosine triphosphate (ATP) production by mitochondria. Energy depletion is the most severe in areas with the lowest residual flow (ischaemic core), in which cell death occurs rapidly. Energy depletion leads to loss in the membrane potential that results in depolarisation of neurones and glia. Subsequently, pre-synaptic Ca^{2+} channels are activated and excitatory amino acids such as glutamate are released to the extracellular space (Dirnagl *et al.*,1999). Glutamate accumulation in the pre-synaptic space is further increased by a loss in energy dependent re-uptake processes (Choi and Rothman, 1990). These events lead to excitotoxicity.

Excessive extracellular accumulation of glutamate is a major factor contributing to the demise of tissues in areas of less severe ischaemia; the ischaemic penumbra. Overactivation of both N-methyl-D-aspartate receptor (NMDA) and α-amino-3-hydroxy-5-methyl-4-isoxazolepropionic acid (AMPA) glutamate receptors leads to significant influx of calcium, sodium and water into

neurones (cellular oedema) (Simard *et al.*, 2007). Cellular oedema not only impairs local perfusion to the core region of ischaemic tissues but also affects other brain regions via increased intracranial pressure, vascular compression and herniation (Dirnagl *et al.*,1999). Meanwhile, calcium influx initiates cellular catabolic processes mediated by catalytic enzymes such as proteases, lipases and nucleases (Ankarcrona *et al.*, 1995). Proteolytic enzymes degrade important cellular protein such as actin and spectrin that make up the cytoskeleton as well as extracellular matrix proteins, such as laminin (Furukawa *et al.*, 1997). Cell membranes are damaged by lipid peroxidation due to the activation of phospholipase A2 and cyclooxygenase enzymes. The damage is exacerbated by the fact that brain tissue is more susceptible to radical-mediated attack due to poor antioxidant defence (Adibhatla and Hatcher, 2010). Calcium overload results in generation of free-radical species that further impairs endogenous free-radical scavenging system (Dirnagl *et al.*,1999).

Ischaemia and reperfusion causes accumulation of reactive oxygen species (ROS) such as superoxide, hydrogen peroxide and hydroxyl; all are powerful mediators of ischaemic injury. Studies have shown that mitochondria and the enzyme NADPH oxidase (NOX) generates the majority of ROS during ischemia (Brennan *et al.*, 2009). Another source of free radicals includes neurones which synthesize nitric oxide (NO), by the neuronal nitric-oxide synthase (NOS), that reacts with superoxide anions to form the highly reactive species, peroxynitrite that further promotes tissue damage (Iadecola et al. 1997).

Acute ischaemia does not affect all brain regions homogeneously. In the core, where blood flow is at levels of less than 20% of baseline, cells have lost their membrane potential, there is failure of metabolism with rapid and irreversible neuronal death (Lo, Dalkara and Moskowitz, 2003). However, in the penumbra where some perfusion is preserved, the neurones are able to repolarise but at the expense of further energy consumption, and oxygen extraction levels are increased to compensate for the reduction in cerebral blood flow (CBF) (Dirnagl *et al.*,1999). Once repolarised, neurones are capable of further depolarisation in response to high extracellular glutamate and potassium concentrations. This repetitive process is termed peri-infarct depolarisation (PID) and accounts for secondary mechanisms that can contribute

to the expansion of the ischaemic lesion. The occurrence of PIDs has been well documented in animal stroke models where an increase in the frequency of PIDs is associated with greater infarct growth (Gill *et al.*, 1992) (Strong *et al.*, 2000). These events lead to necrosis or programmed cell death (apoptosis) depending on the severity of the ischaemic insult and the metabolic state of the neurones. Necrotic cell death predominates in the ischaemic core, while majority of cell death resemble apoptosis in ischaemic penumbra (Dirnagl *et al.*,1999).

The release of 'danger' signals from dying and dead cells activates the immune system. A robust inflammatory response begins within a few hours of the onset of ischaemia. Both resident brain cells (microglia) and circulating leukocytes participate in the response (Benakis *et al.*, 2014). Microglia have been shown to contribute to post-ischaemic inflammation by producing tumour necrosis factor (TNF), interleukin-1 beta (IL-1b), ROS and other pro-inflammatory mediators. Preventing microglial activation has been shown to significantly reduced the infarct volume and improve the neurological deficit scores following cerebral ischaemia in mice (Zhang *et al.*, 2005). The expression of adhesion molecules on the endothelial cell surface initiates influx of peripheral leukocytes into the brain parenchyma causing microvascular obstruction. Furthermore, cytokines and ROS produced both in the vascular and parenchymal compartments, induce the disruption of the blood brain barrier (BBB) facilitating further infiltration of circulating monocytes, neutrophils and lymphocytes. Preclinical studies suggest that therapeutically targeting neuroinflammation, reduces the progression of brain damage that occurs during the late stages of cerebral ischemia (Iadecola *et al.*, 2004). However, the concern is that although counteracting the inflammatory response to ischaemic injury may ameliorate the tissue damage in the acute phase, it may also compromise repair mechanisms and worsen the long-term outcome of the injury (Iadecola and Anrather, 2011).

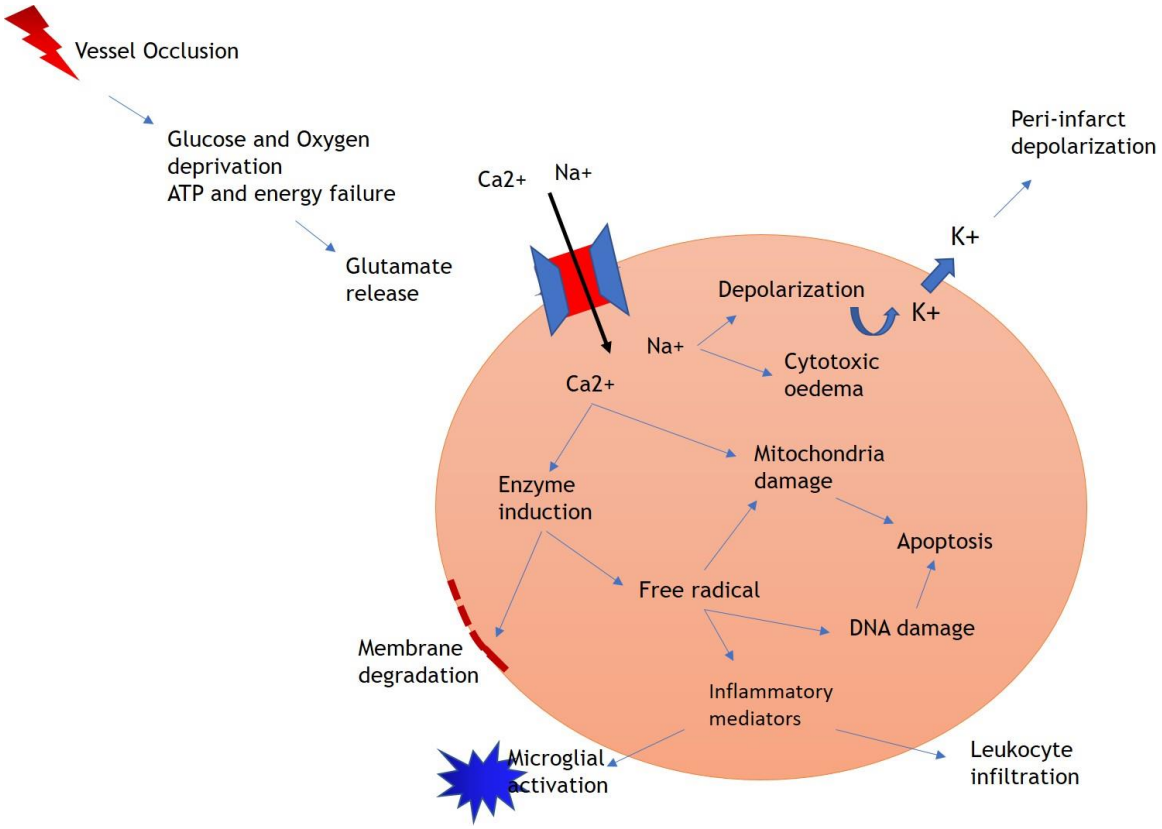

Figure 1.5 Pathophysiological mechanisms following focal cerebral ischaemia. Major events following vascular occlusion includes energy and pump failure, which activates glutamate receptors and increase in intracellular Ca^{2+} and Na^{+}, efflux of K^{+} and peri-infarct depolarization. Cellular damage is potentiated by free radical production, release of catabolic enzymes and membrane degradation. Secondary events such as immune activation further exacerbate ischaemic injury, leading to cell death (apoptosis). Adapted from (Dirnagl *et al.*,1999).

1.3 The Ischaemic Penumbra

The concept of the penumbra as tissue at risk, but potentially salvageable has been of a major target in neuroprotective studies. The ischaemic penumbra has been well characterised in animal studies and defines as “ischaemic tissue which is functionally impaired and is at risk of infarction and has the potential to be salvaged by reperfusion and/or other strategies. If it is not salvaged this tissue is progressively recruited into the infarct core which will expand with time into the maximal volume originally at risk”(Donnan *et al.*, 2007). Nevertheless, identifying the factors that could hasten the penumbra demise is equally important. The following section will discuss on the factors that can potentially exert an adverse effect on penumbra tissues and thereby might provide the basis for risk identification and preventive strategies.

1.3.1 Cerebral Blood Flow

Early restoration of CBF is crucial in the management of acute ischaemic stroke. Therefore, understanding the physiological control of normal CBF and the pathophysiology of ischaemic injury is crucial for planning effective strategies to minimise the consequences of cerebral ischaemia. Under normal physiological conditions, CBF is kept constant and closely maintained within a narrow range in order to sustain a continuous energy supply. The process of maintaining CBF during physiological changes in blood pressure is termed autoregulation. Autoregulation refers to the physiological mechanisms (myogenic, neurogenic and metabolic) that maintain CBF at a constant level during changes in cerebral perfusion pressure (CPP) provided CPP is within the range of 50-150mm. Autoregulation modulates changes in cerebral vascular resistance with regards to variations in CPP. CPP is defined as the difference between mean arterial pressure (MAP) and intra cranial pressure (ICP). In normotensive adults, CBF is maintained at ~50 mL per 100g of brain tissue per minute, provided the CPP is within 60 to160 mmHg (Phillips and Whisnant, 1992). Compensatory mechanisms following reductions in CPP include: vasodilatation, increase in regional cerebral blood volume, increased oxygen extraction from blood and stimulation of anaerobic glycolysis (Kohno *et al.*, 1995). Brain injury may occur when there is

significant failure of cerebral autoregulatory mechanisms due to severe reduction in CBF (Kendal *et al.*, 2000).

1.3.2 Ischaemic Core, Penumbra and Benign Oligaemia

Positron emission tomography (PET) studies have identified three major compartments within the hypoperfused tissues following cerebral blood flow reduction (Heiss, 2012). The region with the most severe reduction in blood flow is referred to as the ischaemic core. In humans, this region corresponds to a region with CBF below a value of approximately 12ml/100g/min. Cells within the core are irreversibly damaged as permanent anoxic depolarization begins to develop within minutes of the onset of ischaemia. The penumbra defines the region surrounding the ischaemic core with less severe reduction in blood flow range from 12-22ml/100g/min. The penumbra is a highly dynamic region in which the tissue will be progressively recruited into infarct core if reperfusion and/or treatment strategies are not established within the critical time window (Touzani *et al.,* 2001). Brain tissues in which CBF above 22ml/100g/min (benign oligemia) is the hypoperfused tissues that does not usually progress to infarction (Heiss 2000) (Figure 1.6). However, with pre-existing pathological conditions such as hypertension and hyperglycaemia, vascular response to ischaemia in this area may have been compromised, and tissues are susceptible to ischaemic injury despite modest reduction in CBF.

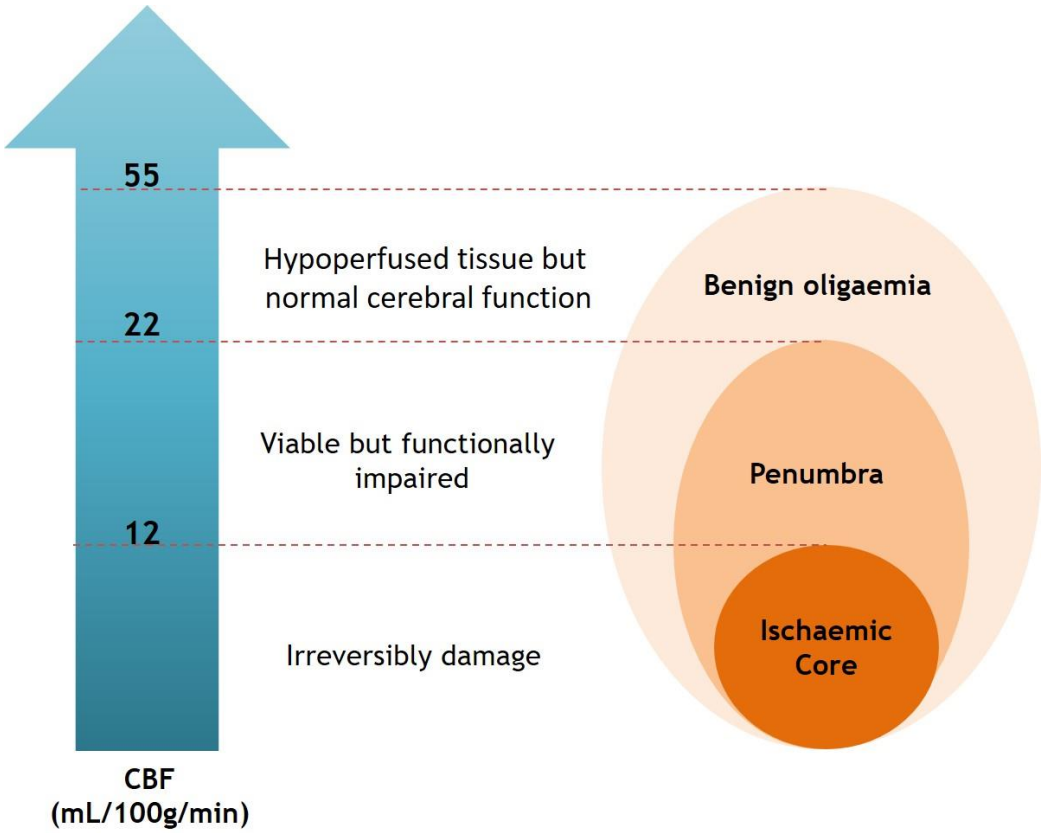

Figure 1.6 Threshold in cerebral blood flow and topographical brain regions following ischaemia. The fate of penumbra depends on rapid restoration of sufficient cerebral blood flow provided within a time window, without which the progression into ischaemic core is inevitable. Cerebral blood flow values adapted from (Heiss 2000).

1.3.3 Factors That Influence Penumbra Demise

Factors influencing the penumbra evolution could exert damaging effects through mechanisms in the cerebral vasculature, brain parenchyma, or both. The knowledge of factors contributing to the evolution of the penumbra is of major interest in the clinical setting; information on penumbral volumes have been used to guide patient selection and therapeutic intervention in clinical practice (Jung *et al.*, 2013).

Many of the established stroke risk factors such as high blood pressure and diabetes have a profound effect on the structure and functions of the cerebral vasculature, such that without reperfusion these can further accelerate penumbra evolution into ischaemic core. Hypertension promotes formation of atherosclerotic plaques in cerebral arteries and arterioles, which predispose to arterial occlusion and ischaemic injury (Dahlöf, 2007). Moreover, hypertension also induces fibrinoid necrosis (lipohyalinosis) of penetrating arteries and arterioles supplying the white matter, resulting in small white matter infarcts (lacunes) or brain haemorrhage (Lammie, 2002). Chronic vascular injury and remodelling alter vascular structure by promoting atherosclerosis and stiffening of arteries, hence promote narrowing, thickening and tortuosity of arterioles and capillaries (Allen and Bayraktutan, 2008). In the brain, the changes in vascular morphology impair CBF autoregulation and its ability to maintain stable blood flow in the event of compromised cerebral circulation (Iadecola and Davisson, 2008). Impaired autoregulation increases susceptibility to ischaemia and leads to more severe ischaemia after arterial occlusion. This is true in the case of middle cerebral artery occlusion in spontaneously hypertensive rats, which demonstrates larger infarcts compared to normotensive rats (Nishimura *et al.*, 2000).

Experimental studies demonstrate that genetic hypertension can influence the amount and lifespan of penumbral tissue. The diffusion-perfusion mismatch method has been used to provide an index of the extent of the penumbra. Spontaneously hypertensive stroke-prone rats (SHRSP) had significantly more ischaemic damage and less penumbral tissue than did normotensive control, Wistar Kyoto Rats (WKY) within 1 hour of MCA occlusion (McCabe *et al.*, 2009).

This finding has an important implication in the management of patients with pre-existing risk factors and suggests that ischaemic damage could progress at a faster rate in hypertensive individuals. In stroke-sensitive animals such as spontaneously hypertensive rats (SHR) and SHRSP, several anatomical and physiological factors have been implicated to increased stroke sensitivity. The impact of collaterals has been addressed by some studies and good collaterals are considered to protect the penumbra (Shuaib *et al.*, 2011)(Zhang *et al.*, 2010). Smaller internal diameter of anastomoses between the anterior cerebral and middle cerebral artery has been identified in the SHRSP rat compared to its reference strain WKY. With increasing age (49-60 weeks old) larger branches of anterior and middle cerebral arteries become narrower. Hence, hypertensive rats are more susceptible to infarction than normotensive rats due to increase resistance in collateral vessels and impaired vasodilator reserve (Coyle and Heistad 1987).

High oxidative stress levels are also thought to contribute to increased sensitivity to experimental stroke in hypertensive rats. Higher production of vascular and brain superoxide anions have been observed in both SHR and SHRSP rats compared to normotensive control WKY rats contributing to increased oxidative stress (Suzuki *et al.*, 1995) (Kishi *et al.*, 2004). Furthermore, ROS such as superoxide anions and hydroxyl radicals have been implicated in the pathogenesis of hypertension (Kerr *et al.*, 1999). In addition to increased levels of oxidative stress, exaggerated inflammatory responses have been reported in hypertensive rats following an immune challenge. Hypertensive rats produced more tumour necrosis factor-α (TNF-α) and platelet activating factor in circulating blood and cerebrospinal fluid in response to provocative doses of lipopolysaccharide than normotensive rats (Sirén *et al.*, 1992). These pro-inflammatory mediators lead to increased adhesion of circulating lymphocytes and transformed the endothelial surface from an actively anti-coagulant to a procoagulant state, thereby increasing stroke susceptibility.

With regards to hyperglycaemia, several mechanisms have been identified through which hyperglycaemia could aggravate cerebral damage in ischaemic stroke. Post-stroke hyperglycaemia is associated with higher mortality and poor functional outcome (Muir et al. 2011). Hyperglycaemia at the time of ischaemic

stroke is associated with increased mortality and morbidity and blood glucose levels over the first 72 hours correlate with growth of the MRI-defined ischaemic lesion (Baird *et al.*, 2003). In type 2 diabetic patients, Ribo and co-workers showed that acute hyperglycaemia at the time of stroke was associated with lower tissue-type plasminogen activator (TPA) recanalization rates, suggesting an impairment of the fibrinolytic system by hyperglycaemia (Ribo *et al.*, 2005). Our in-house data demonstrated that clinically relevant level of hyperglycaemia increased final infarct size and exacerbated early ischaemic lesion growth after permanent middle cerebral artery occlusion in rats (Tarr *et al.*, 2013). Hyperglycaemia also has a profound effect on reperfusion following transient focal cerebral ischaemia, indicated by poor restoration of cerebral blood flow; less than 50% of normoglycaemic rats (Kawai *et al.*,1997). Fructose-fed spontaneously hypertensive stroke-prone (SHRSP) rats, which exhibit features of metabolic syndrome, have shown larger diffusion-weighted imaging (DWI) lesions and final infarcts compared to controls (Tarr *et al.*, 2013). In addition, obesity has been shown to potentiate brain microvascular disruption after experimental stroke causing increased infarct volume in obese mice as compared to lean littermate mice (McColl *et al.*, 2010).

Recently, studies have observed a common feature among co-morbidities presented in stroke patients (i.e. hypertension, diabetes, atherosclerosis, obesity); an elevated inflammatory profile (Dandona *et al.,* 2004)(Hansson and Libby, 2006). Systemic concentrations of inflammatory markers such as C-reactive protein (CRP) and interleukin 6 (IL-6) have been associated with stroke incidence (Muir et al. 2007)(Rodríguez-Yáñez and Castillo, 2008). A study in mice suggested that a systemic challenge with interleukin-1 (IL-1) just prior to MCAO affects reperfusion following transient cerebral ischaemia. Perfusion deficits were observed as early as 180 min after stroke compared to vehicle due to mechanical obstruction by platelet aggregation in the capillaries (Burrows *et al.*, 2016).

1.3.4 Stroke and Disruption of Circadian Rhythm

Epidemiological studies have identified obesity, hypertension, diabetes, atherosclerosis and inflammation as significant risk factors for stroke onset and poor outcome (Baird *et al.*, 2002; Murray *et al.*, 2013). The incidence and overall disease burden of stroke is predicted to rise as these risk factors extend across the developing world (Feigin *et al.*, 2014). In 2007 more than half the global population lived in a city and this is predicted to reach 70% by 2050. Risk factors for stroke are strongly associated with urbanisation mediated through a complex interaction of lifestyle factors including high-energy diets, pollution, sedentary lifestyles and disruption in circadian rhythmicity (Danaei *et al.*, 2013).

1.4 Circadian Rhythm

Experimental studies in both humans and animals associate increased prevalence of cardiovascular and metabolic diseases with disruption in circadian rhythms. Circadian disruption occurs when the internal timing system of the body is asynchronous to the light/dark cycle. Shift work is one example where disruption in the light/dark cycle (photoperiod disruption, PD) occurs chronically and has been associated with principal risk factors for stroke: insulin insensitivity, obesity and hypertension (Scheer *et al.*, 2009). Circadian disruption has a profound effect on the body and brain and induces a proinflammatory state comparable to that associated with diabetes and obesity (Gibson *et al.*, 2010)(Fonken *et al.*, 2013). In addition, these metabolic or physiological changes (i.e. hypertension, hyperglycaemia) have the potential to adversely modify the ischaemic penumbra. To date, little is known about the impact of circadian disruption on sensitivity to stroke and how it influences outcome after stroke. The following section will discuss the impact of circadian disruption on cardiovascular and metabolic disturbances and the potential mechanism that can lead to increased stroke sensitivity.

1.4.1 The Body Clock

The word circadian derives from the Latin *circa* (around) and *dies* (day). The term circadian rhythm was described by Hallberg and is defined as a rhythm in behavioural and physiological parameters that is generated endogenously and displays a length of approximately 24 hours. It persists in the absence of external stimuli, yet can be entrained to daily environmental cues such as light, food or activity (Rüger and Scheer, 2009). Circadian rhythms are present in prokaryotes, fungi, algae, plants and all mammals. Temporal organization within an organism is critical for maintenance of homeostasis as well as adaptation to changing environmental conditions.

In mammals, the circadian timing system is comprised of a master and peripheral circadian clocks. Numerous aspects of physiological functions such as temperature regulation, hormonal control, autonomic tone, and metabolism are regulated by the master clock in interaction with peripheral oscillators (Buijs and Kalsbeek, 2001)(Hastings *et al.,* 2003)(Figure 1.7). The master clock has been identified in the bilaterally paired suprachiasmatic nuclei (SCN) located in the anterior hypothalamus of the brain (Moore 1996). This master pacemaker has anatomical connections with other regions of the brain involved in the control of appetite, energy expenditure regulation and behavioural activity, namely with the supraventricular area, the arcuate nucleus and the lateral hypothalamic area (Saper *et al.,* 2005). Under normal conditions, molecular and behavioural rhythms remain synchronized by the SCN to the light/dark cycle. As the SCN is heavily reliant on the light stimuli as the cue giver, shifting the light exposure resets the clock mechanism in the SCN as well as its downstream molecular and behavioural output. In constant darkness when no time cues are available (i.e. from light) the SCN will autonomously cycle with a period of about 24 hours (e.g. 23.5 – 24.5 hours).

Peripheral clocks are molecular mechanisms that operate in a cell autonomous fashion in most, if not all peripheral tissues such as heart, lungs, adipose tissue, liver, muscle and an extra-SCN regions of the brain (Figure 1.7). (Nagoshi *et al.*, 2004) (Yoo *et al.*, 2003). Peripheral clock genes serve as critical regulators of cellular metabolism such as those involved in glucose and lipid

homeostasis (Marcheva *et al.*, 2010). Despite the autonomous rhythm of the peripheral clocks, they are synchronised to the 24-hour day by the SCN. Nevertheless, recent studies have shown that behaviour such as feeding can directly influence the expression of circadian clock genes within peripheral tissues and potentially overrides the input from SCN; acting as a stronger cue giver (Arble *et al.*, 2010).

At the molecular level, SCN output is generated by a cell autonomous transcriptional auto-regulatory feedback loop which is composed of the transcriptional activators CLOCK and BMAL1 and their target genes: Period (*Per*) and Cryptochrome (*Cry*). Briefly, clock proteins CLOCK and BMAL1 heterodimerize to induce transcription of PER and CRY genes. *Per* and Cry proteins form a complex that translocate back to the nucleus to inhibit CLOCK: BMAL1-mediated gene expression to inhibit their own transcription. This feedback loop produces rhythmic outputs of neural and hormonal signals and gene transcripts and takes approximately 24 hours to complete (Richards *et al.*, 2014).

Due to the earth's rotation around its axis, the SCN is heavily reliant on the light signal as *Zeitgeber* or 'time giver'. Light entrains the master pacemaker in the SCN, which in turn synchronizes extra-SCN and peripheral clocks. Therefore, light acts as the strongest *Zeitgeber* due to its direct influence on the neuronal activity in the SCN. Light information perceived by retina is captured by a specialised intrinsic photosensitive retinal ganglion cells (ipRGCs). The signal is directly transmitted to the SCN via the retino-hypothalamic tract. Once activated, neuronal activity in the SCN coordinates multiple output signals by means of neuro-hormonal pathways to other brain structures and peripheral oscillators in the body (Figure 1.7)(Vosko *et al.*, 2010). Brain clock outputs include behavioural rhythms (i.e. sleep and feeding), whereas peripheral clock outputs include metabolic rhythms such as glucose and lipid homeostasis (Bass and Takahashi, 2010). Together, they optimally regulate much of our physiology and behaviour across the 24 hours day and optimise survival by ensuring internal timings are synchronized to daily variations in the light/dark cycle (Arble et al. 2010).

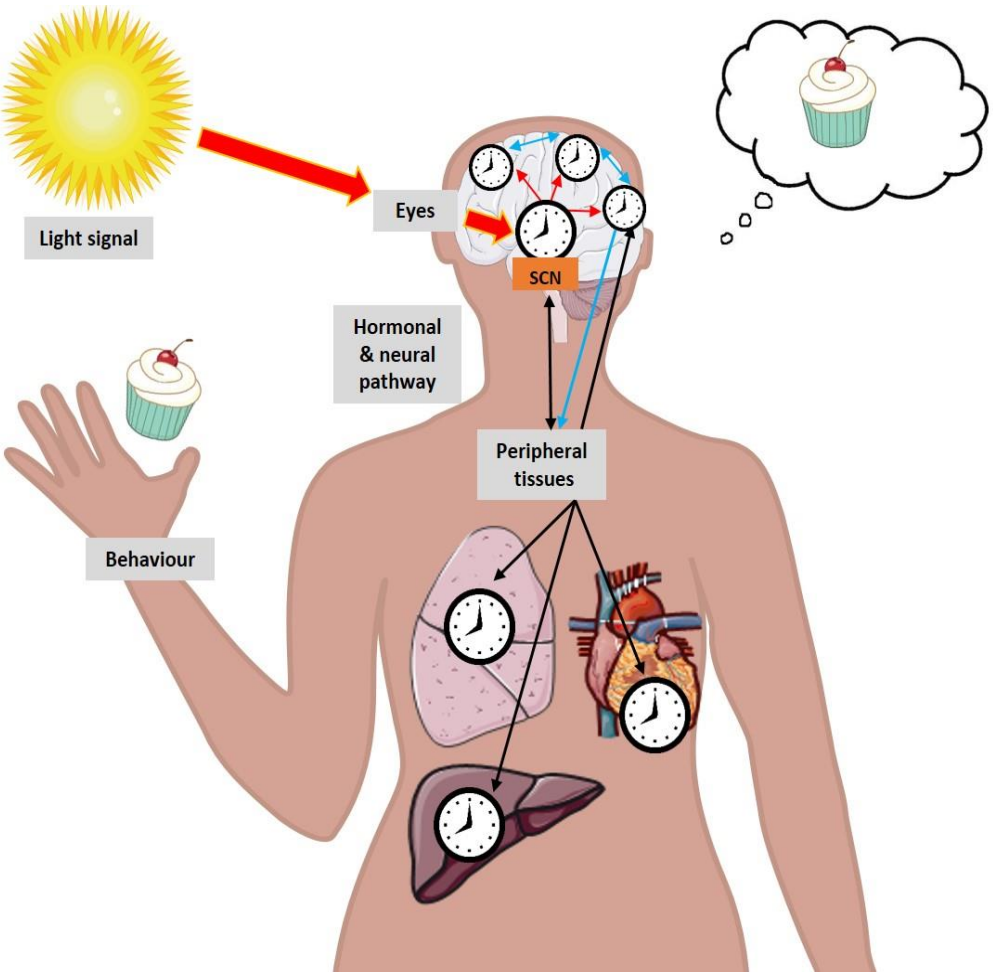

Figure 1.7 Regulation of circadian rhythm by the central circadian clock in the suprachiasmatic nucleus (SCN) of the hypothalamus. Light signal from the retina gives information regarding time of the day. The SCN then synchronises the timing with other extra SCN region in the brain. These brain regions can then influence one another, cause behaviour changes and send timing cues to peripheral tissues via neuro-hormonal pathways. Feeding behaviour can also directly influence the expression of circadian clock and clock controlled genes within peripheral tissues. Hormones and neural signals originating from the periphery can then feedback to the SCN and other brain regions to influence circadian rhythms and genes. Adapted from (Arble et al. 2010).

1.4.2 Circadian Control of Metabolic Function

Delivering adequate oxygen and nutrients to the body is a critical function of the cardiovascular system. Similarly, energy is kept in balance via metabolic processes in vital organs such as liver, pancreas and muscles. The demands on the heart and the local blood flow change dramatically based on our behaviour such as rest/activity, fasting/feeding, as well as with the postural changes. Circadian rhythms allow the cardiometabolic system to anticipate these changes and prepares the body to function effectively.

Glucose homeostasis is subject to strong, endogenous circadian regulation (la Fleur et al. 2001). Nagai and Nakagawa first reported the involvement of SCN in regulation of plasma glucose and insulin daily rhythm, whereby lesioning the SCN abolished the circadian rhythm in both parameters (Yamamoto *et al.*, 1987). Plasma glucose level peaks near the onset of activity in human and rodents. The role of the SCN in glucose homeostasis is further supported by the findings from studies using SCN-lesioned rats which demonstrate disrupted rhythm in 24-hour plasma glucose and insulin levels (La Fleur et al. 1999).

Importantly, daily blood glucose homeostasis also involves control by peripheral clocks in the liver, pancreas, muscle and white adipose tissue (Eckel-Mahan and Sassone-Corsi, 2013). Findings suggest role of food as the strongest cue to the peripheral clock. For example, the circadian clock within the pancreatic ßeta cells directly regulates insulin gene and protein expression, likely in anticipation of increased requirement for insulin secretion upon feeding (Allaman-Pillet *et al.*, 2004). A study in mice employing a restricted feeding protocol demonstrated that feeding time can affect the phase of circadian liver gene expression. Feeding restricted to during the resting phase (day for mice) uncoupled circadian liver gene expression from circadian gene expression in the SCN. In this case, when food is only available during the phase at which the animals are normally inactive (light phase in nocturnal animals), signals triggered by food processing act as dominant *Zeitgebers* on the oscillators of peripheral tissues (Damiola, 2000a). The disturbed phase relationship between the SCN and peripheral oscillations is known as internal desynchronization and this mechanism has been associated with many metabolic related disorders.

1.4.3 Circadian Control of Cardiovascular Function

Numerous markers of cardiac function and metabolism exhibit an endogenous circadian rhythm in humans. The presence of a daily rhythm in heart rate, blood pressure (BP), platelet function and endothelial function has been reported (Martino et al. 2008). Circadian variation in cardiovascular events including ischaemic strokes, myocardial infarction, sudden cardiac death and ventricular arrhythmia has been shown to have peak incidence in the morning hours (Marsh *et al.*, 1990). The SCN control of the cardiovascular rhythm has been suggested by the findings from Scheer et al which demonstrated multiple neural projections from SCN to the heart muscle that involved the autonomic nervous system (Scheer *et al.*, 2003). The SCN also shares direct, reciprocal neuronal feedback circuits with the nucleus tractus solitarius (NTS), that have functional effects on the regulation of vascular reactivity and blood pressure regulation. In this way, the SCN receive BP information directly from the NTS enabling it to react to haemodynamic perturbations, suggesting the role of SCN in BP homeostasis (Buijs et al. 2014).

Despite the belief that SCN is the sole controller of the heart, various neurohumoral factors have been reported to entrain peripheral circadian clocks (Young and Bray, 2007). Recent developments propose that rhythmicity in cardiac processes is mediated by a complex interaction between extracardiac (i.e. behaviours and associated neural and humoral fluctuations) and intracardiac influences such as metabolism and contractile function of myocardium (Martino and Young 2015). Marked oscillations in the expression of circadian clock genes for hearts and blood vessels (i.e. aorta) isolated from rodents at different times of the day have been reported (Young, 2006). Studies have shown that the function of circadian clock within components of cardiovascular system such as vascular smooth muscles cells (VSMC) and cardiomyocytes are affected by different *Zeitgebers*. Nonaka et al. have shown that angiotensin II acts as a *Zeitgeber* for the circadian clock within VSMC in vitro, through an angiotensin II type 1 receptor-dependent mechanism. In this study, brief treatment of VSMC with angiotensin II induced a robust increase in clock gene expression (Nonaka *et al.*, 2001).

1.4.4 Impact of Circadian Disruption on Cardiometabolic Function

The world nowadays has transformed into a 24-hour society that demands late working hours and wakefulness during the night. Shifts in diurnal lifestyles to nocturnal ones has an impact on sleep/wake cycles (Wyse *et al.*, 2014). Metabolic and physiological parameters showing circadian fluctuations such as BP and blood glucose could be affected by circadian misalignment. The latter occurs when the internal timing system is asynchronous with the behavioural cycle (sleep/wake, feeding/fasting) resulting in metabolic disturbances, loss of homeostasis and diseases (Wyse et al. 2011).

Some studies demonstrated a relationship between circadian disruptions, such as occur as a consequence of shift work, with metabolic alterations. Rotating shift work involves photoperiod disruption such that exposure to light/dark cycles are regularly altered compared to normal day/night schedules. In this paradigm, circadian rhythm is chronically disrupted with intermittent periods of re-entrainment to the stable light/dark cycle (Deibel *et al.*, 2014). Among shift workers the risk of developing metabolic syndrome, which represents a combination of metabolic disorders including central obesity, raised plasma glucose and triglycerides, increased blood pressure and reduced high density lipoprotein (HDL) cholesterol has been attributed to physiological maladaptation to sleeping and eating at abnormal circadian phases (Scheer *et al.*, 2009).

Recent epidemiological studies associate shift work with increased risk of cardiovascular and cerebrovascular disease such as myocardial infarction and ischaemic stroke (Vyas *et al.*, 2012). Rotating shift work disrupts circadian rhythms and in humans; exposure to a light/dark cycle lengthened to 28 hours has been shown to increase blood glucose levels, insulin and mean arterial pressure (Scheer et al. 2009). Studies in Japanese male workers, also suggested a positive association between rotating night shift and increased risk of impaired glucose metabolism and diabetes compared with day workers (Morikawa et al. 2005). Another longitudinal study investigating the effects of alternating shift work in male Japanese workers revealed a significant increase in blood pressure from baseline (Suwazono et al. 2008). It has been proposed that endothelial

dysfunction presented by reduced peripheral arterial tone observed in this population may explain the increased cardiovascular risk among shift workers (Suessenbacher *et al.*, 2011).

While epidemiological studies have established important associations between shift work and circadian disruption, *in vivo* studies demonstrated important mechanisms in cardio-metabolic disturbances associated with light/dark cycle manipulation (i.e. photoperiod disruption). Altering the light/dark cycle is one of the mechanisms to induce circadian disruption in experimental animals. In experimental studies modelling shift work or jet lag, animals are shifted and are re-entraining constantly to a new light/dark cycle (Arble *et al.*, 2010). Studies in rodents subjected to experimental shift work showed diminished rhythms of glucose and locomotor activity, and increased body weight caused by food intake during the resting phase (Salgado-Delgado et al. 2010). However, shifting food intake back to the active phase restored metabolic rhythms and body weight in these same animals (Salgado-Delgado et al. 2010). Food intake in the rest phase leads to desynchronization, characterized by misaligned temporal patterns of clock genes and metabolic genes within the liver (Salgado-Delgado et al. 2013). These findings suggest that normal alignment of feeding in addition to the environmental light/dark cycle is critical to maintaining energy homeostasis and that the metabolic consequences of circadian disruption could be rescued by food timing. Furthermore, an experimental shift work in diabetic prone rats has resulted in hyperglycaemia secondary to pancreatic Beta cell loss and dysfunction (Gale *et al.*, 2011). A summary of the metabolic consequences of photoperiod disruption is given in Figure 1.8.

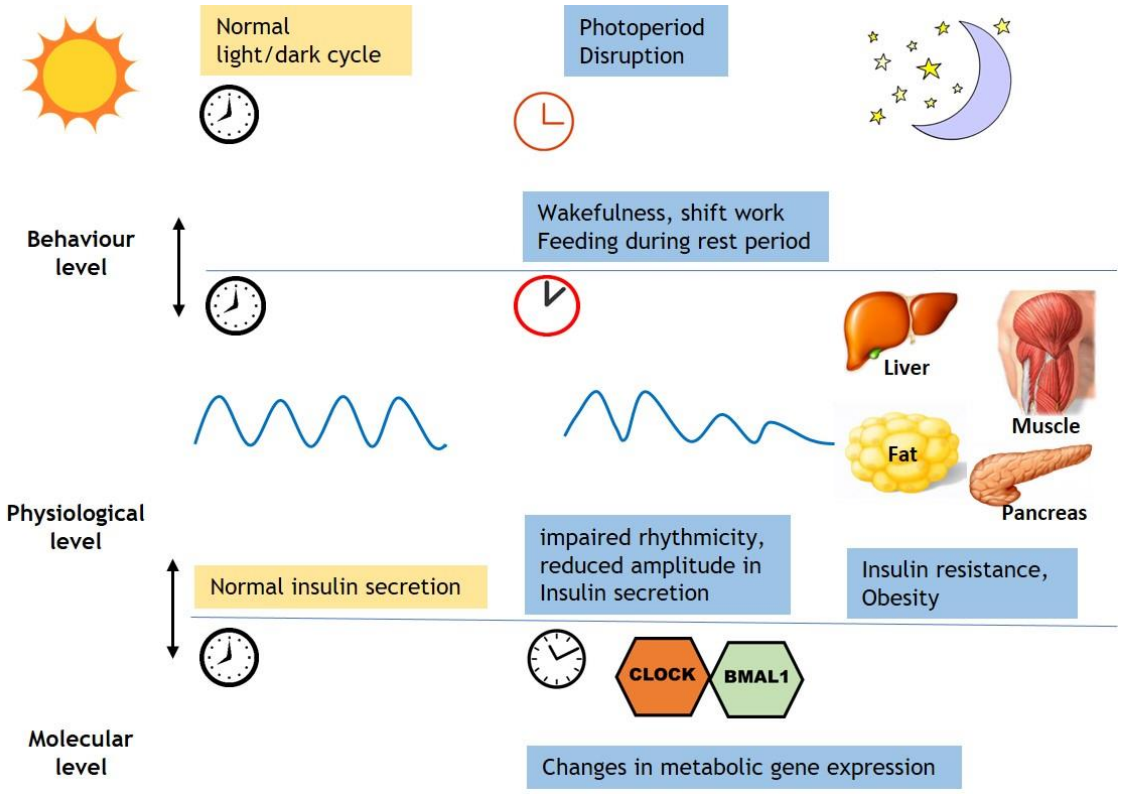

Figure 1.8 Metabolic consequences of photoperiod disruption. Circadian and physiological system together with molecular clock functions are interconnected and synchronised to the changes in environmental light/dark cycles. Oscillations within some peripheral tissues, such as in the liver, fat, muscles and pancreas are largely affected by feeding as a stronger *Zeitgeber*. Wakefulness and night time feeding contributed to metabolic changes that leads to the development of insulin resistance, obesity and changes in metabolic gene expression. Adapted from (Kurose *et al.*, 2014).

Several studies suggest that circadian clock gene mechanisms underlie cardiovascular pathology. For example, mice lacking the clock gene BMAL1, exhibit loss of diurnal variation in heart rate and BP and develop dilated cardiomyopathy (Curtis *et al.*, 2007)(Lefta *et al.*, 2012). In addition, BMAL1-knockout mice exhibited impairment of normal protective endothelial responses to vascular injury, and demonstrated intensified pathologic remodelling and predisposition to vascular thrombosis (Anea et al. 2009). Durgan and colleagues have shown that the circadian clock within cardiomyocytes is responsible for myocardial metabolic gene expression which mediates tolerance to myocardial ischemia/reperfusion (Durgan *et al.*, 2011). Per2 knockout mice (Per-/-) showed impaired glycolytic capacity and myocardial adaptation to ischaemia, leading to larger infarct size after myocardial ischaemia/reperfusion compared to wild-type mice (Eckle *et al.*, 2012). Photoperiod disruption in mice has been reported to impair vascular adaptive response to pathological insult secondary to aortic constriction. In this instance, disrupted mice showed significantly less compensatory hypertrophy despite the increased in blood pressure than the control mice. Importantly, the adverse remodelling was alleviated upon returning the animals to their normal diurnal cycle (Martino et al. 2007). This study also demonstrates the importance of synchrony between the intrinsic circadian period and the external light/dark cycles, implicating the role of circadian disruption in the pathogenesis of heart disease.

1.4.5 Circadian Disruption and Ischaemic Brain Damage

The metabolic and physiological aberrations (such as hyperglycaemia and hypertension) induced by PD could exert damaging effects in the penumbra. Impairment of collateral vessel dilation after arterial occlusion is a potential mechanism leading to increased severity of ischaemia. Remarkably little information exists on the influence of PD on responses to brain ischaemia but effects in the cardiovascular system lend plausibility to the suggestion that cerebrovascular effects could occur. Furthermore, the role of SCN in the regulation of vascular reactivity and blood pressure (Buijs et al. 2014) provide physiological evidence that disruption of circadian clock function could affect vascular response following ischaemic stroke and support the hypothesis that PD will affect cerebrovascular response to ischaemic stroke.

Disruption of cerebral blood flow triggers the onset of ischaemic cascades in which excitotoxicity and oxidative damage are major factors contributing to the demise of brain tissues (Dirnagl *et al.*,1999). The production of antioxidants and protective enzymes, have been reported to be regulated and expressed in rhythmic fashions (Wilking *et al.*, 2013). The circadian clock was recently shown to regulate a major antioxidant pathway (nuclear factor erythroid 2-related factor (NRF2)/glutathione), and disruption of this regulation induced oxidative stress and pulmonary fibrosis (Pekovic-Vaughan *et al.*, 2014). Similarly, the clock gene BMAL1 regulates cerebral redox homeostasis and mice with BMAL1 deletion exhibit high ROS levels in brain and increased neuronal oxidative damage (Musiek *et al.*, 2013). Similarly, increased oxidative stress in the brain has been observed in animals exposed to PD (Kishi and Sunagawa 2011). Taken together, such evidence lends plausibility to the concept that disruption of circadian clocks increases the sensitivity of brain tissue to ischaemia such that the ischaemic cascade is amplified, and tissue damage is greater.

1.4.6 Hypothesis Addressed in The Thesis

Circadian rhythms optimise survival by synchronising physiology and behaviour to environmental variation. There is evidence from human associational studies of a link between circadian disruption and risk factors for stroke. Many of the reported metabolic or physiological changes in PD, e.g. hypertension, diabetes, have potential to adversely modify the ischaemic penumbra. However, little is known on how PD could affect cardiovascular and metabolic parameters hence modify stroke sensitivity and severity. The studies in this thesis aimed to test the hypothesis that PD increases sensitivity to focal cerebral ischaemia. The information will raise awareness of how environmental conditions involving constantly changing patterns of light/dark cycles could influence the severity of stroke therefore, proper intervention can be implemented in a high-risk population.

1.5 Thesis Aims

1. To determine if photoperiod disruption induced in rats by recurrent phase advance of the light/dark cycle, influences the sensitivity of the brain to ischaemic damage induced by permanent MCAO.

2. To characterise and optimise the animal model for transient focal cerebral ischaemia.

3. To determine the impact of photoperiod disruption on sensitivity to focal cerebral ischaemia in spontaneously hypertensive rats and microglia activation.

Chapter 2 - Methods

2.1 Animals

Adult male Sprague-Dawley, Wistar or spontaneously hypertensive rats (SHR) were obtained from Envigo (UK) and housed in an animal care facility at the University of Glasgow. On arrival to the University all rats were acclimatised for 2 weeks before experimentation. Rats were housed in groups of 2-4 rats or singly (for studies in Chapter 3) per cage and were maintained on a 12:12 hour light/dark cycle. Water and food (standard rat chow) were available *ad libitum*. All experiments and surgical procedures in Chapter 5 were performed under license from the UK Home Office. Surgical procedures for Study 1 in Chapter 4 were carried out by Lindsay Gallagher. Middle cerebral artery occlusion surgery in Chapter 3 was performed by Dr Lisa Roy. Animals were excluded from the study and data analysis following failed middle cerebral artery occlusion (MCAO) evident by no obvious infarct assessed by T2 magnetic resonance imaging, died during the MCAO surgery or within 24 hours of surgery.

2.2 Surgery

2.2.1 Animal Preparation

All experiments in this thesis were performed with strict adherence to the National Centre for the Replacement, Refinement and Reduction of Animals in Research (NC3R's) ARRIVE (Animal Research; Reporting In Vivo Experiments) guidelines (http://www.nc3rs.org.uk/arrive-guidelines). On the day of surgery rats were transferred from the animal housing unit to the operating theatre and weighed prior to induction of anaesthesia. Aseptic techniques were maintained throughout the surgery. Prior to the surgical procedure, operating table was properly cleaned and disinfected with chlorhexidine-containing disinfectants (Hibiscrub). Surgical instruments and consumables were sterilised in an autoclaved. All surgical equipment including surgical instruments, sutures and swabs, sterile saline, as well as other consumables required for surgery were set up in advance prior to the start of surgery.

2.2.2 Induction and Maintenance of General Anaesthesia

Rats were initially anaesthetised in an anaesthetic chamber using 5% isoflurane (Baxter Healthcare Ltd, UK) in nitrous oxide: oxygen mixture (70:30). Once deeply anaesthetised the rat was removed from the chamber and immediately transferred to a designated area within the operation theatre where the fur overlying any planned incision sites was shaved using electric clippers (Wella, Germany) and cleared using a handheld vacuum (Black & Decker, USA). The depth of anaesthesia during surgical procedures was assessed at regular intervals by means of the withdrawal reflex, where the footpad of a hind limb is tightly squeezed to evoke withdrawal of the foot. Absence of withdrawal reflex ensured adequate depth of anaesthesia.

2.2.3 Surgical Tracheotomy and Oral Intubation

A surgical tracheotomy was performed in all experiments where animals were not allowed to recover following surgery. Following removal from the anaesthetic chamber, delivery of anaesthesia was continued via face mask at 2.5%–3% isoflurane in the nitrous oxide: oxygen mixture (70:30). The neck area, was cleaned with 70% alcohol and a small incision was made through the skin and fascia of the neck. Blunt dissection technique was used to expose the trachea and separate the overlying connective tissue and musculature. The connective tissue surrounding the trachea was carefully isolated using small round forceps and two ligatures of 2-0 thread (Sofsilk, Tyco Healthcare, USA) were placed under the trachea and loosely tied around the proximal and distal ends approximately 1.5cm apart. An incision was made between rings of tracheal cartilage using micro scissors (World Precision Instruments, UK) and a ventilation tube (Linton Instruments, UK) was quickly inserted into the trachea approximately 2.0cm towards the bronchi. The ventilation tube was then connected to the ventilator (Ugo Basile, Linton Instruments, UK) where the stroke volume was set to 2.5 to 3ml at a frequency of 45 strokes per minute to maintain anaesthesia. The ligatures at both ends of the trachea were tied firmly around the trachea and ventilation tube to hold it in place and the neck was stitched using 4-0 silk suture (Softsilk™, Covidien, USA).

In experiments where the animal was allowed to recover following surgery, artificial ventilation was maintained by oral intubation. Following the initial induction of anaesthesia, animals were transferred to a cork board. A loop of 4-0 silk thread (SoftsilkTM, Covidien, USA) pinned to the board was placed around the upper incisors of the animal and used to lift the animal into a vertical position. A fibre optic light (Schott, USA) was positioned over the neck of the animal to get a clear view of the vocal cords and trachea. The tongue was pulled to one side and a 16-gauge catheter (MillPledge Veterinary, UK) attached to a guide wire was then advanced into the trachea. Once passed the vocal cord, the guide wire was then removed and the catheter was attached to a ventilator at a stroke volume of 2.5-3ml and 60 strokes per minute. Correct placement of tube was confirmed by equal chest expansion. In order to ensure the intubation tube remained secure during anaesthesia and transfer to MRI scanner it was sutured to the side of the mouth using 4-0 silk suture. Depth of anaesthesia was regularly assessed throughout the duration of anaesthesia.

2.2.4 Femoral Artery Cannulation

In Chapter 4, cannulation of the right femoral artery was performed to allow continual monitoring of mean arterial blood pressure (MABP) and blood gases. The right groin region was shaved and sterilised with 70% alcohol. A small incision was made over the region of femoral vessel followed by blunt dissection and femoral artery was carefully isolated from the femoral vein and nerve by blunt dissection using small curved and straight-edged forceps. Two ligatures of 4-0 silk thread were securely fastened around the distal end and loosely tied around the proximal end, approximately 2cm apart. The ligatures were gently pulled and secured to the corkboard by using a masking tape. Using a micro-scissors, small incision on the artery was made at midway between the 2 ligatures. With the aid of right-angled sharp forceps, a 30cm length of polythene catheter (external diameter 0.96mm; internal diameter 0.58mm, Smiths Medical International Ltd) attached to a 1ml syringe filled with 1% heparinised saline (1000units/ml, Wockhardt UK Ltd, UK) was inserted into the vessel. Tension on the proximal tie was released to allow catheter advancement of approximately 2-3 cm along the vessel. Ligatures were secured tightly around the vessel and the inserted catheter. The catheter was connected to a pressure transducer

linked to a computer where physiological parameters including heart rate and blood pressure were recorded using Biopac software.

2.3 Middle Cerebral Artery Occlusion

2.3.1 Distal Diathermy Method

The surgery for this was carried out by Dr Lisa Roy. Animal was placed in a lateral position with the side of head in clear view. The fur between the left eye and ear was shaved using electric clippers and the area was cleaned with alcohol swabs. The left eye was sutured closed (6-0 thread, Sofsilk, Tyco Healthcare, USA) to prevent it from drying out during surgery. A skin incision was made at the midpoint between the left eye and auditory canal with sharp-ended scissor and the temporalis muscle was carefully separated. Metal retractors were used to expose the skull area below the temporalis muscle. The surrounding connective tissue and muscle was further removed from area and protected from drilling using pieces of absorbent sponge (Surgiswabs, John Weiss International). Using a dental drill (Volvere Vmax, Nakanishi Inc) with a round diamond bur (Wright Cottrell, UK) the skull was thinned in order to expose the MCA. Drilling was performed across the entire area of exposed skull in an up and down motion, with regular application of sterile saline (0.9% Baxter Healthcare Ltd) to ensure the underlying brain was cooled throughout. Drilling was continued until the MCA and inferior cerebral vein (ICV) were visible through the skull. The remaining thin layer of bone was removed using needle point forceps. Direct access to the MCA was achieved by removing the dura mater using a modified dura hook (constructed in-house by bending the tip of 21-gauge needle), in a region where there were no visible blood vessels. Bleeding from small vessels was minimised and cleared by flushing the area with sterile saline. If bleeding failed to stop, gentle pressure with absorbent sponge was applied or the vessels were electrocoagulated with diathermy forceps or by reducing the mean arterial pressure to approximately 70-80mmHg via increasing the isoflurane concentration. The point at which the MCA crosses the ICV was identified and the portion of MCA, 2mm distal to the point was electrocoagulated with diathermy forceps (110mm angled, Eschmann, UK). This process was carried out

in saline to prevent diathermy forceps sticking to the vessels. Upon completion of electrocoagulation, the portion of MCA was cut with micro scissors to confirm complete occlusion. Following occlusion, the absorbent sponges and retractors were then removed from surgical area and haemostatic gauze (Surgicel, Ethicon, Johnson & Johnson Medical Ltd 2011) soaked in saline was used to cover the craniectomy site. The muscle was closed over and wound was then sutured using a 4-0 silk suture and the eye suture was removed.

2.3.2 Intraluminal Filament Method

Induction of focal cerebral ischaemia via this method was performed by Lindsay Gallagher for study in Chapter 4 and by me for study in Chapter 5. Transient occlusion of the MCA was performed according to the intraluminal filament model which was first described by Koizumi and co-workers 1986 (Koizumi *et al.*, 1986), with subsequent modifications (Longa *et al.*, 1989) (Figure 2.1). All surgery was performed under a light operating microscope (Zeiss, Germany). In animals where a surgical tracheotomy was performed the common carotid artery (CCA) was isolated through the incision site used for exposing the trachea. If the animals were orally intubated, then the neck area was shaved and sterilised with 70% alcohol prior to midline incision being carried out through the skin and fascia overlying the trachea. The left CCA was exposed by carefully retracting the soft tissues. Curved and straight-edged forceps was used to isolate the left CCA from the surrounding nerves and tissues. Care must be taken to avoid injury to the vagal nerve, which runs next to the CCA. A 4-0 silk thread was securely tied around the CCA ~15mm below the bifurcation of the external carotid artery (ECA) and the internal carotid artery (ICA). A 4-0 silk thread was loosely tied around the CCA immediately below the bifurcation of the ECA and ICA. A loose tie was placed around the ECA above the occipital artery branch but below the ascending pharyngeal artery branch. Another loose tie was placed around the occipital artery and a separate tie was place around the ICA. The pterygopalatine artery was identified and a suture was placed and tied off at its bifurcation from the ICA using a 4-0 silk thread (Figure 2.1). Ties around ECA, ICA and occipital arteries was secured with enough tension to prevent flow. This was achieved by using masking tape to secure the ties to the corkboard. A small incision was made in the CCA just below the bifurcation. The filament was

typically advanced at a distance of 20-22mm from carotid artery bifurcation in rat. The distance was measured from the tip of the filament and a bend was introduced at the point. Filament was gently advance into the vessel to avoid damage to the vascular endothelium. The CCA was cauterized prior to wound closure. For Study 1 in Chapter 4, the intraluminal filament was prepared from a length of 3-0 or 4-0 monofilament nylon suture (Dermalon, Sherwood Medical, USA). The filament was blunted at one end by creating a small bulb using a cauterising pen (Aaron Medical, FL, USA). The diameter of the bulb was measured and this was used to select filaments for use based upon the weight of the animal. For studies in Chapter 4 and Chapter 5, the intraluminal filament was purchased from Doccol (Doccol Corporation, CA, USA).

2.3.3 Physiological Monitoring

Physiological parameters such as heart rate, body temperature, MABP and blood gases were regularly monitored and recorded throughout the period of anaesthesia. Body temperature was maintained within physiological range at 37±0.5 ºC using an angle poise heat lamp and recorded using a rectal thermal probe (Physitemp, New Jersey, USA). Blood gases (blood pH, arterial oxygen pressure (PaO_2) and arterial carbon dioxide pressure ($PaCO_2$) was taken after the induction of anaesthesia and at hourly interval for the duration of the experiment. Blood gases were maintained within physiological range by adjusting the ventilator setting (i.e. tidal volume and rate of respiration). Due to high percentage of oxygen ventilating the animal, a higher PaO_2 value (80-100mmHg) was expected. Mean arterial blood pressure and heart rate data was obtained by connecting the femoral artery catheter to a pressure transducer in combination with an MP150 Biopac system (Biopac systems Inc, USA) and AcqKnowledge software (Linton). The MABP was maintained within the range of 85-100mmHg for normotensive rats by adjusting the isoflurane concentration.

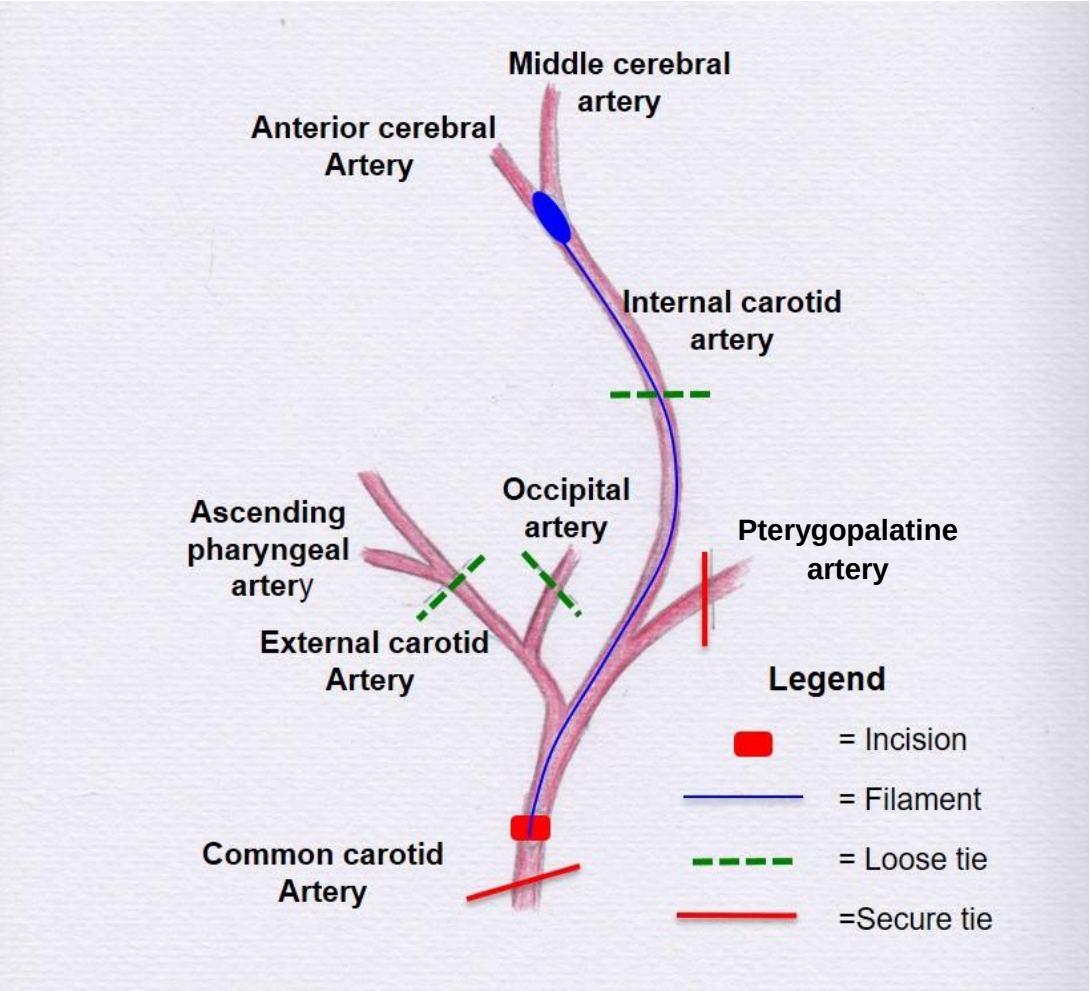

Figure 2.1 The intraluminal filament model of MCAO. Secure ties (red) were placed at the proximal end of common carotid artery and pterygopalatine artery. Loose ties (green) were placed around the external carotid, internal carotid and occipital artery. Gentle tension was applied at these arteries to stop blood flow. A small incision was made on the common carotid artery and filament was advanced along the internal carotid artery until it lodges at the proximal end of the middle cerebral artery.

2.3.4 Recovery from Anaesthesia and Post-Operative Care

Upon completion of surgical procedures, the femoral artery cannula was removed and the small incision in the artery was sealed using diathermy forceps in order to maintain patency of vessel. Surgical site was flushed with sterile saline. To ease pain and discomfort, subcutaneous Ropivacaine (Naropin; at 1-2mg/kg) was given at the surgical before closing the wound with 4-0 suture. Isoflurane was switched off and rats were ventilated with 100% of oxygen until responsiveness to foot pinching was observed and breathing against the ventilator. At this point the animal was disconnected from the ventilator and the intubation tube was removed. The animal was supplemented with 100% oxygen via a facemask until breathing became steady and the animal started to regain consciousness.

The animal was transferred to a clean cage lined with soft absorbent pads containing softened food and water available ad libitum. The cage was transferred to a recovery room maintained at ~25°C and the animal was housed there until it was killed. During the first 24 hours, animal may exhibit behavioural changes, lethargy, altered consciousness or seizure episode with large infarct. Therefore, animal was closely monitored 3 times per day, for the next 3 days and details of the condition was recorded on recovery sheet. To aid recovery, animal was kept adequately hydrated with subcutaneous fluid and soft diet. Subcutaneous sterile saline was administered at 5 ml/kg on each side of the body for 3 days and soft diet (softened rat chow, baby food or Complan) was given to aid recovery.

2.4 Brain Processing

2.4.1 2,3,5-triphenyltetrazolium Chloride (TTC) Staining and Quantification of Ischaemic Damage

Tetrazolium salt such as 2,3,5-triphenyltetrazolium chloride (TTC) has become a convenient marker for detecting infarcts in tissue slices. TTC is a colourless water soluble salt which is reduced by dehydrogenase enzymes to a lipid soluble, bright red formazan. This staining method is easy to apply and is effective in

assessing the infarct volume at 24 hours after permanent and transient ischaemia (Hatfield et al. 1991; Popp et al. 2009). The staining properties based on the function of mitochondrial system. In undamaged tissue, TTC is oxidised by mitochondrial dehygrogenases to a lipid soluble bright red formazan. Whereas in damaged/infarcted tissue, TTC remains colourless so no staining is observed (Figure 2.2). Following decapitation, brain was removed and kept in a minus 20 freezers for 20-30 minutes, to ease the slicing process. The brain was removed from the freezer and using the matrix (World Precision Instruments, Hertfordshire, UK) as a guide the brain was sliced at 2mm apart, one slice at a time using a single razor blade. Slicing the brain with brain matrix was not performed as the fragile brain slices often fragment and difficult to remove intact. The brain sections were then immersed in 2% TTC (Sigma-Aldrich, Switzerland) prepared in phosphate buffered saline in a cell culture dish. As the TTC is light-sensitive, the dish was covered with an aluminium foil and incubated in the oven at 37°C for 15 min. TTC staining after 24 hours of focal ischaemia displays deep red staining of normal brain tissue and pale non-staining of ischaemic brain tissue with a distinct border. The slices were transferred into fixative solution 4 % paraformaldehyde (PAM) for 24 hours before quantification of ischaemic damage. Digital photographs of both sides of the slices were taken with a Canon Camcoder Mv750i. The areas of the infarct, ipsilateral (ischaemic) and contralateral (non-ischaemic) hemispheres were measured on both sides of each slice using image analysis software (ImageJ, http://rsb.info.nih.gov.ij). Infarct volume was calculated by summing the individual areas and multiplying by the slice thickness. Infarct volume was corrected for ipsilateral brain swelling (Swanson et al., 1990). Volume of each hemisphere calculated as follows:

Corrected infarct= volume	Volume of contralateral - hemisphere	(Volume of ipsilateral - hemisphere	Lesion volume)

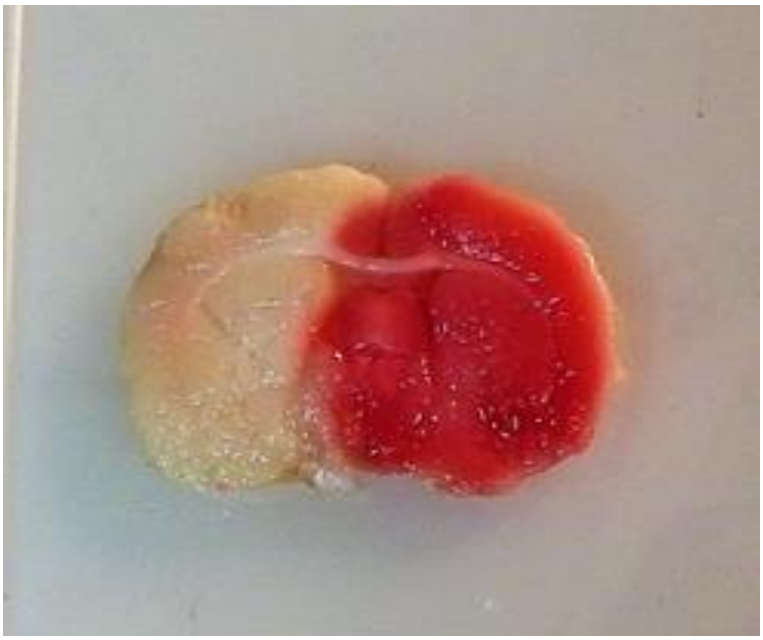

Figure 2.2 Representative coronal brain slice stained with TTC, 24 hours after permanent MCAO. Image depicts coronal level 3 (Osborne *et al.*, 1987). The infarct is well demarcated and represents by pale area in cortical and subcortical regions.

2.4.2 Perfusion Fixation

Prior to opening of chest cavity, animals were deeply anaesthetised with 4-5% isoflurane in anaesthetic chamber delivered in a 30:70 mixture of oxygen and nitrous oxide. Animal was transferred to an absorbent tray and anaesthesia was continued via a face mask. An incision was made below the sternum and the ribcage was cut on both sides to expose the viscera of the chest cavity. Using forceps, the beating heart was held gently and pulled down to allow visualisation of the aorta. A blunt-ended 16-gauge needle, connected via a pressurised system to a sphygmomanometer and three-way taps to either a flask of 0.9% saline containing heparin (10ml/Litre) or a flask containing 4% PAM (in 50mM phosphate buffer), was inserted into the base of left ventricle and advanced into the aorta. The needle was clamped to secure it in place and the right atrium was cut to allow blood to drain out of the heart. Perfusion was carried out via a sphygmomanometer and was maintained at physiological levels (around 100-120mmHg) with approximately 200-250ml of heparinised saline. Once the blood ran clear from the body, PAM was perfused at the same pressure. Spontaneous movement and a lightened colour of the liver were indicative of a successful perfusion fixation. After fixation rats were decapitated and the heads post-fixed in 4 % PAM for 24 hours. After 24 hours of post-fixation brains were removed and subsequently post-fixed in 4% PAM for a further 24 hours before tissue processing.

2.4.3 Tissue Processing, Embedding and Sectioning

Following perfusion fixation brains were transferred to an automatic tissue processor (Tissue-Tek VIP, Miles Scientific). The process involves multiple dehydration cycles through alcohols and then into xylene which acts as a clearing reagent. Brains were then submerged in liquid paraffin wax at 60°C. The entire process takes 59 hours to complete (Table 2.1). The brains were then removed from the processor and individually housed in small containers where they were embedded in liquid paraffin wax and left to cool. Once the paraffin had set, the embedded brains were removed from their containers and mounted onto wooden blocks. Each brain was cut coronally into 5µm sections using a microtome (Leica, UK). The sections were stretched by surface tension on a

water bath (approximately 40°C) and mounted onto poly-l-lysine coated glass slides. Slides were dried on a hot-plate and then sorted at room temperature in protective cases until required for Iba-1 immunohistochemistry staining as described in Chapter 5.

Stage	Solution	Temperature	Time (hours)
1	70% alcohol	35°C	2
2	80% alcohol	35°C	3
3	96% alcohol	35°C	4
4	Absolute alcohol	35°C	4
5	Absolute alcohol	35°C	5
6	Absolute alcohol	35°C	5
7	Absolute alcohol	35°C	6
8	Xylene/Absolute alcohol	35°C	4
9	Xylene 1	35°C	5
10	Xylene 2	35°C	5
11	Paraffin wax 1	60°C	5
12	Paraffin wax 2	60°C	5
13	Paraffin wax 3	60°C	6

Table 2.1 Tissue processing schedule for rat brains.

2.5 Magnetic Resonance Imaging (MRI)

2.5.1 Magnet Specifications

MRI scanning took place at the Glasgow experimental MRI centre (GEMRIC) based within the University of Glasgow. All animals were scanned in a Bruker Pharmascan 7T system equipped with a 4-channel phased array surface coil and a 72mm birdcage resonator for brain imaging. MRI scanning was performed by staff within the centre: Jim Mullin, Dr Chris McCabe and Lindsay Gallagher.

2.5.2 Physiological Monitoring During MRI Scan

Animals were transferred to the MRI scanner and put in prone position a Perspex rat cradle and the head was restrained using tooth and ear bars. A 4-channel phased array surface receiver coil was placed on the rat's head before the cradle was placed inside the scanner. During MRI scanning, anaesthesia was either maintained via face mask for animals which have been recovered from MCAO or via a ventilator for acute MRI scanning during MCAO. Anaesthesia was delivered at 2-2.5% isoflurane in a 70:30 mixture of nitrous oxide: oxygen throughout the scanning. Respiratory rate was monitored with a pressure sensitive pad placed under the rat's chest and connected to a Biopac system. A rectal thermocouple probe was inserted for continuous temperature monitoring and the body temperature was maintained within physiological range (37±0.5°C) using a temperature controlled water jacket.

2.5.3 Diffusion-Weighted Imaging (DWI)

Technical Specifications

In Chapter 5.2.2, diffusion-weighted imaging was performed at 25 min post-MCAO to assess the early ischaemic lesion. Spin Echo-Echo Planar Imaging (SE-EPI) diffusion-weighted scans consisted of eight contiguous coronal slices of 1.5mm thickness which were generated with an in-plane resolution of 260μm. The field of view was 25 x 25mm^2 and the matrix size was 96 x 96mm. The gradient strengths (B values) were 0 and 1000s/mm2 and gradient directions

were x, y and z. The repetition time (TR) was 4000.3ms and the echo time (TE) was 22.9ms. The DWI scan took approximately 3 mins.

Post Processing

Quantitative ADC (apparent diffusion coefficients) maps (mm^2/sec) were generated for each of the 8 continuous coronal brain slices (Figure 2.3A). Raw datasets were initially processed using Paravision v5 software (Bruker Biospin). Subsequent analysis of ADC maps was carried out using ImageJ (http://rsb.info.nih.gov.ij) software. To calculate ADC lesion volume an abnormal diffusion threshold was applied to all ADC maps (Figure 2.3B). ADC threshold values are described in detail in Chapter 5.

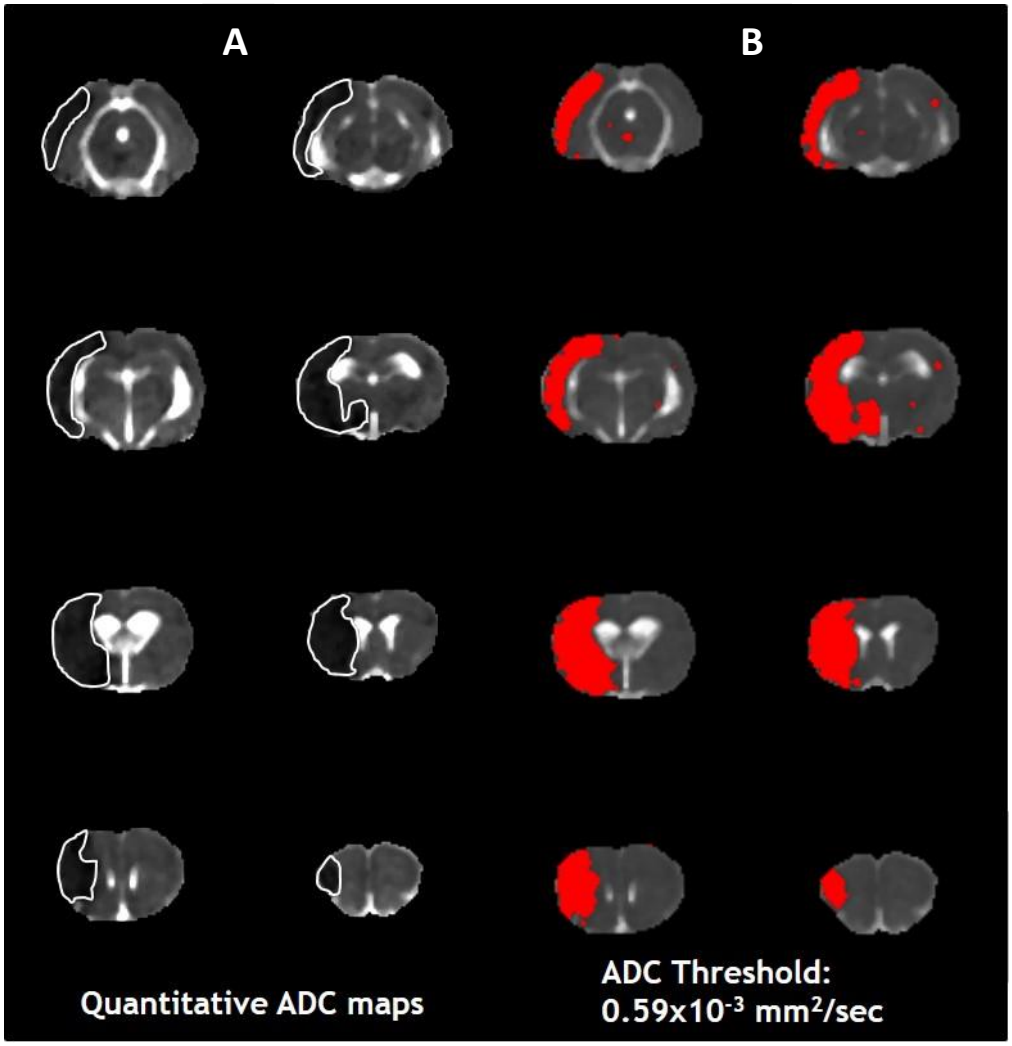

Figure 2.3 (A) Quantitative ADC (apparent diffusion coefficient) maps on 8 contiguous coronal slices of the rat brain (caudal to rostral) and (B) strain-specific ADC thresholds (coloured in red) for hypertensive rats was applied to each of ADC maps obtained following 25 minutes MCAO for assessment of acute ischaemic injury.

2.5.4 RARE T_2 Weighted Imaging

In all experiments, infarct volume was determined using MRI RARE (rapid acquisition with refocused echoes) T_2 weighted imaging. A coronal RARE T_2 weighted sequence (effective TE: 100ms, TR: 6000ms; in plane resolution of 97um; 16 slices of 0.75mm thickness) was used to determine final infarct volume at 7 days post MCAO (Figure 2.4A).

Image J was used to measure the areas of infarct by manually delineating the hyperintense area on all 16 coronal slices (Figure 2.4B). Infarct volume was calculated by summing the total area across all 16 slices and multiplying by the slice thickness (0.75mm). The areas of the ipsilateral and contralateral hemispheres on each slice were also measured and these were used to calculate the volume of each hemisphere. Infarct volume was corrected for oedema using published equations (see below) that take into account both the compression of the contralateral hemisphere (Gerriets *et al.*, 2004) and swelling of the ipsilateral hemisphere (Swanson *et al.*, 1990).

Following equation was used for calculation of infarct volume corrected for swelling of ipsilateral hemisphere:

Corrected Lesion Volume = volume of contralateral hemisphere – (volume of ipsilateral hemisphere – lesion volume)

A correction factor which accounts for compression of the contralateral hemisphere is calculated by the following equation:

Compression Factor = (ipsilateral volume + contralateral volume)/(2 x contralateral volume)

For calculation of final infarct volume that is corrected for both ipsilateral swelling and contralateral compression, the follow equation was used:

Infarct Volume = corrected lesion volume x compression factor

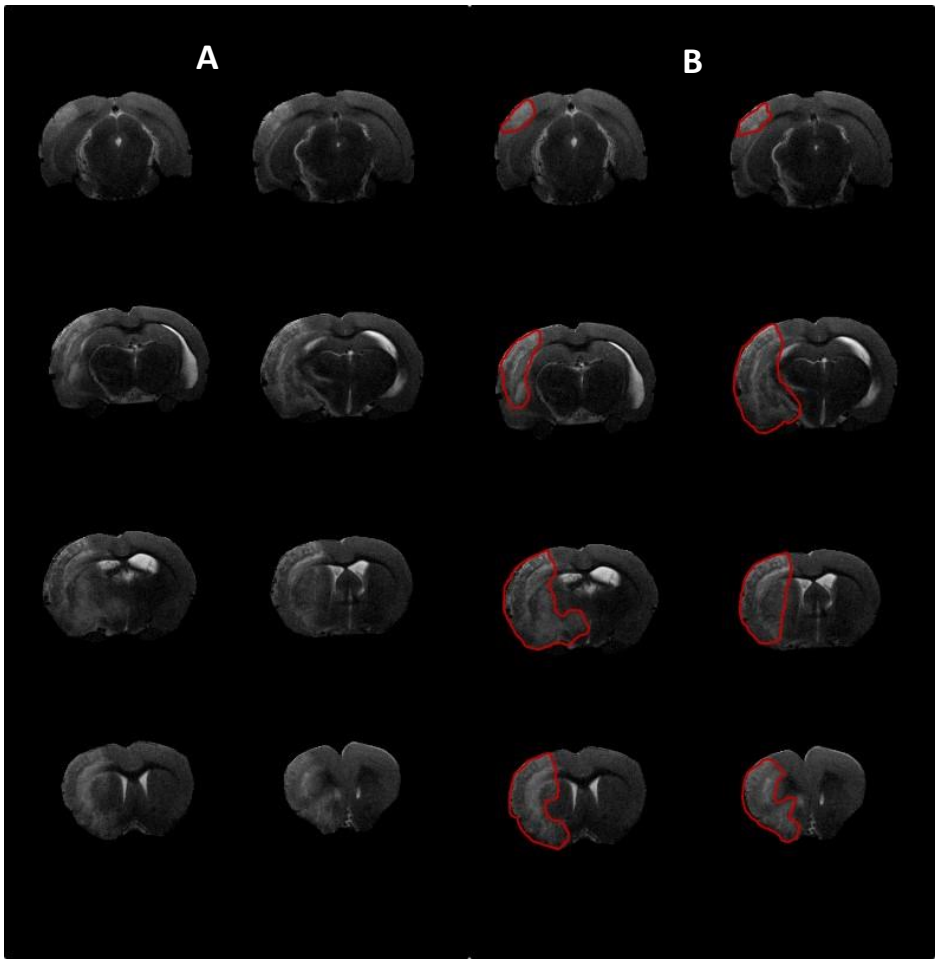

Figure 2.4 MRI RARE T_2 images from a representative SHR rat acquired at 7 days following transient occlusion of the middle cerebral artery. Column (A) shows 8 coronal slices and ischaemic damage appears hyperintense within the ipsilateral hemisphere. Extensive swelling of the ipsilateral hemisphere and compression of contralateral hemisphere was also noted. Image J software was used to delineate the infarcted tissue, as shown in column (B). Infarct volume was corrected for both ipsilateral swelling and contralateral compression using published equations by (Swanson *et al.*, 1990; Gerriets *et al.*, 2004).

2.6 Neurological score

An 18-point composite neurological score was used to assess the functional outcome in rats following MCAO. The score includes 6 neurological tests that assessed spontaneous activity, symmetry in limb movement, forepaw outstretching, body proprioception, response to vibrissae touch and climbing ability. Test was conducted 3 days prior to induction of cerebral ischaemia for assessment of baseline performance and then at different time point post MCAO (i.e. day 1, 3 and 7) for the assessment of neurological deficits. Scores for each test were summed up to generate the overall neurological core. The maximum score of 18 indicates no obvious deficit and the minimum score of 3 indicates the most severe neurological impairment (Table 2.2).

2.6.1 Spontaneous Activity

This was assessed with the rat in its own home cage with the cage top removed and rat was observed for a period of 5 minutes. The rat's spontaneous activity was scored from 0 to 3 based on its ability to approach walls of the cage. A score of 3 indicates that rats has moved around in the cage and approached at least three walls of the cage. A score of 2 was given when rat did not approach all four walls but has moved around although it eventually reached at least one upper rim of the cage. A score of 1 indicates that the rat barely moved in the cage and did not rise up on his hind limbs to approach any of the cage walls and a score of 0 was given if the rat did not move at all during the observation period.

2.6.2 Symmetry in The Movement of Four Limbs

The test was carried out by suspending the rat in the air by holding the base of its tail. A score of 3 was given if all four limbs extended symmetrically and score of 2 was given when the limb of the affected side (contralateral) extended less or more slowly than the unaffected side (ipsilateral). A score of 1 was assigned if minimal movement was observed on contralateral limb and 0 if the contralateral limb did not move at all.

Test	Neurological Score			
	0	1	2	3
Spontaneous activity (in cage for 5 min).	No Movement	Barely Moves	Moves and reaches at least 1 upper rim of the cage	Moves and approaches at least 3 sides of cage
Symmetry of movements (four limbs).	Contralateral side: no movement	Contralateral side: slight movement and splays to side a lot resulting in sideways movement	Contralateral side: moves slower & splays to side. General movement still forward	Both sides: Move symmetrically
Symmetry of forelimbs (outstretching to bench-top while held by tail).	Contralateral side: no movement, no outreaching	Contralateral side: slight movement to outreach	Contralateral side: moves & outreaches less than ipsilateral side	Symmetrical outreach
Reaction to touch on either side of trunk.	…	Contralateral side: no response	Weak response on contralateral side	Symmetrical response
Response to vibrissae touch.	…	Contralateral side: no response	Weak response on contralateral side	Symmetrical response
Climbing wall of wire cage	…	Fails to climb	Contralateral side is weak	Normal climbing

Table 2.2 A composite 18-Point Neurological Score is performed to assess neurological deficit following transient focal cerebral ischaemia in rodent. Six tests comprise of sensory and motor component are each given a score up to 3. Overall score is each test scores added up where minimum of 3 indicates severe neurological impairment and the maximum score of 18 indicate no obvious neurological deficit. Adapted from (Garcia *et al.*, 1995)

2.6.3 Forepaw Outstretching

The rat was held by its tail so that it had to walk along the surface of the table using its forelimb only. The hind limbs were kept in the air and the symmetry in the outreaching of both forelimbs was observed. Scores were assigned as follows; 3, both forelimbs were outstretched and rats walked symmetrically on forepaws; 2, contralateral forelimbs outstretched less than ipsilateral forelimbs, indicating impaired forelimb walking; 1, was given when contralateral forelimb exhibited minimal movement; and 0, when no movement was observed on contralateral forelimb.

2.6.4 Climbing

The rat was placed on grid wire and was then pulled off the wire by gripping the base of the tail and the strength of attachment was noted. A score of 3 was given if rat climbed easily and gripped tightly to the wire. The rat scored 2 if the grip on contralateral side was impaired and weaker than the ipsilateral side. Score of 1 indicates that the rat failed to climb or tended to circle instead of climbing.

2.6.5 Body Proprioception

The test assessed the rat's ability to react to stimulus when each side of the body was prodded with a blunt wooded pencil. A score of 3 was given when the rat reacted by turning its head and was equally startled by the stimulus on both sides. A score of 2 indicates that the rat reacted slowly to the stimulus on the contralateral side and score of 1 was given if the rat did not respond at all to the stimulus on contralateral side.

2.7 Adhesive Label Test

Adhesive label test was used to determine the extent of forelimb-use asymmetry displayed by the animal (Schallert and Whishaw, 1984). During this test, the rat was removed from the home cage and a circular adhesive test label (1.3cm diameter, Avery International, USA) was placed on the hairless radial aspect of each wrist as shown in Figure 2.5. To prevent order of attachment from biasing motor behaviour, label placement was changed for 3 separate trials and the experimenter touched each forepaw simultaneously immediately after the stimuli was attached. The animal was then placed in the observation cage and behaviour was recorded using a video camera (Sony). The trial has to restart if the label fell off without directly being removed by the rat. Each trial ended when both labels have been removed or when the animal failed to contact/remove each label within the 3 minutes' time period. The latency to contact and remove each label by the mouth was assessed by observing the video. For each trial, the difference in contact/removal time between the affected (right) and non-affected (left) paw was calculated to prevent overall activity of the rat from affecting the performance (Stroemer *et al.*, 2009). The rat was returned to home cage for 5 minutes between each trial. This test was performed prior to MCAO (day 0) and post operatively on days 1,3, and 7.

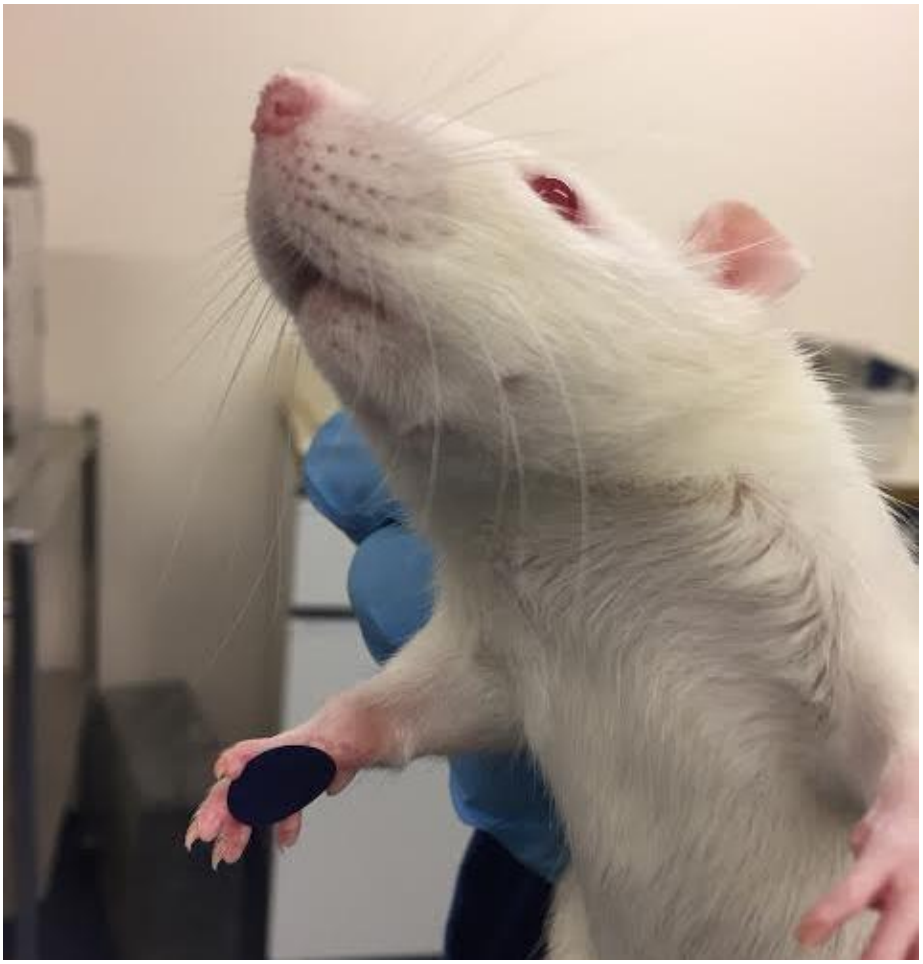

Figure 2.5 An adhesive label was placed on the distal-radial region of each wrist. The latency to contact or remove each label was recorded to assess whether the rat showed bias for the affected or unaffected forelimb.

2.8 Blood Pressure Determination

The tail-cuff method of systolic blood pressure is a non-invasive technique which was developed by the west of Scotland's Department of Clinical Physics and Bioengineering, based at the Southern General Hospital in Glasgow (Evans *et al.*, 1994). An occluding cuff was placed around the proximal end of the rat's tail which is then inflated with air until the vessel was transiently occluded at the point where the pressure in the cuff matches of the tail artery. The absence of pulse then is detected by a pneumatic pulse sensor which is attached to the tail distal to an occluding cuff (Figure 2.6C). The signal is relayed to a central monitoring system which is connected to a laptop (Dell, UK) which then displays the systolic blood pressure reading in mmHg and the cuff is then deflated (Figure 2.6A). The advantage of this technique is that does not involve arterial catheterization as required for direct methods of blood pressure measurement and has been validated against direct measures of blood pressure measurement (Feng *et al.*, 2008). Furthermore, this method enables BP measurements in conscious animals without the influence of anaesthesia on BP, as is the case with invasive methods. However, mild restraint during the procedure may contribute to stress in the animal which will be reflected in the blood pressure measurements but this can be minimised by incorporating a thorough acclimatisation and training period into the regime.

2.8.1 Tail Cuff Apparatus

Prior to BP measurement, the animals must be pre-warmed to induce maximal vasodilatation of the tail artery. This is achieved by placing the animals in an insulated heat box (dimensions 37cm x 35cm x 40cm) (Figure 2.6B) to which the animals had been previously conditioned. The upper surface of the box has a circular opening (diameter 7cm) to allow the box to be warmed to a temperature of 34ºC using a hairdryer (Boots, UK). Once the desired temperature was reached it was maintained by positioning an angle poise lamp over the opening of the box and this was monitored using a thermometer situated on the inner wall of the chamber. The door on the front panel of the heat box allowed easy access to the rat in the chamber and the removable insulating tile on the door could be removed to observe the animal. If the

temperature rose above 35ºC, the insulating tile and angle poise lamb over the upper opening shall be removed to facilitate heat loss.

The tail cuff was constructed by cutting the medial portion of a 5ml syringe (Plastipak, UK) to a length of 2cm. A latex tubing (length 6cm, width 1.5cm) was then inserted into the syringe. A 10-gauge catheter, cut to 4cm in length was inserted into the latex tubing and secured in place by tying 5-0 thread around the tubing. This needs to be done meticulously to prevent any air leak if the seal was incomplete. The opposite end of the latex tubing was turned over to the outer face of the syringe and was secured using a plastic O-ring (1.7cm diameter) (Figure 2.6C).

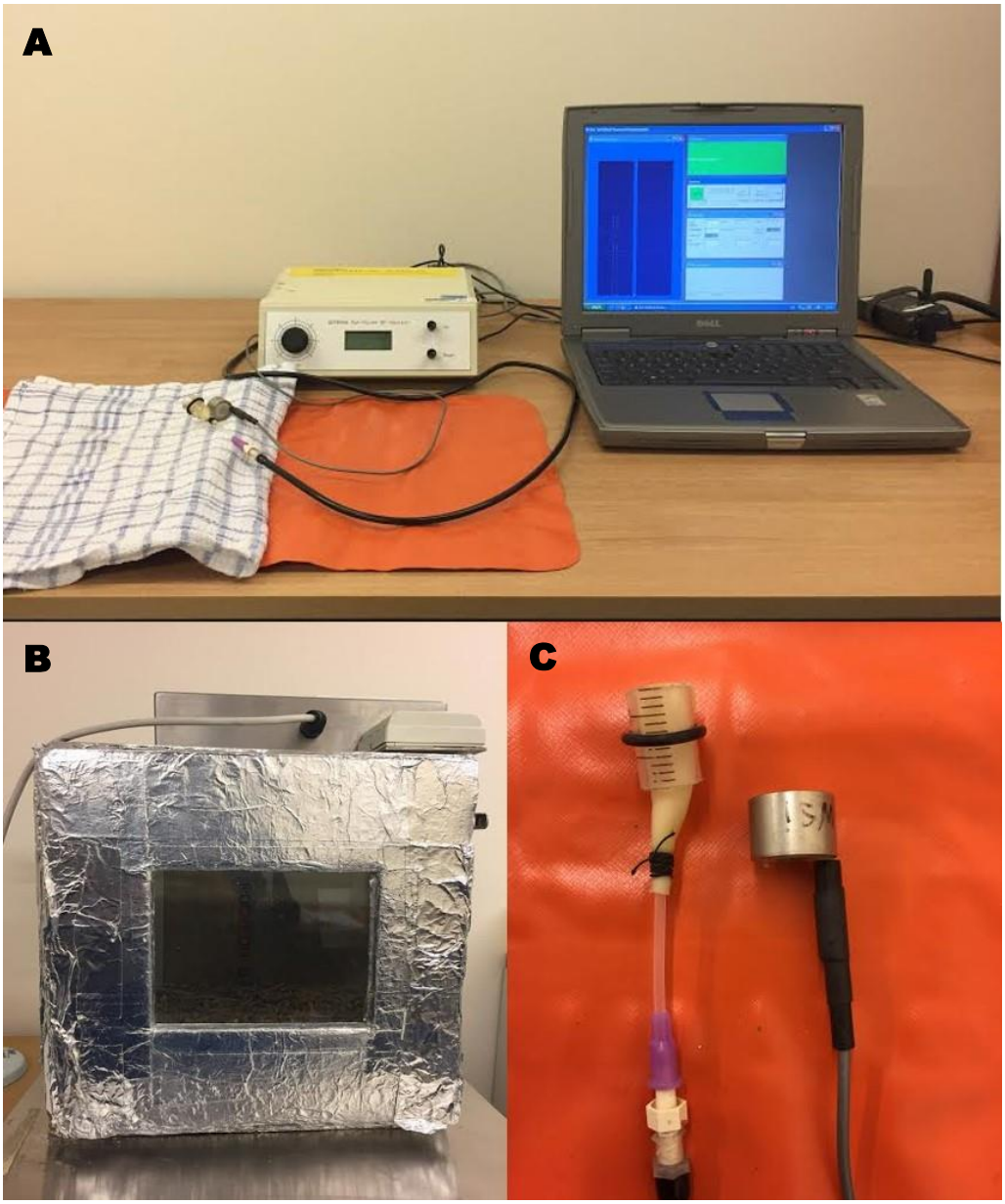

Figure 2.6 The tail cuff plethysmography apparatus. (A) Blood pressure monitoring system connected to a laptop, where the systolic blood pressure measurements are displayed and recorded. A heat mat was used to keep the rat warm and a towel was used to gently restrain the rat. (B) The heat box used to pre-warmed the rats prior to BP measurement. (C) The tail cuff (left) which is placed on the base of the tail and transducer which relays the blood pressure signal to the central blood pressure monitoring system.

2.8.2 Animal Training Procedure

All rats were subjected to an intensive 5 days training period to acclimatise them to handling and the tail cuff apparatus. On day one of training rats were taken to the room where the tail cuff apparatus was set up in their home cage. The animals were then handled for a period of 20-30 minutes and were allowed to explore the table where the tail cuff apparatus was set up. They were also wrapped in a towel to accustom them to mild restraint. On day two, rats were subjected to the same handling procedure as the previous day, with the addition of being placed in the heat box for 10 minutes, which had not been pre-warmed. The training on day 3 was the same as day two, except that the heat box was pre-warmed to 34ºC prior to the animals entering it. On day 4, the training procedure was as described for day 3 and then the tail cuff and transducer were positioned on the rat's tail (Figure 2.7A) whilst the rat was being mildly restrained within a towel. On the final day of training, the tail cuff apparatus was again positioned on the rat's tail following 10 minutes in the heat box and the cuff was inflated and deflated to allow the rat to acclimatise to the pressure of the tail cuff. At the end of each training day, rats were rewarded with a treat of Multi-Cheerios.

2.8.3 Systolic BP Measurement Protocol

The tail cuff method was used to measure systolic blood pressure in Sprague-Dawley and Wistar rats prior to stroke and on specific days following stroke in Chapter 3 and 4 respectively. In Chapter 5 BP measurement was taken 2 weeks prior to the commencement of PD protocol in SHR rats to ensure that rats were hypertensive. BP measurement was performed in the morning between 1000 to 1200, by the same experimenter. BP measurement was not performed on a Monday afternoon, as the rats tended to be more stressed on this day as their cages were cleaned out every Monday.

Rats were placed in the pre-warmed heat box with their cage-mates for 10-15 minutes and no longer than 20 minutes. Care was taken to regularly assess the temperature in the box by looking at the thermometer attached to the inner wall of the box. If the temperature was above 36ºC, then the front panel of the

box was removed to aid heat loss. The front panel of the heat box also allowed the animals to be observed. The rats were deemed to be warm enough when there was very little spontaneous movement and the ears looked very pink. At this stage the rat was removed from the box and swiftly wrapped in a towel with only the tail exposed. The rat was placed onto the heat mat to keep it warm and the tail cuff and the signal transducer were positioned on the tail (Figure 2.7A). Once the rat was settled and was sitting on the heat mat, the restrain was release and BP measurement was taken while the rat wrapped in the towel. The laptop was used to inflate and deflate the cuff in cycles to obtain measurements of systolic blood pressure. This was repeated until 8-10 consistent measurements of systolic BP were acquired and the mean and standard deviation were then calculated. Only the most consistent measurements were used to calculate the mean systolic BP for each animal. Measurements which were acquired when an animal was visibly stressed were excluded. After the tail cuff procedure, the rats were returned to their home cage and were rewarded with Multi-Cheerios.

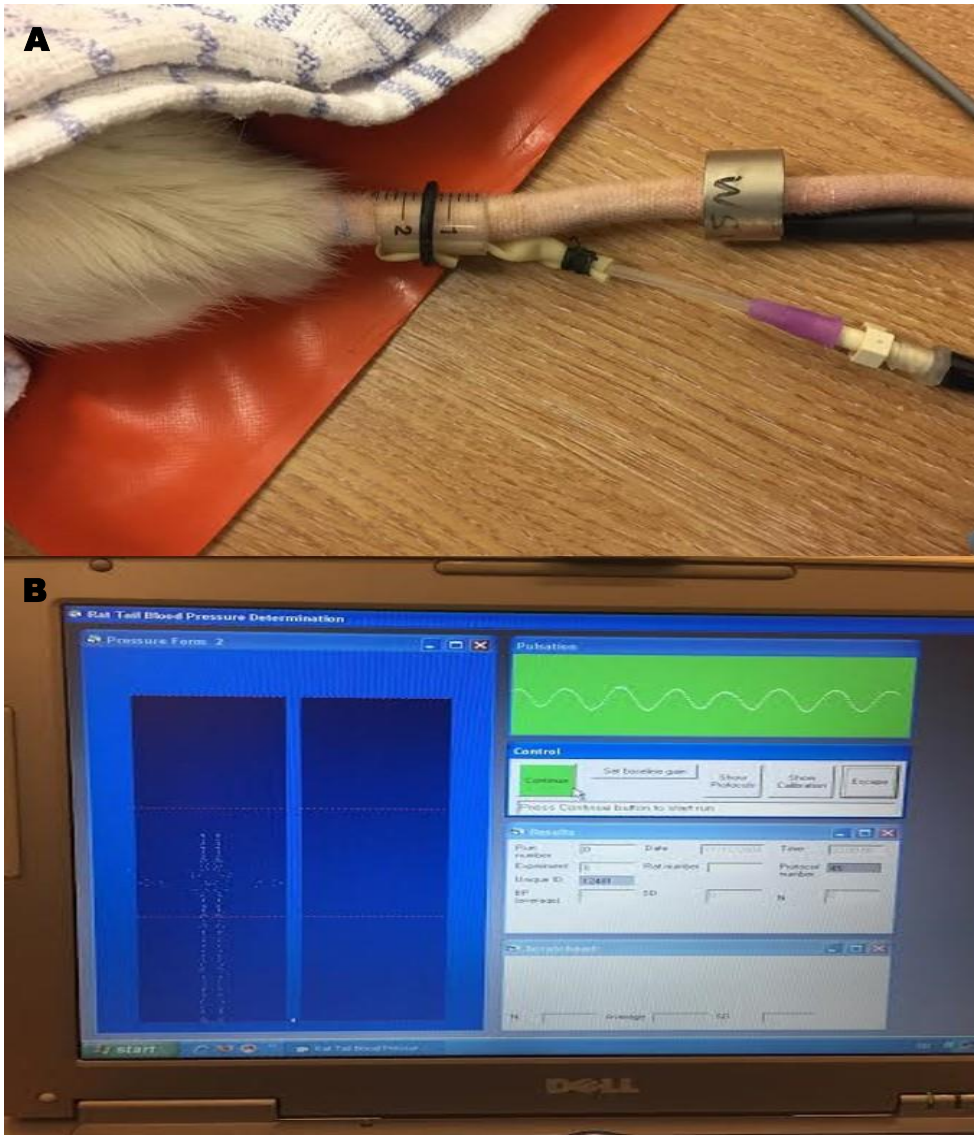

Figure 2.7 Non-invasive blood pressure measurement via tail-cuff method. (A) The positioning of the tail cuff and the signal transducer on the tail of the rat, where the cuff is positioned at the base and the transducer is placed distal to the cuff. (B) The computer screen as displayed when blood pressure measurements are being recorded.

2.9 Photoperiod Disruption Protocol

In Chapter 3 and 5, photoperiod disruption by manipulating the timing for light exposure was used to modulate shift work in rats. Control rats were housed in a room with a standard 12:12 light/dark cycle for 9 weeks. Light intensity in the room housing the control rats was measured with a lux meter at the beginning of the study (~150 lux). PD rats were housed singly in a well-ventilated light-tight box that accommodated 2 cages per shelf; and allowed for alterations in the light/dark cycle using a digital timer. Lights in the box were switched on 6 hours earlier than in the previous photoperiod every 3 days for 9 weeks as has been described previously to simulate shift work, where it was shown to induce perturbations of circadian biomarkers (melatonin) and changes in blood glucose and insulin in diabetic-prone rats (Gale *et al.*, 2011). A schematic representation of photoperiod disruption protocol employed in the study is illustrated in Figure 2.8. With this protocol rats in the PD group returned to the "original" baseline LD cycle (lights on at 0700 hour, lights off at 1900 hour) every 15 days. Light intensity in the box was maintained at ~150 lux similar to that experienced by the control animals. The temperature and humidity in the light-tight box were closely monitored and maintained at 20-21°C and 35%-40% respectively during the duration of study.

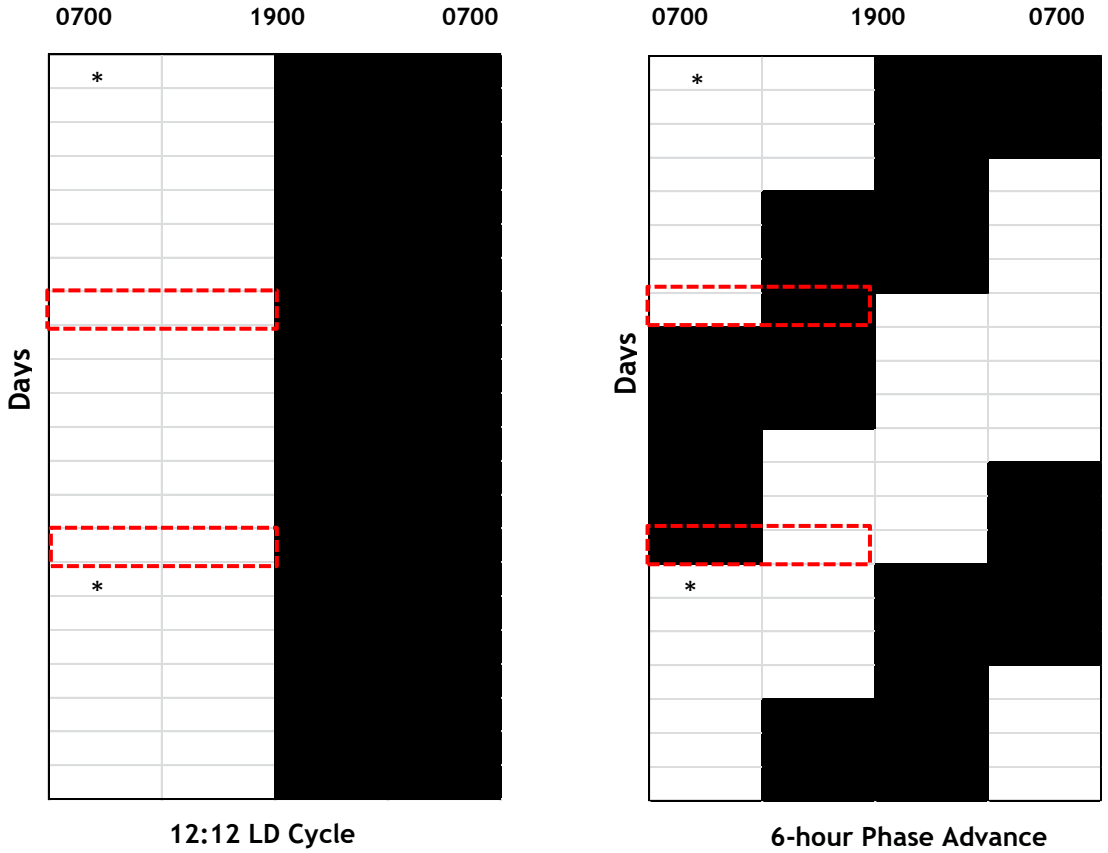

Figure 2.8 Schematic representation of 2 light/dark cycles employed in this study; 12:12 LD cycle (lights on at 0700 h, lights off at 1900 h) for 9 weeks and 6 h phase advance of the LD cycle every 3 days for 9 weeks. Red rectangle represents under what light conditions food intake, and body weight measurement were performed both experimental groups, * and ** indicates the day for first and second batch of rats (n=2-3/group) entering the protocol respectively. Surgery for MCAO was performed at the end of 9 weeks during the light phase.

2.10 Locomotor Activity Monitoring

Rat's locomotor activity for studies done in Chapter 3 and 5 was monitored to demonstrate disruptions of circadian rhythms as well as to determine patterns of activity in response to LD cycle. Activity monitoring was conducted only in the PD rats due to limited access to sufficient number of activity monitors. Baseline locomotor activity was recorded 2 weeks prior to the commencement of 9 weeks' phase advance protocol, in which the rats were maintained under standard 12:12 light/dark cycle and for the subsequent 9 weeks period of PD. Therefore, the activity analysis was based on intra-subject design comparing baseline activity (during normal LD cycle) with activity in PD period in the PD group.

Activity was measured in each individual cage using a passive infra-red sensor connected to a relay and then to a PC via a 56 channel interfaces (ClockLab CL200) that counted events on the relays in 1 min bins. The sensors were positioned above the cage at a distance that was optimised for detection of movement in all quadrants and for insensitivity to movements outside the cage (Figure 2.9). Data were acquired using ClockLab software (Actimetrics, Illinois, United States) and were expressed in units of beam breaks per min. Disruption of circadian rhythmicity in locomotor activity was quantified using parameters described for assessment of fragmentation of human rhythmicity.

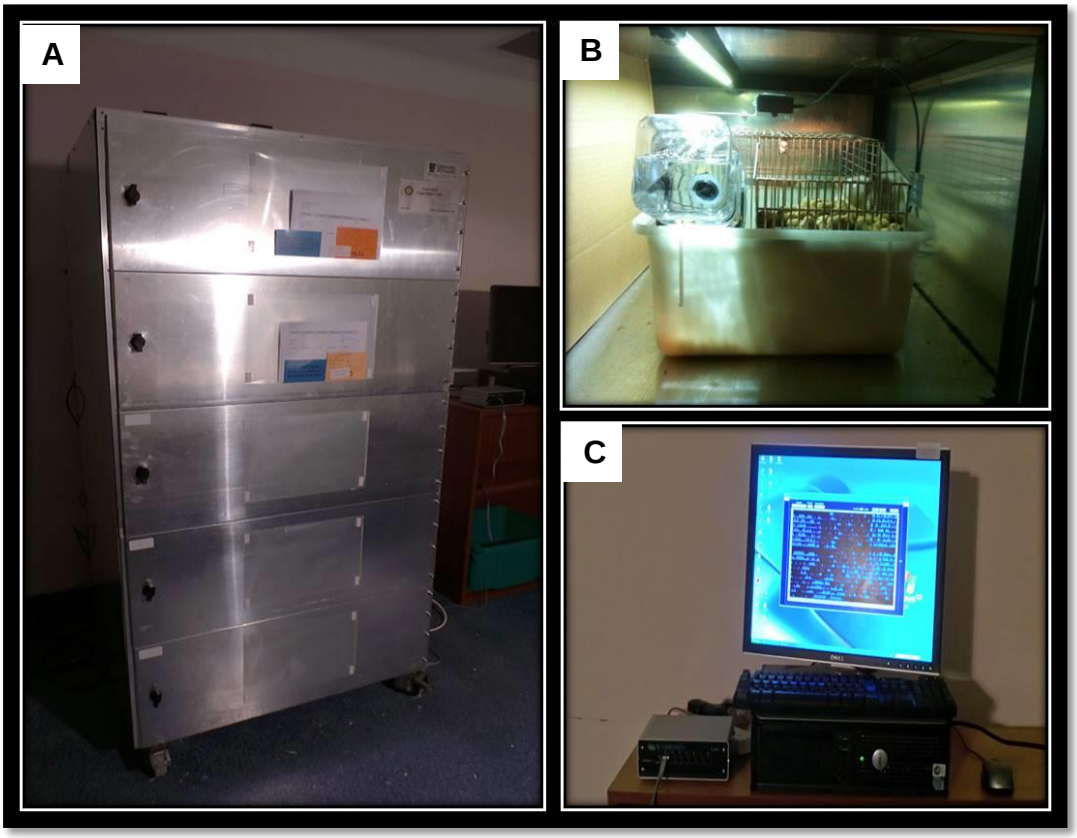

Figure 2.9 The room set up for circadian study. (A) Light/dark box which accommodate 2 singly housed rats per shelf with maximum capacity of the unit is for 10 rats. (B) Infra-red movement sensor positioned at distance optimised for detection of movement in all quadrants and (C) double-plotted actogram presenting locomotor activity data.

Chapter 3-The Effect of Chronic Photoperiod Disruption on Outcome Following Permanent Focal Cerebral Ischaemia

3.1 Introduction

Epidemiological studies have identified obesity, hypertension, diabetes, atherosclerosis and inflammation as significant risk factors for stroke onset and poor outcome (Baird *et al.*, 2002; Murray *et al.*, 2013). The incidence and overall disease burden of stroke is predicted to rise as these risk factors extend across the developing world (Feigin *et al.*, 2014, 2015). In 2007 more than half the global population lived in a city and this is predicted to reach 70% by 2050. Risk factors for stroke are strongly associated with urbanisation mediated through a complex interaction of lifestyle factors including high-energy diets, pollution, sedentary lifestyles and disrupted circadian rhythmicity (Danaei *et al.*, 2013).

Circadian rhythms optimises health by ensuring that the internal rhythms of metabolism and cardiovascular physiology are synchronised to daily variations in the light/dark cycle (Arble *et al.*, 2010). Erratic cycles in the light/dark cycle, food availability or social interaction can affect the alignment between endogenous clocks and the environment, a condition associated with detrimental effects on metabolic and mental health. Around 20% of workers in the developed world are required to undertake shift work which involves chronic disruption of circadian rhythms and shift work is strongly associated with metabolic dysfunction and increased risk of cardio and cerebrovascular diseases (Scheer *et al.*, 2009).

Animal studies suggest potential links between disrupted rhythmicity and ischaemic stroke. The spontaneously hypertensive rat (SHR) showed a disrupted circadian phenotype with impaired capacity to maintain robust rhythms (Sládek *et al.*, 2012) while a progressive desynchronization of rhythms in behaviour and drinking was reported to be a prodromal sign of impending stroke in these animals (Minami *et al.*, 1985). In healthy individuals, blood pressure and vascular contractility show strong daily rhythmicity which indicates underlying clock control, and disruption of these rhythms is an early sign of cardiovascular diseases in humans (Gönenç *et al.*, 2013) and animals (Shimamura *et al.*, 1999). Disruption of clock function by exposure of animals to disrupted photoperiods is used as a model of circadian

disruption, and negatively affects vascular rhythmicity, function and vulnerability to ischaemia in organs other than the brain. For example, PD decreased survival in a hamster model of cardiomyopathy (Penev *et al.*, 1998) and a mouse model of myocardial infarction (Alibhai *et al.*, 2014) and compromised vascular adaptive responses to aortic constriction in mice (Martino *et al.*, 2007). Furthermore, mice with genetic clock lesions (BMAL1 knockout) had impaired pathological remodelling in response to ligation of the carotid artery, enhanced vascular injury and impaired endothelial function (Anea *et al.*, 2009) and importantly, increased cell death in the hippocampus following transient forebrain ischaemia (Wiebking *et al.*, 2013). Together with the increased vulnerability of clock disrupted animals to cardiovascular ischaemic injury, this suggests that PD might have an adverse impact on cerebral ischaemic damage.

Some of the reported metabolic or physiological changes associated with PD such as hypertension and diabetes have the potential to adversely impact on stroke. The adverse effect of hyperglycaemia on outcome after stroke or infarct size after MCAO in rodents is well documented (MacDougall and Muir, 2011; Tarr *et al.*, 2013) while co-morbidities such as genetically determined hypertension, diabetes or insulin resistance hasten the demise of the penumbra and increased infarct volume(McCabe *et al.*, 2009)'(Tureyen *et al.*, 2011). We therefore hypothesise that PD will alter key physiological variables such as blood pressure and blood glucose, and increase vulnerability to focal cerebral ischaemia. The primary objective of the present study was to determine if rats subjected to recurrent phase advance of the light/dark cycle for 9 weeks had larger infarcts compared to animals maintained on a normal light/dark cycle following permanent MCAO.

3.1.1 Study Aims

The primary objective of the present study was to determine if PD induced in rats by recurrent phase advance of the light/dark cycle for 9 weeks, influences the sensitivity of the brain to ischaemic damage induced by permanent MCAO.

3.2 Methods

3.2.1 Animal

All animals were obtained from Envigo (UK) and housed in Veterinary Research Facility (VRF) at the University of Glasgow. Experiments were carried out under license from the UK Home Office and were subject to the Animals (Scientific Procedures) Act, 1986. The report was carried out in accordance with the ARRIVE guidelines (http://www.nc3rs.org.uk/arrive). A total of 24 male, adult Wistar rats (8-10 weeks) weighing 210-290g were entered into the study. Rats were singly housed under a standard 12:12 light/dark cycle (lights on at 0700, lights off at 1900) for two weeks prior to allocation into one of two experimental groups. All rats had *ad libitum* access to water and standard rat chow.

3.2.2 Sample Size Calculation and Blinding

Sample size calculation was performed using equation for sample size calculation for continuous variable (Snedecor and Cochran, 1989) as provided in Table 3.1. Group sizes were based on previously published data from our research group that used the same model of MCAO and was able to detect 50% change in infarct volume due to acute hyperglycaemia (Roy, 2015). In previous experiments, the difference in mean (d) T_2-derived infarct volume between vehicle and glucose treated was 33mm^3, with a standard deviation (s) of 22mm^3. Given the sample size calculation was based on an 80% power (1-ß) and 95% significance level (α), the number of animals needed for each group is 7 to detect the difference in infarct volume. From this, it was decided that the optimum group size would be 12 rats per group, which is necessary to detect a 39% increase in infarct volume.

It was not possible to randomise rats to the two groups due to the limited number of stroke surgeries that could be carried out per day at the end of the 9 weeks' protocol. All animals were allocated to control and PD groups in equal numbers when batches of 4 rats were entered into the 9 weeks' protocol described below with the total number of 12 animals per group. Surgery for MCAO was carried out by a surgeon (Dr Lisa Roy) who was blinded to the experimental groups. Similarly, data analysis for infarct volume was carried out in a blinded manner.

A

$$n = 1 + 2C\left(\frac{s}{d}\right)^2$$

B

		α	
		0.05	0.01
1-β	0.8	7.85	11.68
	0.9	10.51	14.88

Table 3.1 (**A**) Sample size calculation using equation for an experiment that designed to measure continuous variables. (**B**) C is dependent on values chosen for significance level (α) and power (1-ß)

3.2.3 Photoperiod Disruption Protocol and Locomotor Activity Monitoring

Photoperiod disruption and locomotor activity monitoring were carried out as described in detail in Chapter 2.9 and 2.10.

3.2.4 Food Intake and Body Weight

Weekly food intake and body weight of rats were measured every Monday at regular time point (from 0900-1000). For PD rats, if the measurement of food intake and body weight of rats was during the dark cycle then this was conducted under the red light in the dark room. In all rats, body weight and food intake were measured at baseline (week 0) and thereafter on a weekly basis for 9 weeks. Food intake was calculated by weighing the amount of food given each week and calculating the difference from the previous week. Both measurements were performed at the same time of the day in each group as illustrated by red rectangle in Figure 2.8 on Chapter 2.

3.2.5 Tail Cuff Plethysmography

In all rats, systolic BP was recorded by tail cuff plethysmography at baseline and at the end of 9 weeks' protocol prior to MCAO. All animals had been previously conditioned to the indirect blood pressure set up prior to the study as described in Chapter 2.8. Blood pressure was measured by same experimenter at approximately the same time of the day on every occasion. To facilitate vasodilatation, animals were placed in an insulated heat box at 35-36°C for 10 min. Eight to ten successive BP readings at each session were recorded and the average calculated.

3.2.6 Surgical Procedures

At the end of 9 weeks, all rats in control and PD groups were subjected to permanent MCAO by the same experimenter who was blinded to the animal identity. Animals were initially anaesthetised in an induction chamber with 5% isoflurane in a 70% nitrous oxide and 30% oxygen mixture. Oral intubation was performed and animals were mechanically ventilated with 2% to 3% isoflurane in a nitrous oxide: oxygen mixture (70:30). A digital blood glucose

meter (Accu-Check Aviva, Roche, Germany) was used to measure blood glucose (non-fasting) sampled from the tail vein immediately following induction of anaesthesia. Body temperature was monitored by a rectal probe and maintained at 37±0.5°C using a heat lamp throughout surgery. Permanent focal cerebral ischemia was induced by distal occlusion of the MCA using diathermy method adapted from Tamura et al. 1981 as described in detail in Chapter 2.3.1. After recovery from anaesthesia, animals were returned to their home cage and kept in the recovery area where their general well-being and body weight were closely monitored 3 times daily. Animals received soft diet and fluid, in order to aid recovery.

3.2.7 Blood Glucose Measurement

Blood glucose was sampled from rat tail vein following induction of anaesthesia and intubation. The tail vein was heated using a single head poised lamp to facilitate vasodilatation and identification of sampling point. The right or left tail vein on either side of the artery (that was located on the mid dorsal side of tail vein) was identified and the target area was wiped with 2% chlorhexidine antiseptic solution. A small gauge needle (25G, BBraun Sterican**)** was used to puncture the vein. A test strip (Accu-Chek® Aviva) was placed in the meter, and a drop of blood from tail vein was placed at the tip of the test strip. The glucose value in mmol/L was displayed on the meter and was recorded. Gentle pressure was applied to the vena puncture area for 1-2 mins with sterile gauze to stop the bleeding. To ensure reliability of the results, the glucose meter machine was calibrated regularly using Accu-Chek® Aviva control solutions in accordance with the manufacturer's instructions.

3.2.8 MRI Scanning Protocol

At 48 hours after MCAO rats were re-anaesthetized and placed in Bruker Pharmascan 7T MRI scanner. Rats were maintained under anaesthesia with 2% to 3% isoflurane in nitrous oxide–oxygen (70:30) using a face mask throughout the scanning process. Rats were placed into a rat cradle, the head secured and a phased array surface coil was positioned above the head. Body

temperature was maintained at 37±0.5°C during scanning using a temperature-controlled water jacket. A RARE (rapid acquisition with refocused echoes) T_2-weighted sequence was acquired (TE=100ms, TR=6000ms, matrix=256x256, 16 coronal section slices; 0.75mm thick) to image the infarct.

3.2.9 Infarct Volume Measurement

Infarct volume was measured at 48 hours following permanent MCAO as described in Chapter 2.5.4. Infarct volume analysis was performed using Image J software (NIH, Bethesda, MD, USA) and the assessor was blinded to the experimental group. Infarct area was calculated by manually delineating the hyper-intense regions on T_2-weighted images. Infarct volume was calculated by summing the infarct area on each slice and multiplying by slice thickness (0.75 mm). Correction for oedema was performed to account for brain swelling at 48 hours after stroke using previously described method (Gerriets *et al.*, 2004).

3.2.10 Plasma Fructosamine

The bonding of glucose to plasma proteins produces fructosamine and plasma fructosamine levels are proportional to the average glucose concentration over the previous 2-3 weeks prior to the measurement. Blood for measurement of plasma fructosamine was collected at 48 hours after MCAO. Whole blood was withdrawn from the heart (via cardiac puncture) and collected into EDTA-treated tubes (1.5ml). Samples were processed immediately by centrifugation for 10 min at 1,000xg using a refrigerated centrifuge. Samples were stored at -80ºC and analysed at the end of the study. The fructosamine assay uses the rate of formation of formazan from nitrotetrazolium blue in an alkaline environment at 546nm(Johnson, Metcalf and Baker, 1983). Reagents were provided by Horiba ABX and the analysis was performed on the Olympus AU 640 chemistry analyser.

3.2.11 Hair Corticosterone

Hair corticosterone levels have been validated as reliable biomarker for chronic stress. Study by (Scorrano *et al.*, 2015) demonstrated that hair corticosterone level in male rats properly reflects their plasma level after exposure to chronic stress protocol (intermittent restraint) for 14 days. This method is less intrusive compared to blood and saliva corticosterone measurement that could be confounded by stress secondary to sampling procedure.

Hair samples taken from dorsal aspect of the body at the termination of the experiment was weighed, placed in a sterile plastic wrap and kept at room temperature until further analysis. On the day of analysis, hair samples from each rat (70mg) were transferred into 2.5 ml tubes and labelled. Sample was washed twice with 1000ul isopropanol (Sigma) to remove surface contaminants, using a mini Rocker-Shaker (PMR-30, Grant Instruments (Cambridge) Ltd UK) for 3 minutes at room temperature. Excess isopropanol was discarded. Samples were then left to dry under clean protected fume hood at room temperature for 5 days, to allow evaporation of isopropanol.

Dried hair was grinded to fine powder using a Retsch ball mill (mixer mill MM 200; 5.0 ml stainless steel grinding jars; single 5.0 mm stainless steel grinding balls) for ~4 min in bead mill at 30 Hertz (4 x 50s; 20s rest in between). Approximately 50 mg of powdered hair was weighed out and carefully placed into a 2ml micro centrifuge tube and 1.5 ml of methanol was added to each sample. Tubes were incubated at room temperature for 24 hours with slow rotation for the extraction of steroids. Following extraction, samples were spun at 10,000 rpm (Jouan BR4i, DJB Labcare ltd, England) for 5 min and 1 ml supernatant was transferred to clean 1.5ml tube. Supernatant was spun again at 10,000 rpm for 5 min. 900ul supernatant was transferred to clean tube and placed in vacuum evaporator (Thermo-Scientific) to remove methanol. Following evaporation of the solvent, extract was reconstituted in assay buffer, and corticosterone concentration was determined by using Corticosterone ELISA Kit (Enzo Life Sciences ltd, Exeter, UK) according to

manufacturer's instruction. ELISA plates were read at 405nm on a plate reader.

3.2.12 Statistical Analysis

Data are expressed as mean ± standard deviation (SD). All statistical analyses were performed using GraphPad Prism software v6 (GraphPad, La Jolla, CA). Food intake data were plotted over time and area under the curve was calculated. Data were analysed using a 2-way ANOVA and an unpaired Student's t-test, respectively. An unpaired Student's *t* test was used to compare final infarct volume, blood glucose, % increase in body weight, % change in BP, plasma fructosamine and hair corticosterone level between the groups. A probability value of 0.05 or less was considered statistically significant.

3.3 Results

3.3.1 Mortality

A total of 24 Wistar rats that were included in the study completed the entire experimental protocol. There was no mortality following MCAO in both either PD or control groups.

3.3.2 Photoperiod Disruption Results in Disruption in Locomotor Activity and Rhythmicity for The Duration of PD Intervention

Rats showed a strong circadian rhythm for locomotor activity in the baseline 12:12 light/dark period that was disrupted on commencement of the phase advance protocol (Figure 3.1A). Loss of circadian rhythmicity during the PD period was confirmed by changes in the rhythmicity parameters; inter-daily stability (IS) and intra-daily variability (IV) between these periods.

The inter-daily stability was calculated as the ratio between the variance of the average 24-hour pattern around the mean and the overall variance, and reflects the predictability of the diurnal pattern over sequential days. The IS was significantly decreased in the PD period

compared to baseline; 0.76 ± 0.08 and 0.06 ± 0.04 (arbitrary units), mean ± SD for baseline and PD periods respectively (P < 0.0001, Student paired t-test; Figure 3.1C).

The intra-daily variability index was measured as an indicator of the fragmentation of the rhythm, with high values indicative of multiple transitions between periods of rest and activity. Variability within days was increased by PD as indicated by significant increases in the IV compared to the baseline period; (0.75 ± 0.16 and 1.18 ± 0.09 (arbitrary units), mean ± SD for baseline and PD periods respectively (P < 0.0001, Student paired t-test; Figure 3.1C). The mean effect of PD on the rhythmicity of all animals is illustrated in Figure 3.1B which shows that both IS and IV deviated from baseline values when PD commenced, and that baseline values were not recovered. Therefore, locomotor activity rhythmicity remained profoundly disrupted for the duration of the PD intervention.

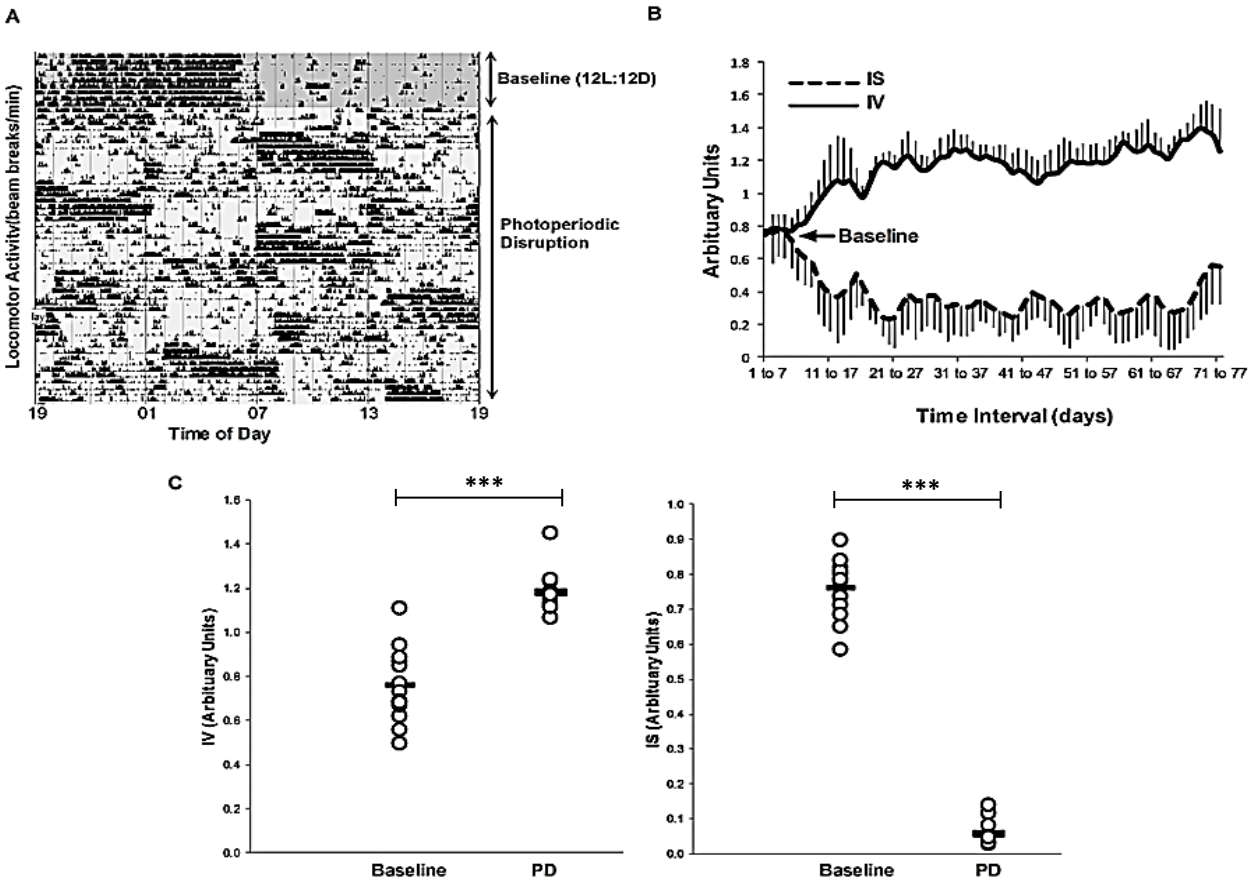

Figure 3.1 (A) Actogram from a single animal showing disrupted rhythmicity in locomotor activity during chronic photoperiodic phase advance. (B) Mean rhythmicity indices (IS and IV) calculated over the duration of the baseline and PD periods for all animals, shows significant increase in IV from baseline (C) indicates increased fragmentation of the daily rhythm in locomotor activity. The IS was decreased from baseline indicating disrupted stability of rhythmicity between days (Student's paired t-test, $P<0.000$, $n=12$).

3.3.3 Food Intake and Body Weight

Control and PD groups consumed 21 ± 0.3 and 19.5 ± 0.9 g/day respectively (daily food intake was calculated by averaging the weekly intake). Weekly food intake in control and PD rats over 9-week period is shown in Figure 3.2A. As a summative measure for food intake from baseline to week 9, an area under the curve was calculated for each rat. Despite statistically significant reduction of food intake in PD rats (control, 1331 ± 96.4 g; PD,1227 ± 100.5 g P= 0.02, Figure 3.2B), the reduction was not biologically significant as the % increase in body weight from baseline was comparable in both groups at the end of 9 weeks (control, 41.39 ± 17.16%; PD, 37.37 ± 15.03%, P= 0.60, (Figure 3.3B). Body weight data also shows that both groups were matched for body weight at baseline (control, 247.8 ± 18.6 g; PD, 243.3 ± 18.3 g) and the % increase of body weight increased steadily over time (Figure 3.3A).

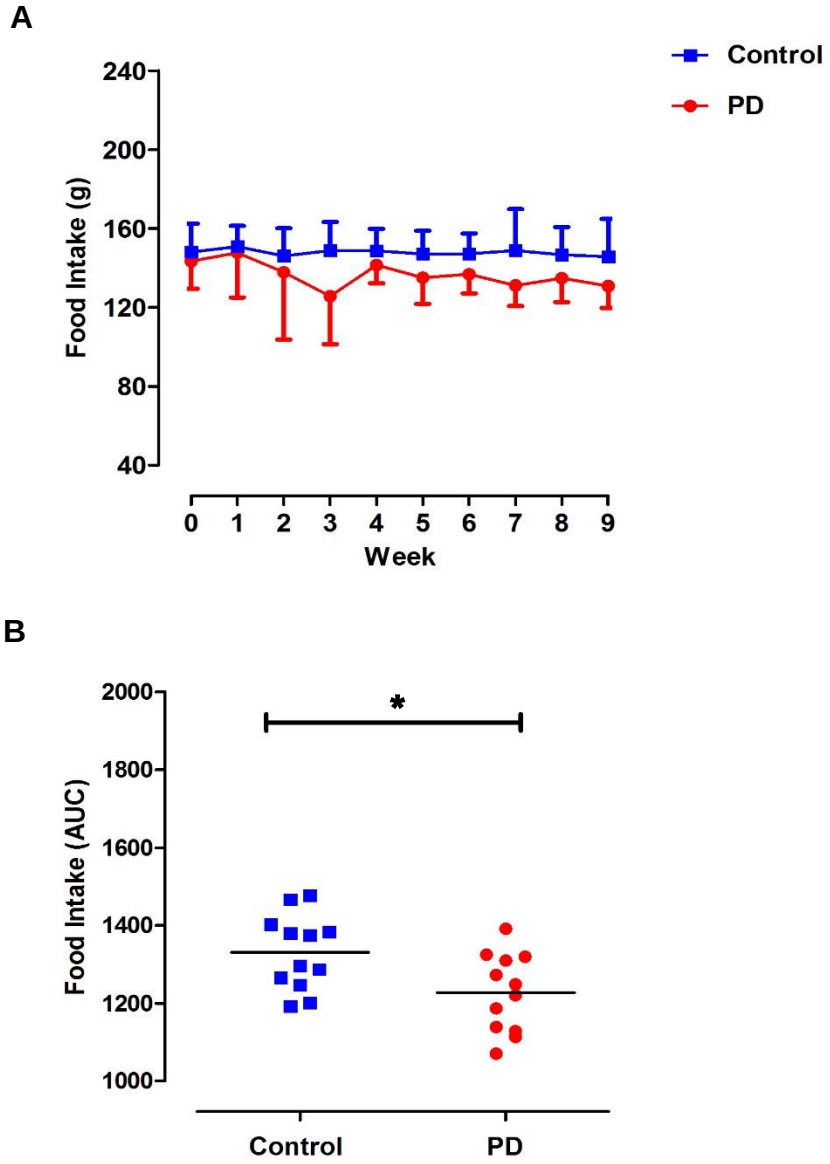

Figure 3.2(A) Weekly food intake in control and PD rats over the entire 9-weeks protocol and (B) the weekly food intake calculated as area under the curve for each individual rat for the control and PD groups. The data in (A) expressed as mean ± standard deviation. The data in (B) are expressed as AUC for each animal. Horizontal bar indicates the mean. Data in (B) analysed using a Student's unpaired t-test, P=0.02, n=12.

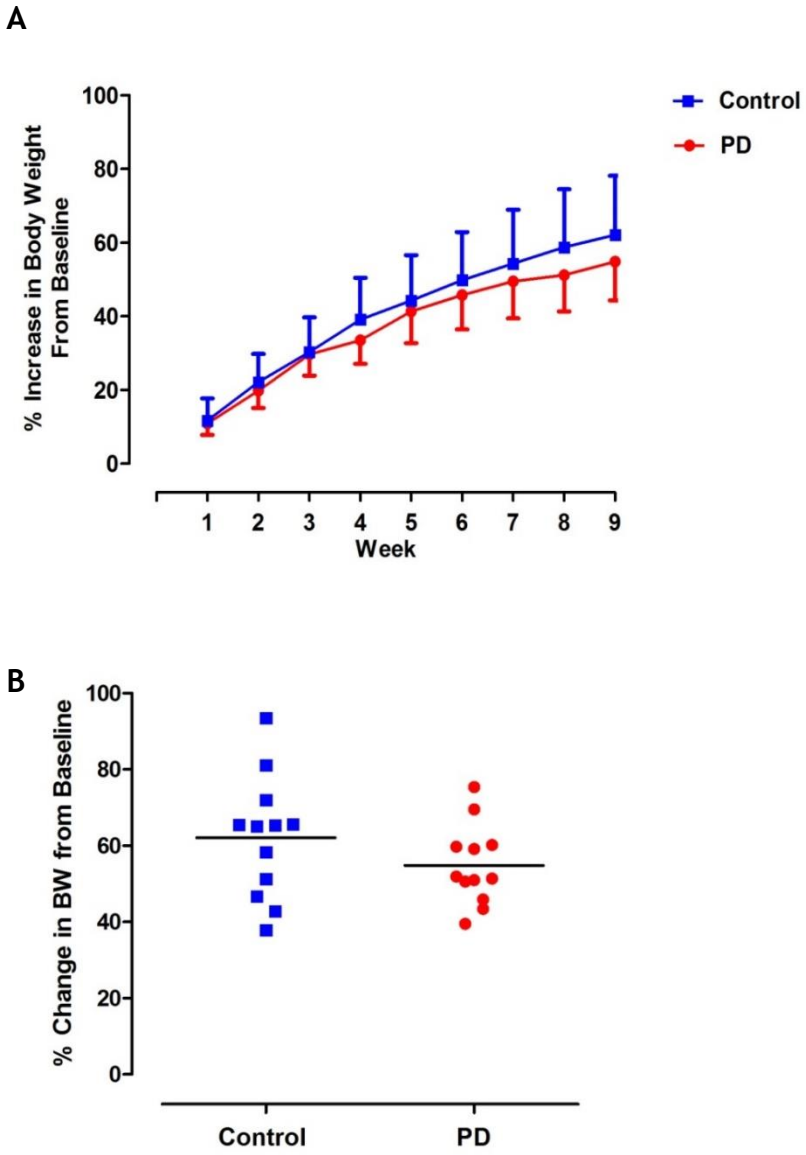

Figure 3.3 (A) Weekly % increase in body weight from baseline in control and PD groups. (B) Scatter plot showing the % change in body weight from baseline to week 9 for both control and PD group. Data points indicate individual rats and the horizontal bar represents the mean, and analysed using Student's unpaired t-test P=0.20, n=12.

3.3.4 Blood Pressure Were Unchanged by PD Intervention

The baseline systolic BP for control and PD groups was 99 ± 9.5 mmHg and 106 ± 13.2 mmHg respectively. At 9 weeks, no significant difference in BP was observed when compared to baseline measurements in either group (control: 99 ± 13.5 mmHg and PD: 104 ± 11.2 mmHg). There was no difference between control and PD groups in the degree of change in BP over 9-week period (Figure 3.4). Therefore, PD did not significantly alter BP.

3.3.5 PD Did Not Alter Blood Glucose and Plasma Fructosamine Level

Blood glucose was sampled immediately following induction of isoflurane anaesthesia prior to MCAO. Rats were not fasted prior to stroke surgery and blood glucose was sampled from the tail vein. Despite a slightly higher mean blood glucose level in the PD group in comparison to the control group the difference was not statistically significant (Control, 9.783 ± 2.107mmol/L; PD,11.26 ± 1.418mmol/L, P=0.056, Figure 3.5A). As compared to blood glucose, plasma fructosamine is a measure of glycated protein which indicates the average glucose concentration over the previous 2-3 weeks, based on the half-life of the plasma proteins. The fructosamine level at 48 hours after MCAO was not significantly different between control and PD rats (188.9 ± 13.6 μmol/L and 184.5 ± 15.9 μmol/L respectively, P= 0.47 (Figure 3.5B).

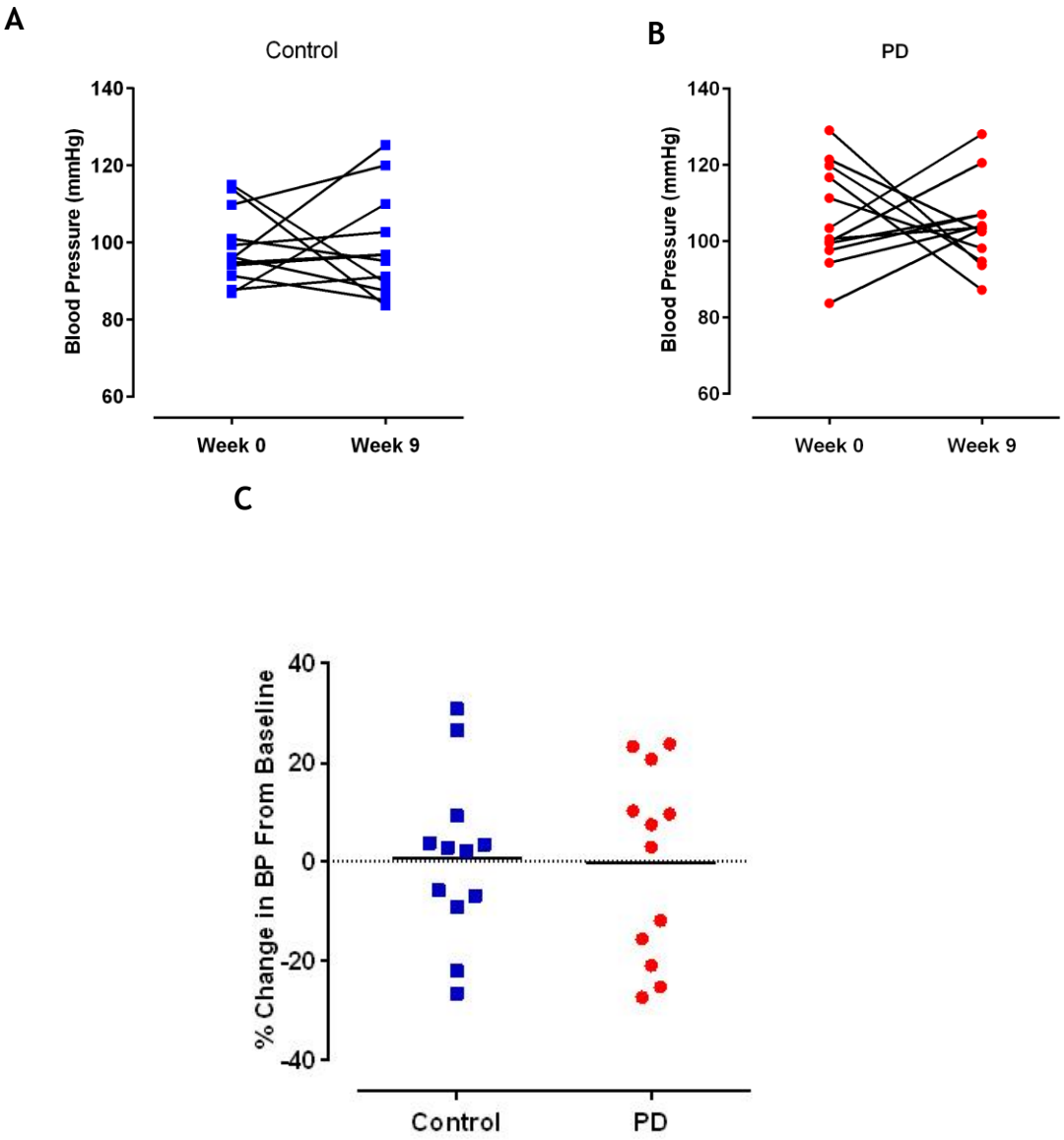

Figure 3.4 Systolic blood pressure at both baseline and at week 9 in individual rats for control (A) and PD groups (B), Student paired t-test, Control: P=0.9729, PD: P=0.71. (C) Scatterplot showing the % change in BP from baseline to week 9 for both control and PD groups. Data points indicate individual rats and the horizontal bar represents the mean, Student unpaired t-test, P=0.90, n=12.

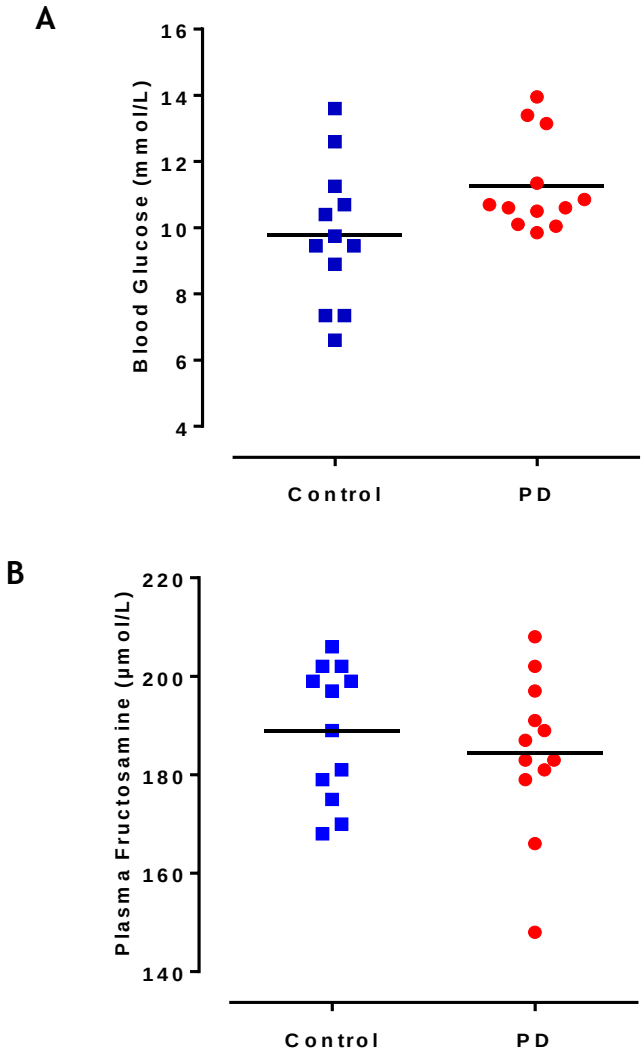

Figure 3.5 (A) Scatter plot showing the individual blood glucose values taken immediately prior to MCAO for both control and PD groups, Student's unpaired t-test, P=0.056, n=12. (B) Scatter plot showing the plasma fructosamine level at 48 hours after MCAO in both control and PD groups, Student's unpaired t-test, P=0.47, n=12. Data points indicate individual rat and the horizontal bar represents the mean.

3.3.6 Hair Corticosterone

Hair corticosterone taken at 48 hours after stroke was comparable between groups. Control: 13.58 ± 3.46ng/ml, PD: 11.96 ± 4.40 ng/ml, P=0.33, Student's unpaired t-test (Figure 3.6)

3.3.7 Infarct Volume Was Not Significantly Larger in PD Group

Infarct volume was assessed by T_2-weighted MRI at 48 hours following MCAO. Representative T_2-weighted MR images from the median animal of each group are presented in Figure 3.7A**.** The area of infarct is represented by hyper-intense region on each slice. In both groups, infarct was located within the cortex with no subcortical damage. The mean infarct volume for control and PD rats was 77.44 ± 34.20mm^3, and 88.36 ± 27.98mm^3 respectively and T_2-derived infarct volume was not significantly different in PD rats at 48 hours following permanent MCAO (P=0.34, Figure 3.7B). The correlation between infarct volume at 48 hours post-MCAO and blood glucose levels immediately prior to MCAO was also evaluated (Figure 3.8A) and no significant correlation was noted (r^2=0.08, P=0.18).

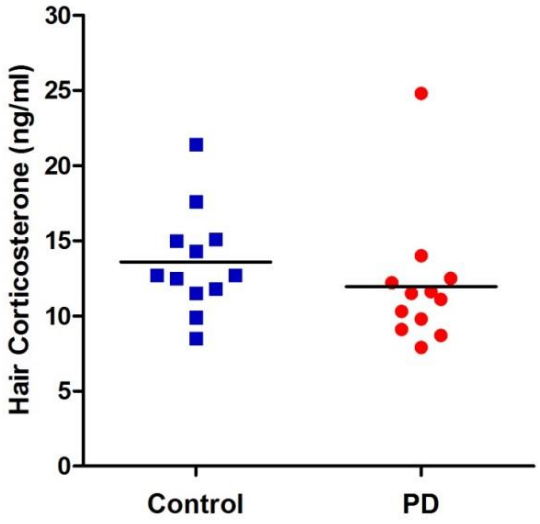

Figure 3.6 Hair corticosterone levels measured from hair samples taken at 48 hours after MCAO in both control and PD groups. Student's unpaired t-test, P=0.33, n=12 for each group.

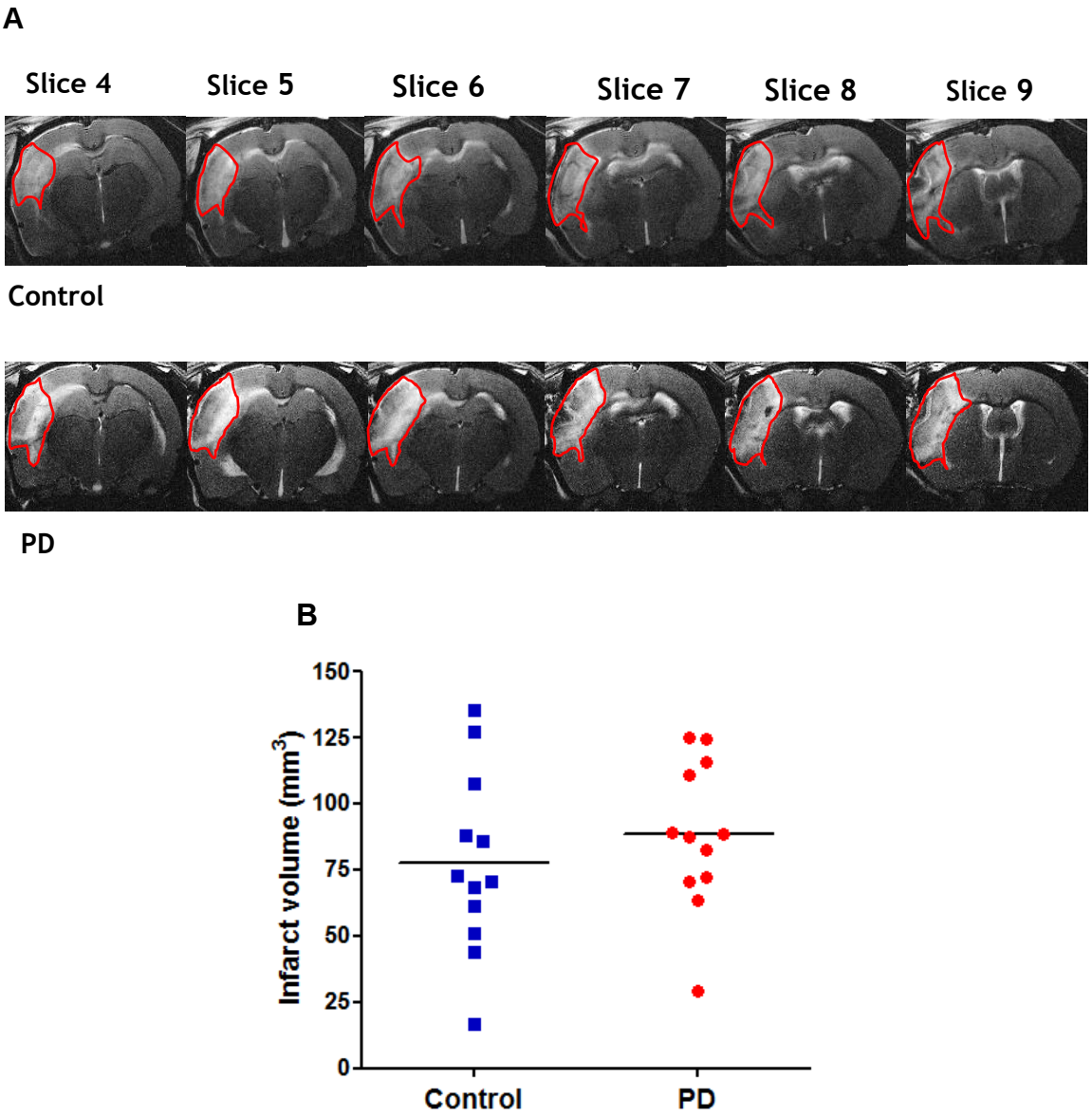

Figure 3.7 (A) T_2-weighted MRI images taken at 48 hours post MCAO showing hyper-intense (highlighted) region as infarcted area. Representative slices from median animal demonstrate comparable ischaemic damage in both groups. (B) Scatter plot illustrating infarct volume at 48 hours post MCAO. Data points indicate individual rats and the horizontal bar represents the mean (Student unpaired t-test, P= 0.34, n=12).

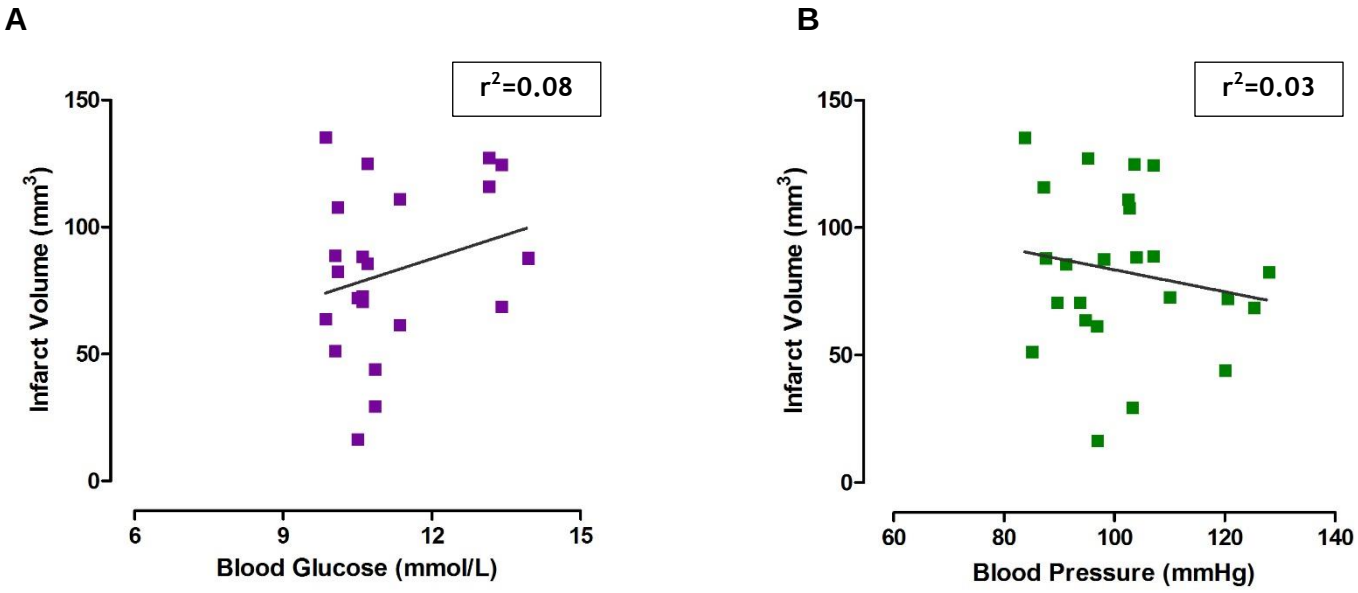

Figure 3.8 (A) The correlation between physiological parameters immediately prior to MCAO and T_2-derived infarct volume at 48 hours post MCAO. No significant correlation was found between blood glucose and infarct volume in all animals, r^2=0.08, P=0.18. (B) Similar observation noted in blood pressure with infarct volume, r^2= 0.03, P=0.42.

3.4 Discussion

Rotating shift work results in photoperiod disruption such that exposure to light/dark cycles are regularly altered compared to normal day/night schedules. In this paradigm, circadian rhythms are chronically disrupted with intermittent period of re-entrainment to the stable light/dark cycle (Deibel *et al.*, 2014). Altering the light/dark cycle is one of the mechanisms to induce circadian disruption in experimental animals. In this instance, light stimulation on SCN results in rapid changes in physiology and behaviour (Arble *et al.*, 2010). To elucidate the potential impact of PD on outcome after ischaemic stroke, we examined two groups of animals under different light/dark conditions. Based on associations made between shift work and metabolic dysfunction in humans (Scheer *et al.*, 2009) we hypothesised that a chronic period of PD would have an adverse effect on infarct size after permanent MCAO in rats.

Locomotor activity is one of the most commonly used measures of circadian rhythmicity (Deibel *et al.*, 2014). Under baseline conditions consisting of the standard 12:12 light/dark cycle, PD rats exhibited clear rhythms that were entrained to the light/dark cycle. When these light/dark cycles were adjusted during the phase advance protocol there was a clear disruption of circadian rhythmicity as could be seen when assessing locomotor activity. However, our data clearly demonstrate that while PD rats exhibited chronic disruption of locomotor activity rhythms over 9 weeks, this did not result in an increased sensitivity to ischaemic damage following MCAO when compared to control rats. Consistent with the lack of effect of PD on infarct size was the lack of effect on physiological parameters which can influence stroke outcome: body weight; blood pressure and blood glucose.

3.4.1 PD Did Not Alter Food Intake and Body Weight

The metabolic effects of PD in experimental studies are notably inconsistent. This study and others (Bartol-Munier *et al.*, 2006; Gale *et al.*, 2011) did not observe changes in metabolic parameters reported previously such as increased body weight gain and food intake (Tsai *et al.*, 2005). Differences in the protocols used to induce PD could partly account for the heterogeneity of the study

results; it is likely that phase advance/delay, constant light and photoperiod less than 24 hours affect both circadian rhythms and metabolism in different ways and it is not clear which intervention most closely represents disrupted rhythmicity in humans. Furthermore, the impact of PD on cardiometabolic function might further depend on the wavelength and intensity of light exposure (Turin *et al.*, 2012) that are not easily compared between studies. This is supported by a study employing different light/dark manipulations in diabetic prone rats which demonstrated various degrees of metabolic disturbances. Higher mean blood glucose level was observed in diabetic prone rats exposed to constant darkness protocol as compared to 6 hour phase advance protocol for 10 weeks (Gale *et al.*, 2011). In similar experiment, 5% increase in body weight was observed in rats exposed to a constant darkness. Dose dependent stimulatory effect of light has been elicited in another study such that subjects exposed to higher light intensity (800 lux) developed larger increase in heart rate (Scheer, van Doornen and Buijs, 1999).

Environmental entrainment is a complex parameter and differences in the degree of secondary disruption of food and social rhythmicity might further contribute to these discrepancies between studies. Indeed, PD is just one component of the multiple conflicting social, stress and food-related disruptions to the lifestyle of the shift worker. In addition to light-entrainment through the SCN, emerging evidence supports a strong impact of food intake on the control of peripheral rhythms (Salgado-Delgado, Nadia, *et al.*, 2010; Salgado-Delgado *et al.*, 2013). In nocturnal animals, restricting the time for food intake to the rest phase changed clock gene expression in liver and pancreas but not in the SCN (Damiola, 2000) and caused increased in body weight (Salgado-Delgado *et al.*, 2013). In this case, weight gain is due to uncoupling between peripheral clocks and light signal from the central pacemaker (Patton and Mistlberger, 2013). In the present study, animals had free access to food at all times of the day and it is possible that they maintained synchronization of food intake to the disrupted light/dark cycles, and that enabled them to accommodate the challenge of PD without comprised metabolic function.

Animals subjected to PD in the laboratory may maintain overall synchronisation if food rhythms remain intact, and further studies that measure

temporal aspects of food mediated cues are required to resolve this issue. The rhythmicity of the shift worker is different to that of their family and friends, while in rats, all of the animals share the same (disrupted) photoperiod. This important difference between circadian disruption in the laboratory, and in real life might account for the inconsistent reports of the impact of PD on metabolic health. The findings that animals in some laboratories were able to maintain metabolic health despite PD indicate that unidentified factors may protect animals from the detrimental effects of light disruption. Future studies should focus on identifying if entrainment to social or food-related *zeitgebers* can help animals to accommodate PD, and if similar interventions can attenuate the risks of shift work for metabolic and vascular health in humans.

3.4.2 PD Did Not Alter Physiological Parameters; Blood pressure, Blood Glucose and Plasma Fructosamine

Significant time-of-day-dependent variations are observed in multiple cardiovascular parameters, such as blood pressure and heart rate suggesting circadian rhythmicity (Molcan et al. 2013). Young, normotensive Wistar rats were used in the present study and chronic PD had no impact on BP which is concordant with similar findings in normotensive Wistar rats subjected to 8 hours photoperiod disruption for 12 weeks (Molcan *et al.*, 2013). Their study demonstrated dampening of circadian rhythms in BP, interpreted as diminished spectral circadian power. Nevertheless, PD for 12 weeks did not result in any increase in blood pressure. The study also concludes that circadian rhythms in BP are less sensitive to photoperiod disruption than heart rate (evidenced by smaller decrease in spectral power for circadian rhythm in BP as compared to heart rate). Circadian rhythm of the heart rate is controlled mainly via sinoatrial node pacemaker cells and autonomous nervous system branches (Mighiu and Heximer, 2012) which are under direct influence by the SCN (Buijs *et al.*, 2003) and therefore is more sensitive to light/dark manipulation.

While light is the primary *zeitgeber* for the central clock in SCN, peripheral clocks in the heart and blood vessels are mainly influenced by neuro-humoral factors; namely changes in autonomic, sympathetic, and adrenergic stimulation, nutrients (i.e. glucose, fatty acids, lipoproteins), circulating

hormones (i.e. insulin, cortisol, adipokines)(Young and Bray, 2007). To date, investigators reported several *zeitgebers* exist for different types of cells in cardiovascular system. Nonaka and colleagues have shown that Angiotensin II, the primary vasoconstrictor in BP regulation acts as a *zeitgebers* for the circadian clock within vascular smooth muscle cells through an Angiotensin II type 1 receptor-dependent mechanism (Nonaka *et al.*, 2001). Durgan and colleagues reported that norephinephrine acts as a *zeitgeber* for the circadian clock within the cardiomyocyte, suggesting the influence of sympathetic stimulation (Durgan *et al.*, 2005). This observation suggests that BP is partially regulated by peripheral clock mechanism, thus less strongly influenced by light-dark manipulation.

One of the advantages of the above-mentioned study by Molcan and colleagues was the usage of radio-telemetry that provides continuous monitoring of blood pressure and heart rate thereby allowing assessment of the daily rhythms of these variables. With regards to our experiment, tail cuff measurement of systolic BP provided a single measure at a specific time of day and therefore did not provide any information on the daily changes in the rhythm parameters (amplitude or loss of rhythmicity) that might be missed during the duration of PD intervention. The outcome measure in this study however, was to investigate the cumulative effect of PD on blood pressure near the time of stroke, which was shown to have no effect.

Gale et al. in 2011 suggest that the interaction of genetic predisposition with an environmental trigger (such as PD) further accelerates early development of hyperglycaemia in diabetic prone rats compared to the wild type (Gale *et al.*, 2011). Other studies demonstrate that 12 hours phase shift in the light/dark cycle on a weekly basis causes a significant reduction in survival time in cardiomyopathic hamsters (Penev *et al.*, 1998) and a higher mortality rate in aged mice (Davidson et al. 2006). Thus, the adverse effects of PD on health may be manifested in the context of existing factors such as advanced age, hypertension, insulin resistance or genetic variation.

Blood glucose and plasma fructosamine data obtained from this study indicates that PD for 9 weeks was not associated with increased glucose level.

Blood glucose measured immediately prior to MCAO reflects an acute glycaemic status prior to stroke, whereas plasma fructosamine measurement taken at 48 hours after stroke indicates the average glucose concentration over the previous 2-3 weeks. Since blood glucose was measured at a single time point in this study that was immediately prior to MCAO, the level could be influenced by various factors such as stress-induced hyperglycaemia secondary to handling (i.e. intubation) and Isoflurane anaesthesia.

Rats were not fasted prior to glucose measurement and anaesthesia was induced by inhalation of Isoflurane. Saha and colleagues reported two important factors which could affect blood glucose level in animal models under anaesthesia; choice of anaesthesia and fasting/feeding states of the animal. They reported that administration of Isoflurane (1.5% to 2%) for 3 h produced acute and sustained hyperglycaemia in non-fasted rats. In contrast, fasted rats displayed normal and stable blood glucose level during the 3 h study period (Saha *et al.*, 2005). In view of this, plasma concentration of fructosamine was measured to reflect blood glucose level over the past 2-3 weeks prior to MCAO, which was not increase in PD group.

3.4.3 Hair Corticosterone

Single housing of rats for long periods is not ideal due to possible confounding effects (e.g. stress-induced by social isolation). In this experiment, rats were housed individually for measurement of rat activity in the PD group. Since all rats in the study were housed singly, any adverse effects would have been experienced by both PD and control groups and our data have shown that hair corticosterone was indifference between groups. It is possibly explained by the fact that auditory and olfactory social contacts were still present among animals. Despite being singly housed, the rats were not totally isolated as rats were kept in the same shelf in the pair of 2.

The rhythmic release of glucocorticoids are under control of the SCN, and bilateral lesion of the SCN has been shown to abolish the rhythms (Cascio et al., 1987). Since corticosterone secretion in rats was driven by SCN, manipulation in light-dark cycle has been reported to disrupt its diurnal variation. Deibel and co-

workers had shown that plasma corticosterone was elevated following 64 days of photoperiod shifting in female rats (Deibel *et al.*, 2014). With regards to our data, hair corticosterone level was not elevated in PD groups. However, this finding does not exclude the possibility of any changes in rhythm parameters (i.e. dampening or shifting of the rhythm) since the temporal data for corticosterone level over the period of 24 hours was not demonstrated. Perturbation in the circadian patterns of corticosterone is best demonstrated by timed blood sampling over 24 hours period. This pointed to our study limitation in which regular blood sampling in the same animal would have compromised the animal's physiology (i.e. by lowering blood volume and possibly on the outcome after stroke). The purpose of the study however, was to examine the cumulative effect of PD on physiology at the time of MCAO which was unaffected.

3.4.4 PD Did Not Exacerbate Ischaemic Damage

This study demonstrates that PD alone was not sufficient to increase vulnerability to stroke in young rats without stroke co-morbidities. Previous laboratory studies reported the presence of co-morbid factors in experimental animals such as genetically determined hypertension, diabetic prone, or rats modelling metabolic syndrome have increased sensitivity to ischaemic damage and less potentially salvageable ischaemic penumbra (McCabe *et al.*, 2009). In the case of stroke-prone spontaneously hypertensive rats (SHRSP) an increased sensitivity to experimental stroke may be attributed in part to increase oxidative stress and poor collateral flow (Coyle and Jokelainen, 1983). Another study found that hyperglycaemia at clinically relevant levels increased early lesion volume following MCAO in both normal rats and those with the features of metabolic syndrome (Tarr *et al.*, 2013).

Study by Earnest and colleagues however reported conflicting findings; photoperiod shifting for 8 weeks exacerbated stroke outcomes in both male and female rats (Earnest *et al.*, 2016). In contrast to our experiment, this study employed slightly different photoperiod shifting protocol; 12 hours phase advance every 5 days for 8 weeks duration. As mentioned in the early part of the discussion, differences in PD protocols could partly account for the heterogeneity in the study results. However, the striking difference was in the

model of MCA occlusion. Adult male rats were used in both studies, and rats were 21-23 weeks old and 30-38 weeks old at the time of MCAO (our study vs Earnest's respectively). In Earnest and colleagues' MCAO was induced by endothelin-1 injection which stated longer reperfusion time (16 hours in cortex and 7 hours in striatum). The exact time of reperfusion however was not confirmed in this study as they utilised prior information from previously published paper by (Biernaskie et al. 2001). Apart from increased in infarct volume, higher mortality rate in male rats (70%) was also reported in shifted group.

Nevertheless, in our study distal end of MCA was permanently occluded by electrocoagulation that resulted in small cortical infarct. It is likely that less severe stroke outcome was partly explained by smaller initial lesion and MCAO model used in our study. The fact that chronic PD did not significantly increase infarct size in our study fits in our finding on blood pressure and blood glucose such that PD did not result in alteration that could potentially increase the sensitivity to ischaemic damage. On the other hand, changes in the parameters that could potentially impact on stroke outcome were not demonstrated by Earnest's and colleague. Furthermore, the increase in infarct volume observed in shifted female rats in their study was proposed due to the loss of neuroprotective effect evident by abolished oestrous cyclicity and decrease in IGF-1 levels. These examples may indicate that depending on the ischaemic model used, strain, age and gender differences, the observable effect of PD can be largely different.

One potential caveat of the present study is that it was not sufficiently powered to detect an effect of PD on infarct volume. When designing the study the original sample size was calculated based on previous data from our laboratory using the same model of MCAO and strain of rat which detected a 50% increase in infarct volume associated with hyperglycaemia (Roy, 2015). Using the data obtained from control group in the current study a group size of 14 is predicted necessary to detect a 50% increase in infarct volume and so it does not appear likely that an effect of PD was missed due to a Type II error.

3.4.5 Summary

In summary, the present study demonstrated that PD for 9 weeks did not impact on physiological parameters near the time of stroke and increase infarct size in young normotensive rats. We conclude that young healthy individuals may be resilient to any impact PD, as a consequence of shift work or other environmental influences, may have on sensitivity to stroke. However, the potential adverse impact of PD on stroke outcome in the context of concomitant disruption of food or social *zeitgebers* or additional pathological challenges from a sedentary lifestyle, a high fat/high sugar diet, ageing or pre-existing co-morbidities warrant future investigation.

Chapter 4 -Characterisation and Optimisation of Animal Model for Transient Focal Cerebral Ischaemia

4.1 Introduction

In the previous Chapter the effects of PD on permanent focal cerebral ischaemia were examined. Permanent MCAO is a good approach for investigating potential influences on the evolution of ischaemic damage when reperfusion, either spontaneous or therapeutically-induced, does not occur. The choice of stroke model for a particular study must consider the strength and weaknesses of the different models in relation to the experimental aims and research question (Howells *et al.*, 2010). Human stroke generally involves a degree of reperfusion either spontaneously or following thrombolysis. Increasingly in the future, more patient will benefit from reperfusion following mechanical thrombectomy as this therapy becomes more widely available (Muir, 2016). Therefore, a question arising from the permanent MCAO study described in the previous Chapter was: does PD exacerbate damage after transient MCAO? Before embarking on a study to address that question a study was performed to characterise the effects of the model of focal cerebral ischaemia with reperfusion in terms of the size, anatomical location and measurable neurological and behavioural deficits.

For this study, occlusion of the proximal MCA was achieved via the intraluminal filament method (Longa *et al.*, 1989). Technically, this method is less invasive and does not require craniectomy and therefore avoids damage to cranial structures (Macrae, 2011). Importantly, the filament can be withdrawn at any time to permit restoration of blood flow after defined periods of occlusion (Carmichael, 2005). With the intraluminal filament model, reproducible ischaemic infarcts have been reported following arterial occlusion times ranging from 20 min to 2 hours. Depending upon the duration of ischaemia, this method has been shown to induce ischaemic damage in basal ganglia and cortical regions with severe and consistent functional deficits (Liu *et al.*, 2009). In the first part (Study 1) of this characterisation study, a 90 min MCA occlusion time was selected and this was applied in the first instance to normotensive Sprague-Dawley rats. The duration of ischaemia could be altered in future studies depending upon mortality rate, infarct size, distribution and functional deficits.

As human stroke often co-exists with other co-morbid factors, incorporating recognised risk factors for stroke (i.e. hypertension) into animal models provides increased clinical relevance to human stroke. Study 2 of this Chapter was therefore conducted to determine the optimal MCA occlusion time for transient focal ischaemia in spontaneously hypertensive (SHR) rats. The information gained will be used to determine the condition applied in the subsequent study in Chapter 5, investigating the impact of PD on sensitivity to transient focal cerebral ischaemia in the context of existing hypertension. It is hypothesised that PD would increase stroke sensitivity and infarct size in hypertensive rats. Our previous in-house studies of transient focal ischaemia in spontaneously hypertensive stroke-prone rats (SHRSP) demonstrated large areas of ischaemic damage and very little penumbra defined by diffusion-perfusion mismatch, incorporating almost the entire ipsilateral hemisphere as early as 1 hour post occlusion (Reid *et al.*, 2012). Such large initial lesions could therefore restrict the ability to detect a detrimental effect of PD. Therefore, shorter occlusion times (30 min and 45 min) were chosen in this pilot study to determine which was optimal for subsequent study.

4.1.1 Study Aim

Study 1: Characterise the effect of transient focal cerebral ischaemia in terms of infarct size and distribution and functional deficits in normotensive rats.

Study 2: To determine the optimal MCA occlusion time for transient focal cerebral ischaemia in SHR rats.

4.2 Methods

4.2.1 Study 1: Characterization of the Transient Focal Cerebral Ischaemia Model in Normotensive Sprague-Dawley Rats

4.2.1.1 Animals

All animals were obtained from Envigo (UK) and housed in an animal care research facility at the University of Glasgow. Experiments were carried out on adult male Sprague-Dawley rats, weighing 296-340g (on the day of surgery) and all animals were maintained on a 12:12 hour light/dark cycle. Water and food were freely available.

4.2.1.2 Surgical Procedure

The rats were anaesthetised initially in an induction box (5% isoflurane) and then endotracheally intubated, ventilated and maintained between 2-2.5% isoflurane with a mixture of nitrous oxide and oxygen (70:30). Cannulation of the right femoral artery was performed as described in Chapter 2.2.2 to allow continual monitoring of blood pressure and arterial blood gases. Cerebral ischaemia and reperfusion was achieved by 90 min MCAO with an intraluminal filament (3-0 to 4-0 nylon monofilament) as described in Chapter 2.3.2. The filament was introduced from the bifurcation of internal carotid artery and advanced until resistance (20-22 mm). In the present study, filament diameter was carefully matched to a defined body weight range to ensure adequate occlusion of the origin of the MCA. It was removed after a pre-determined period, depending on the study to establish reperfusion. During anaesthesia, all physiological parameters were maintained within physiological range. Body temperature was maintained throughout the procedure using an angle poise heat lamp and recorded using a rectal thermal probe (Physitemp, New Jersey, USA).

4.2.1.3 Animal Recovery from Surgery

Animals were recovered from surgery as previously described in Chapter 2.3.4. The animal was closely monitored hourly post-operatively for the next 3 hours and details of the animal condition were recorded on the recovery sheets.

4.2.1.4 MRI Scanning Protocol

At 7 days after MCAO rats were re-anaesthetized and placed in a Bruker Pharmascan 7T MRI scanner. Rats were maintained under isoflurane anaesthesia with 70:30 of nitrous oxide: oxygen mixture using a face mask throughout the scanning process. Body temperature was maintained at 37±0.5 °C. The rats were placed into a rat cradle, secured and a surface coil was put above the head before placing them in the MRI scanner. A RARE T_2 weighted sequence was acquired (TE=100ms, TR=6000ms, matrix=256x256, 16 coronal section slices; 0.75mm thick) to allow calculation of final infarct volume.

4.2.1.5 Infarct Volume Measurements

Cerebral infarct volume analyses were performed using Image J software (NIH, Bethesda, MD, USA), in which the assessor was blinded to the experimental groups. Final infarct at day 7 post-stroke was defined as a hyperintense area on T_2-weighted images. The hyperintense area was manually delineated on the T_2 slices and infarct volume was calculated by software as described in Chapter 2.5.4.

4.2.1.6 Neurological Score

Neurological scoring was performed to evaluate sensory and motor functions and the overall neurological deficits. Neurological abnormalities were evaluated with the use of a modified Garcia Score (Garcia *et al.*, 1995) prior to surgery for their baseline performance and then on day 1, 3 and 7 post MCAO. The score given to each rat at the completion of the evaluation is the summation of all six individual tests which separately evaluate spontaneous activity, symmetry in limb movement, forepaw outstretching, climbing, body

proprioception, response to vibrissae touch, resistance to lateral push. The minimum neurological score is 3 and the maximum is 18.

4.2.1.7 Adhesive Label Test

The adhesive label test that was previously used to evaluate the degree of forelimb sensory motor impairment in animals following unilateral lesion involving the sensorimotor cortex, the corticospinal tract, and the striatum was employed in this study (Schallert et al. 2000; Metz 2010). Animals were removed from their home cage and adhesive dots (1.3cm, Avery International) were attached on the hairless aspect of the right and left paw. To prevent bias, the adhesive dots were touched simultaneously before the recording of 3 separate trials and dot placement was alternated after each trial. In the assessment cage, latency to contact and latency to remove the adhesive dot by mouth was recorded by a video camera (Sony). Each trial ended when 3 minutes has elapsed or contact and removal of the adhesive dots had been accomplished. The trial was re-started if the dots came off without prior contact by the animal. Animals were returned to their home cage for 5 minutes before the beginning of next trial.

4.2.2 Study 2: Optimisation of Occlusion Time for Transient Focal Cerebral Ischaemia In Spontaneously Hypertensive Rats

Adult, male spontaneously hypertensive rats obtained from Envigo (UK) and age between 10-12 weeks were randomly assigned to 2 groups with 2 different MCA occlusion times: 30 min (n =8) or 45 min (n=6). Non-invasive blood pressure measurement was performed prior to the commencement of the study to confirm that rats were hypertensive (data not shown). Animals were anaesthetised with 5% isoflurane in a Perspex chamber and then orally intubated. They were then mechanically ventilated with 2.5% isoflurane in a nitrous oxide: oxygen mixture (70:30). A rectal thermocouple probe provided continual monitoring of core body temperature that was maintained at 37±0.5°C via angle poise heat lamp. Animals were recovered as described in Chapter 2.3.4. and were re-anaesthetised for determination of final infarct volume via MRI scanning at day 3.

4.2.3 Statistical Analysis

Statistical analyses were performed using GraphPad Prism software v6 (GraphPad, La Jolla, CA). All data are expressed as mean ± SD or scatterplots with the mean indicated, with the exception of the neurological scores which are expressed as medians. Repeated measures (RM) 1 way analysis of variance (ANOVA) and Dunnett's post hoc test were applied to compare data at each post-MCAO time point with day 0 (pre-MCAO) and assessment of neurological deficits. Non-parametric Spearman's correlation was used to examine associations between infarct volume and neurological score at day 7 post MCAO. Differences are considered significant when $P < 0.05$.

4.3 Results

4.3.1 Study 1: Characterization of the Transient Focal Cerebral Ischaemia Model in Normotensive Sprague-Dawley Rats

4.3.1.1 Mortality

A total of 17 rats were included in Study 1. Five died during the first 24 hours after MCAO. Post mortem examination of the brain revealed large infarcts OR the presence of subarachnoid haemorrhages. Therefore, the final group sizes for analysis was n=12.

4.3.1.2 Physiological Variables

During anaesthesia, the physiological variables were all within the normal physiological range, except for PaO_2 which was elevated. This is likely to be attributed to the anaesthetic gas mixture, where 30% oxygen is used rather than the 21% oxygen found in air.

Physiological variables	
Body weight (g)	308.4 ± 13
Body temperature (°C)	37 ± 0.5
Mean arterial blood pressure (MABP) (mmHg)	86 ± 4
Arterial $PaCO_2$ (mmHg)	43 ± 5
Arterial PaO_2 (mmHg)	121 ± 18
Blood pH	7.4 ± 0.1

Table 4.1 Physiological variables in Sprague-Dawley rats from Study 1. Body weight was taken prior to the surgery, MABP and temperature expressed as mean over the entire surgical period; blood pH, arterial $PaCO_2$ and PaO_2 as measured at the onset of MCAO. Values expressed as mean ± standard deviation.

4.3.1.3 Infarct Volume

Mean infarct volume defined by MRI T_2-weighted imaging at day 7 after MCAO was 100.2 ± 60.7 mm^3 (ranging from 8.91 to 245.8 mm^3). There was notable variation in infarct volumes between rats (Figure 4.1). A caudal to rostral distribution of ischaemic areas of a representative animal defined by T_2-weighted MRI is presented in Figure 4.2A and 4.2B. The hyperintense and highlighted region on each slice in Figure 4.2A represents the area of ischaemic damage which encompasses mainly the subcortical region.

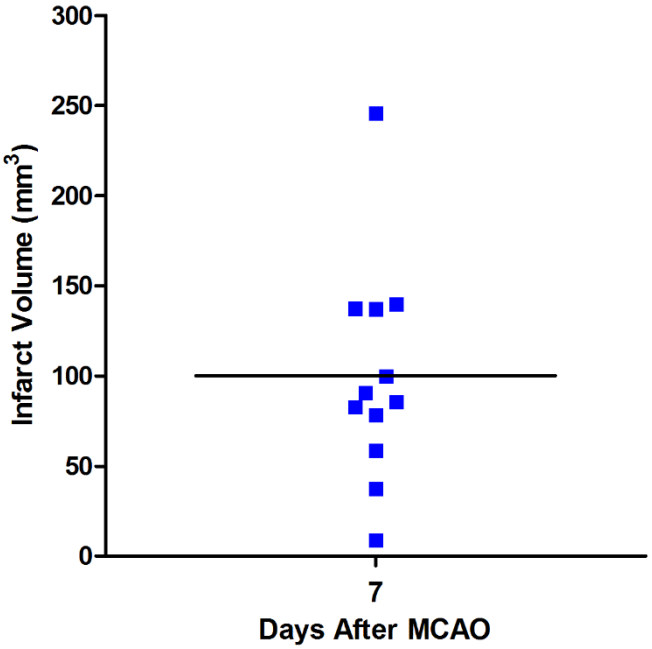

Figure 4.1 Infarct volume from Study 1. Scatterplot illustrating infarct volume at day 7 following 90 min transient MCAO, in individual Sprague-Dawley rats. The horizontal line represents the mean.

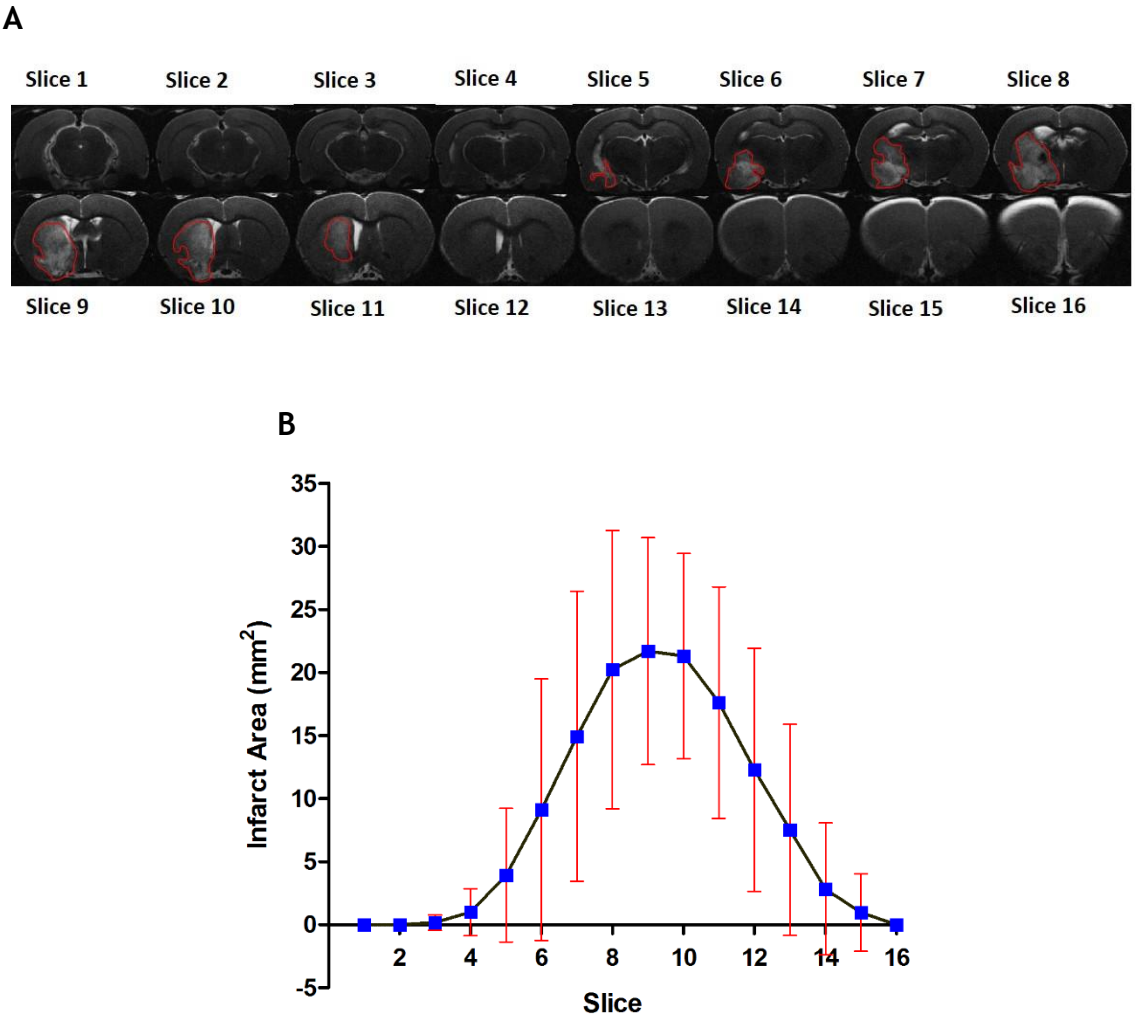

Figure 4.2 The infarct areas at 7 days after 90 min intraluminal-induced transient MCAO in Sprague-Dawley rats. Sixteen coronal slices of T_2-weighted MRI images from the animal with the median infarct volume are shown to illustrate the spatial distribution of the infarct (caudal to rostral). (A) The infarct areas were determined by manually delineating the hyperintense area on each of 16 coronal T_2 slices. (B) The distribution of infarct area in each slice for all 12 rats. Data presented as mean ± standard deviation.

4.3.1.4 Neurological Score

The 18-point neurological score was conducted prior to MCAO with all animals scoring the maximum score of 18. Figure 4.3A shows the mean neurological scores. All animals scored significantly worse than the baseline performance following MCAO. Repeated measures 1 way ANOVA and post hoc comparisons (Dunnett's) revealed that the mean score for each post-MCAO days (day 1, 3 and 7) was significantly reduced ($P<0.001$) compared to the baseline (day 0). However, the mean score at day 7 was higher compared to day 1 post-MCAO indicating a degree of recovery. Using the non-parametric Spearman's correlation, an r value of -0.65 demonstrates that there is an inverse relationship between infarct volume and neurological score; as infarct volume decreases, neurological score increases (Spearman $r= -0.65$, $P=0.02$, Figure 4.3B).

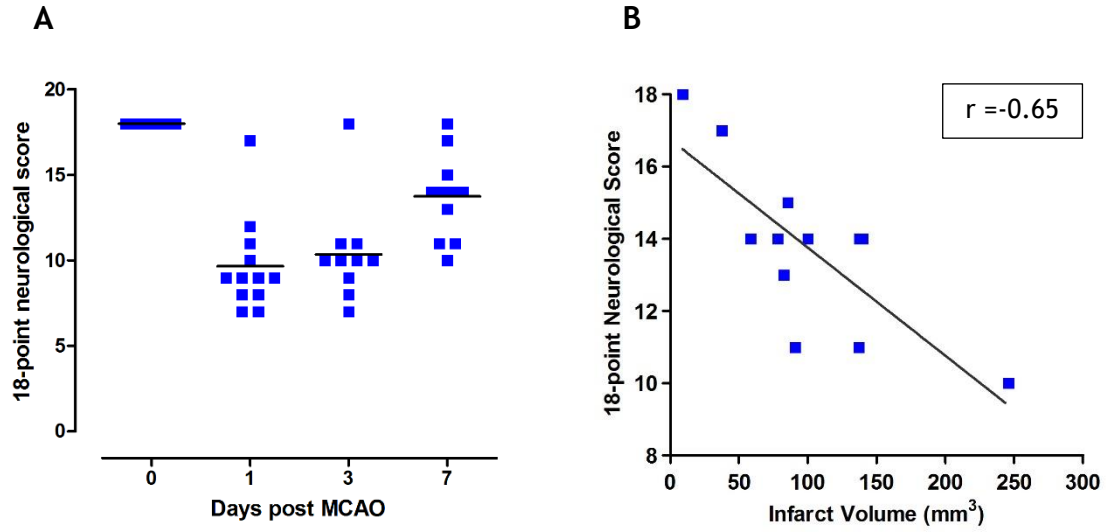

Figure 4.3 (A) 18-point neurological score for individual animals. Prior to MCAO (day 0) all rats obtained the maximum score of 18, after which the scores were reduced. (B) Spearman's correlation between infarct volume and neurological score indicates significant association at 7 days post-MCAO (Spearman r=-0.65, P=0.02, n=12).

4.3.1.5 Adhesive Label Test

For both the time to remove and contact the adhesive dot, the difference between the time for each forepaw (affected-non affected) was calculated to ensure the outcome measures were not affected by overall activity of the animals (Stroemer *et al.*, 2009). The mean differences in contact time between the affected and unaffected paws for each individual rat are shown in Figure 4.4A. Prior to MCAO, all rats exhibited contact difference times close to zero which indicates symmetrical limb contact (and removal) latencies. RM 1 way ANOVA and post hoc (Dunnett's) test showed that the contact difference time was significantly increased at all time point after MCAO compared to their baseline performance (day 0) ($P<0.05$).

Figure 4.4B shows the mean removal difference times for each individual rat. Transient MCAO for 90 min resulted in an increased removal difference time. RM 1 way ANOVA and post hoc (Dunnett's) test showed that the removal difference time was significantly increased at all time points after MCAO compared to baseline (day 0) ($P<0.05$). Although the contact (and removal) difference time was lessened by day 7 compared to day 1, the majority of rats exhibited marked deficits and did not reach their baseline performance (Figure 4.4C and 4.4D).

It was noted that some rats exhibited a complete lack of activity (freezing behaviour) on day 1 and day 3 post MCAO, and remained in the same position for the duration of the trial (180s). Such behaviour would have confounded experimental results (rats have shown zero contact/removal difference time). Therefore, in experiments described in Chapter 5, it was decided not to perform the adhesive label test at those time points and data was only collected at 7 days as freezing behaviour was not observed.

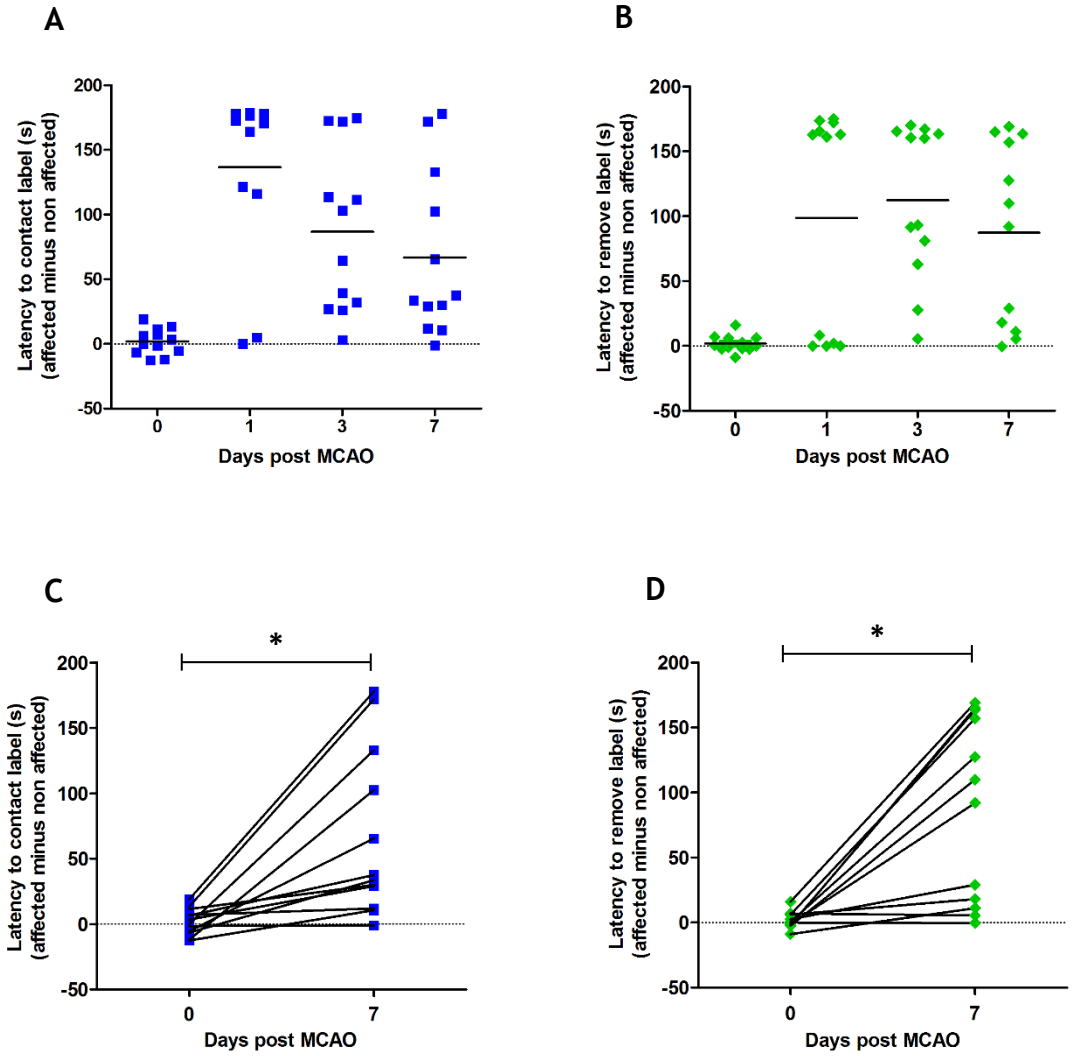

Figure 4.4 Effect of 90 min MCAO on contact (and removal) difference times over 7 days. A scatterplot showing the mean contact (A) and removal (B) difference times data for individual animals which was significantly increased at each time point post MCAO compared to their baseline (RM 1-way ANOVA and Dunnett's post hoc test, $P<0.05$, n=12). The mean difference in contact (C) and removal (D) times at day 7 is highly variable, with the majority of animals showing persistent deficits. The dotted horizontal line indicates zero, which denotes symmetrical limb contact (and removal) latencies. Data points indicated individual rats. Horizontal bar represents the mean.

4.3.2 Study 2: Optimisation of MCA Occlusion Time for Transient Focal Cerebral Ischaemia in Spontaneously Hypertensive Rats

4.3.2.1 Mortality and Excluded Animals

There was no mortality following 30 min or 45 min MCAO. However, 3 animals were excluded from the analysis due to failed MCAO (no evident of infarct assessed by T_2 weighted MRI at day 7).

4.3.2.2 Infarct Volume

The extent of ischaemic damage from representative animals following 30 or 45 min transient MCAO are shown in Figure 4.5A. Infarct area distribution for each coronal slice of T_2 weighted MRI images, from all animals is shown in Figure 4.5B. Data presented as mean ± standard deviation. A 45 min occlusion resulted in more extensive ischaemic damage involving almost the entire ipsilateral hemisphere, in the region supplied by the MCA (Figure 4.5A). Figure 4.6 shows the impact of different occlusion times and rat strains (normotensive vs hypertensive) on the extend of ischaemic damage. The mean infarct volume for 30 min vs 45 min MCAO was 161.2±63 mm^3 and 212.1±55 mm^3, respectively. In hypertensive rats, the ischaemic damage was extensive within 30 min of MCAO suggesting an increased sensitivity to focal ischemia compared with the normotensive rats, such that shorter occlusion time is sufficient to induce a bigger size infarct.

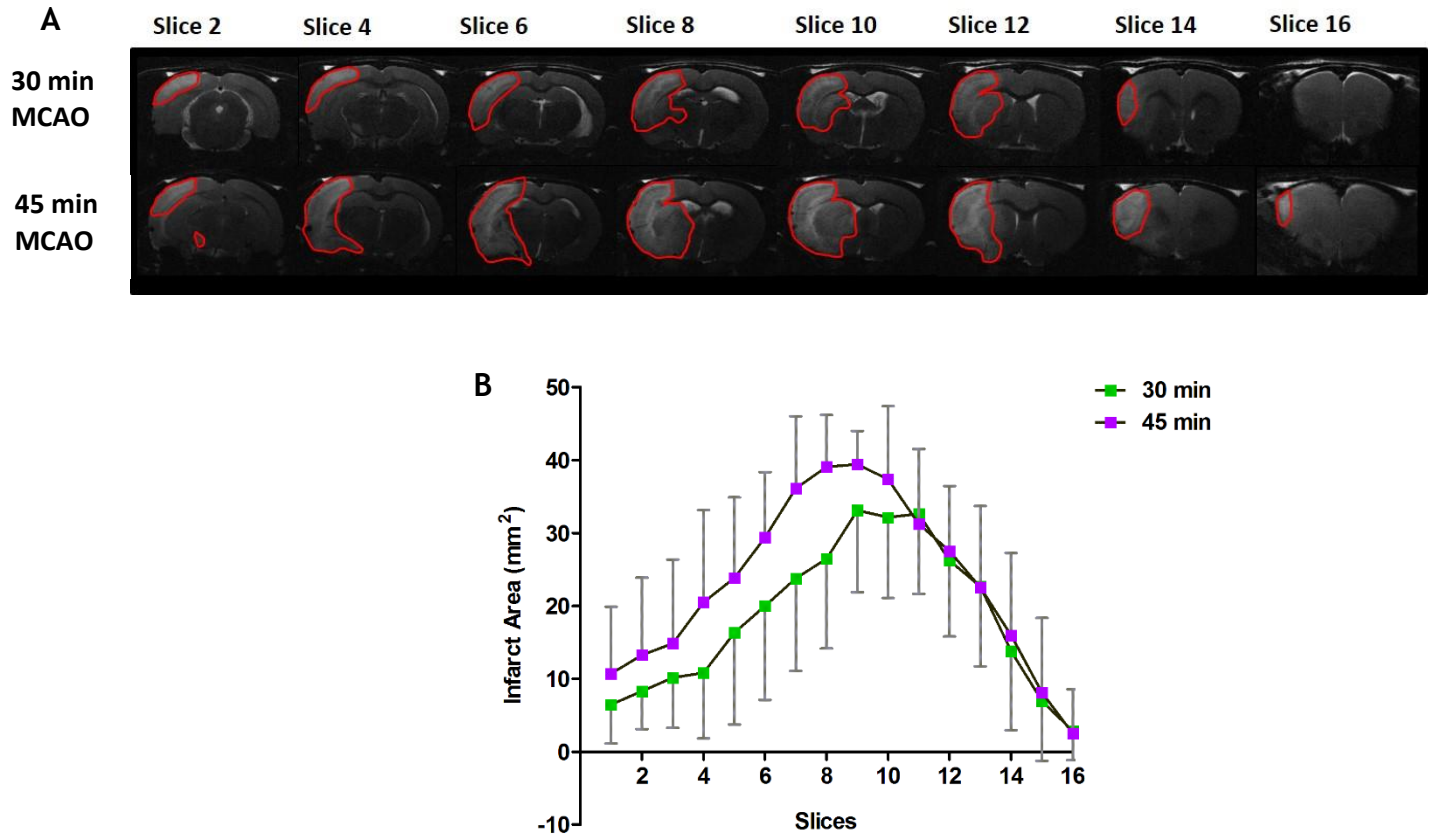

Figure 4.5 (A) Final infarct volume at day 3 after transient MCAO in SHR rats. T_2 MRI images from representative animals following either 30 min or 45 min MCAO showing ischaemic damage across 8 coronal sections. (B) Distribution of infarct areas defined by T_2 MRI, across 16 coronal slices for both MCA occlusion times. Data presented as mean ± standard deviation.

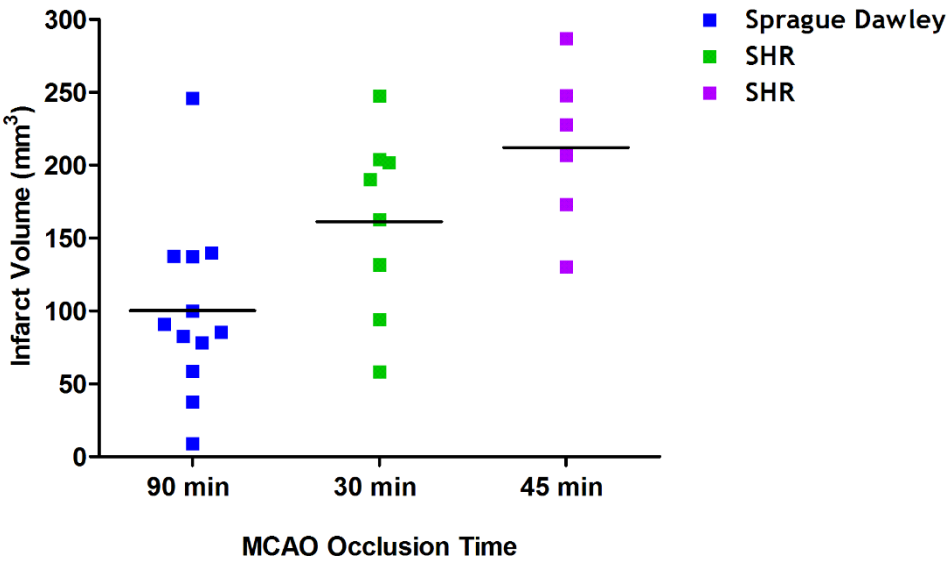

Figure 4.6 Final infarct volume for 3 different MCAO occlusion times in Sprague-Dawley rats (90 min, n=12) and SHR (30 and 45 min; n=8 and n=6 respectively). Each data point represents individual animals and horizontal bar represents the mean.

4.4 Discussion

Pilot studies conducted in this Chapter generated 2 important results in the selection of an appropriate stroke model for subsequent studies of the effects of transient MCAO in animals subjected to PD. Firstly, intraluminal transient MCAO for 90 min in Sprague-Dawley rats resulted in ischaemic lesions involving mainly subcortical areas and behavioural deficits which persisted for 7 days which could be detected by the adhesive label test and neurological scoring. Secondly, intraluminal transient MCAO in SHR rats resulted in more extensive ischaemic damage with only 30 min of MCAO involving both subcortical and cortical regions.

4.4.1 Ischaemic Damage

Since vessel occlusion is seldom permanent in human stroke, many pre-clinical studies incorporate reperfusion (following ischaemia) into the design of the animal model (Macrae 1992). The Sprague-Dawley rat is an outbred strain most commonly used in pre-clinical stroke studies which is considered a standard normotensive rat strain (Howells *et al.*, 2010; O'Collins *et al.*, 2013). Therefore, this strain of rat was selected for Study 1 which aimed to characterise the transient model of focal cerebral ischaemia. One of the major strengths of experimental stroke research is the ability to closely monitor and control the factors that can influence the magnitude of an ischaemic lesion. However, infarct volume data from this study shows that there was substantial variation in ischaemic lesion size within strain. This is in agreement with other studies which have shown that Sprague-Dawley rats displayed a much greater range of infarct sizes following intraluminal MCAO than other strains such as SHR or WKY (Aspey *et al.*, 2000; Howells *et al.*, 2010). Anatomical variation within strain has been shown to contribute to the variability in lesion size (Howells *et al.*, 2010). Fox and colleagues reported that the potential source of variation in Sprague-Dawley rats is due to highly variable origin and branching pattern of the MCA found in this strain (Fox *et al.*, 1993).

Apart from anatomical variation, several other experimental factors can also account for the differences in lesion size induced by intraluminal MCAO.

Physiological variables such as body temperature and arterial blood gases (i.e. $PaCO_2$, PO_2) significantly affect infarct volume and should be kept within a narrow range (Browning *et al.*, 1997; Zausinger et al., 2002). Hyperthermia following cerebral ischaemia is commonly encountered when vessels supplying the thermoregulatory centre in the hypothalamus are affected by infarction (Li, Omae and Fisher, 1999). A brain temperature of 39°C significantly increased the brain infarct volume as compared to the normothermic controls (37°C) (Noor et al., 2003). In view of this, physiological variables and body temperature were closely monitored and maintained within the normal limits throughout the duration of surgery.

Properties of the filament used to occlude the MCA, such as the filament dimension, insertion length and filament coating can have a major influence on infarct size. In Study 1, the intraluminal filament was constructed from a length of 3-0 to 4-0 nylon monofilament. A small diameter bulb was then created using a cauterising pen. This process is operator dependant and therefore may result in inconsistent bulb size and shape. In order to reduce variability, bulb diameter should be matched to the animal weight and also strains (Howells *et al.*, 2010). Silicon coated filaments have been shown to reduce the incidence of subarachnoid haemorrhage and premature reperfusion (Belayev *et al.*, 1996) and produce more reproducible infarcts (Shimamura *et al.*, 2006). Another source of variability is due to the inadequate reduction of cerebral blood flow following filament occlusion. It was unknown whether blood flow reduction induced by intraluminal filament in this study was sufficient to induce infarction as successful occlusion of MCA was not confirmed (i.e. by Laser Doppler flowmetry or MRI angiography). Therefore, it is possible that there will have been some partial occlusions of the MCA, which may explain some of the small infarcts observed at day 7 post MCAO. This would account for the increased variability and is a particular problem in studies where an intervention (i.e. PD or pharmacological treatment) is being assessed between groups.

Data from Study 2 in this Chapter demonstrates the effect of co-morbidities on stroke outcome (infarct volume). A greater susceptibility of hypertensive strains to brain ischemia is well documented in other studies compared to their control strain, WKY (Duverger and MacKenzie, 1988; Reid *et*

al., 2012). In hypertensive rats, a shorter duration of MCAO is sufficient to induce a bigger infarct than in normotensive animals. This has an important clinical implication for management of stroke patients with hypertension and suggests that with pre-existing hypertension, ischaemic damage could progress at a faster rate (McCabe *et al.*, 2009). This pilot study was conducted to optimise the MCAO occlusion time for SHR rats study in Chapter 5. It is hypothesized that adding another factor such as photoperiod disruption (PD), would increase stroke sensitivity in hypertensive rats. The infarct volume data shows that 45 min MCAO resulted in ischaemic damage encompassing almost the entire ipsilateral hemisphere in the MCA territory. Larger infarcts induced by 45 min MCAO in SHR could present a problem as the ability to detect any harmful effects of PD on infarct size may be restricted due to a "ceiling effect". This means that the level of ischaemic damage may be at its maximum and it would be impossible to detect an adverse impact of PD. Therefore, it was decided that 30 min MCAO is the optimal occlusion time to be used for future study in Chapter 5.

4.4.2 Neurological and Sensory Motor Outcome

The effect of focal cerebral ischaemia on functional outcome represents an important component in the pre-clinical setting. The choice of neurological and behavioural tests which involves the assessment of skilled motor functions is of clinical importance as motor deficit after stroke is common, and has a considerable influence on quality of life (Shelton et al., 2001; Macrae, 2011). In the present study, intraluminal occlusion of the proximal end of the MCA induces contralateral limb sensorimotor deficits manifested as impaired detection and removal of adhesive labels placed on the forepaw. This test has previously been shown to detect sensorimotor deficits up to 12 weeks following 60 min transient ischaemia (Modo *et al.*, 2000). Similar functional deficits have been reported in stroke patients and therefore there is a high validity in relating experimental findings to the clinical condition (Rose *et al.*, 1994). In Study 1, MCAO for 90 min was found to induce a measurable sensorimotor deficit that partially recovered over 7 days. The initial loss of function following ischaemia is caused by neuronal death within the infarct core and cellular dysfunction in the hypoperfused ischaemic penumbra (Kriz and Lalancette-Hébert, 2009), which explained the

significant neurological and sensory motor deficits observed on day 1. However, the functional impairment at this acute time point may also be due to lack of activity as animals become very sick following MCAO surgery and anaesthesia, may confound interpretation of the results. As most of the animals demonstrated freezing behaviour on day 1, it was decided that the neurological and sensory motor assessment not be performed until 7 days after MCAO in Chapter 5.

4.4.3 Summary

The data from these characterisation experiments were used to inform the design of the subsequent experiments described in this thesis. The optimal MCA occlusion time to produce infarcts in SHR that was not so anatomically extensive, that they could not be made larger by the adverse influence of PD was 30 min. The functional consequences of transient MCAO could be detected using neurological scoring and the adhesive label test at 7 days after MCAO; a time when animals had recovered from the acute effects of the surgical procedure and the initial effects of ischaemia. In order to overcome any issues relating to variability in infarct volume we opted to carry out acute MRI scanning during MCAO allowing us to confirm successful occlusion of the MCA and to assess the impact of PD on growth of lesion in individual animals. These parameters were applied in the subsequent study described in Chapter 5.

Chapter 5-Impact of Photoperiod Disruption on Sensitivity to Focal Cerebral Ischaemia and Microglia Activation in Spontaneously Hypertensive Rats

5.1 Introduction

In our previous study, we have demonstrated that PD in young healthy rats did not increase sensitivity to permanent focal cerebral ischaemia (Ku Mohd Noor *et al.*, 2016). Circadian disruption has been associated with the pathogenesis of many of the features of metabolic syndrome (i.e. hypertension, obesity, diabetes) (Rüger and Scheer, 2009)(Scheer et al. 2009). Therefore, we hypothesize that PD in the presence of pre-existing hypertension will exacerbate outcome following transient focal cerebral ischaemia. In humans, stroke typically occurs as a result of the cumulative effects of pre-existing risk factors such as hypertension, diabetes, and obesity. A population-based study reported that 37-42% of ischaemic stroke patients presented with diabetes alone or in combination with hypertension (Kissela *et al.*, 2005). Moreover, the incidence rate of ischaemic stroke is now taking a reversing trend: despite a substantial decrease in stroke incidence in the older population, incidence in younger age group (less than 55 years old) is on the rise. In addition, atrial fibrillation, diabetes and hypertension; the leading risk factor for stroke, have also been steadily increasing in younger individuals (Swerdel *et al.*, 2016).

In the setting of acute cerebral ischaemia, many of the reported metabolic or physiological changes in circadian disruption, i.e. hypertension, diabetes, have potential to adversely modify the ischaemic penumbra, and hasten its demise. In preclinical studies, SHR rats has been widely used to evaluate the effect of hypertension on ischaemic stroke (Yao and Nabika, 2012) as it shares many features of human essential hypertension (Amenta et al., 2003). Greater susceptibility to stroke in SHR rats is frequently explained by a deficit in collateral circulation compared to normotensive rats (Grabowski *et al.*, 1993). Moreover, hypertrophic remodelling of cerebral arteries are well known features of vascular changes present in SHRs (Mulvany et al., 1978). Chronic arterial hypertension, genetically determined or renovascular-induced, has been shown to accelerate the evolution of diffusion-weighted imaging (DWI) lesions and increase infarct size after permanent focal cerebral ischaemia (Letourneur *et al.*, 2011) (McCabe *et al.*, 2009). The differences in evolution of ischaemic penumbra observed between SHR and normotensive control, WKY could be

explained by chronic hypertension-induced functional and structural alterations of the brain vasculature (Letourneur et al 2011).

Apart from hypertension, clinical studies indicate that persisting hyperglycaemia influences stroke evolution. For example, post-stroke hyperglycaemia is associated with higher mortality and poor functional outcome (Muir *et al.*, 2011) and blood glucose levels over the first 72 hours after stroke correlate with growth of the MRI-defined ischaemic lesion (Baird *et al.*, 2003). Our in-house data demonstrated that clinically relevant levels of hyperglycaemia increased final infarct size and exacerbate early ischaemic lesion growth after permanent middle cerebral artery occlusion in rat (Tarr *et al.*, 2013). Fructose-fed spontaneously hypertensive stroke-prone (SHRSP) rats, which exhibit features of metabolic syndrome, have shown larger DWI lesions and final infarcts compared to controls (Tarr *et al.*, 2013). Hyperglycaemia also has a profound effect on reperfusion following transient focal cerebral ischaemia, indicated by poor restoration of cerebral blood flow; less than 50% of normoglycaemic rats (Kawai, Keep and Betz, 1997). Given that alterations in circadian rhythm have been shown to be implicated in the pathogenesis of disease such as metabolic syndrome, we hypothesize that cumulative effect of PD in the presence of co-morbid factor (hypertension) will exacerbate damage following stroke.

We also proposed that the downstream mechanism for increased sensitivity to stroke could involve inflammation, as these stroke co-morbidities share a common feature; elevated inflammatory profile (Hansson and Libby 2006). There is emerging evidence that inflammatory events outside the brain occurring prior to, during, and after stroke markedly influence stroke susceptibility and outcome (McColl et al., 2009). In a rat model of transient focal cerebral ischaemia, systemic immune challenge with lipopolysaccharide (LPS) markedly exacerbates ischaemic damage and the severity of neurological deficit (McColl et al., 2007). In fact, systemic inflammation has been shown to significantly increases reperfusion deficits via enhanced platelet aggregation in microvessels and microglial activation following transient ischaemia (Burrows *et al.*, 2016).

A number of immune processes namely toll-like receptor function, cytokine gene expression, lymphocyte proliferation and microglia exhibit daily variations in circadian rhythm (Scheiermann *et al.*, 2013)(Fonken *et al.*, 2015). A role for circadian disruption in brain inflammation has been implicated in mice studies whereby exposure to a dim light at night showed enhanced microglia activation and pro-inflammatory cytokine expression in mice (Fonken et al., 2013)(Phillips et al., 2015). Because the immune and circadian systems are related, it is likely that there are inflammatory consequences of photoperiod disruption. Therefore, in this study we also looked at the impact of PD on the principal immune cell of the brain, microglia.

Microglia, the primary immune cells in the brain, has been shown to possess circadian clock mechanisms that display rhythmic fluctuations in pro-inflammatory cytokines including IL-1ß, TNF-α, IL-6, and IL-1R1 (Fonken *et al.*, 2015). In a setting of acute stroke, activation of microglia is the key initial event for post stroke inflammation (Patel *et al.*, 2013). Animals with higher number of activated microglia displayed greater degree of ischaemic damage, suggesting the role of increased microglial activation in stroke sensitivity (Marks *et al.*, 2001). The importance of microglial activity after ischaemic stroke has been reported in number of studies. In studies where microglia have been ablated, mice had larger infarctions and a doubling of apoptotic neurones after ischemia (Lalancette-Hébert *et al.*, 2012). Furthermore, suppression of microglia activation by Edaravone; a free radical scavenger (Zhang *et al.*, 2005) and hyperbaric oxygen (Günther *et al.*, 2005) resulted in reduction in infarct volume and improvement in functional outcome following MCAO.

We have shown in previous study that PD did not impact on outcome after permanent focal cerebral ischaemia (Chapter 3). Compared to permanent occlusion, transient models better correlate with clinical stroke whereby recanalization was achieved either with treatment-induced or spontaneous thrombolysis. The ischaemic injury following transient ischaemia is an evolving process, therefore the model is suitable for studying the impact of PD on lesion evolution (Williams et al, 2004). In addition, the impact of PD on ischaemic damage may be different in the absence and presence of reperfusion. Having

both transient and permanent models allow us to draw comparison on the effect of PD on both model of focal cerebral ischaemia.

5.1.1 Study Aims

The primary aim was to investigate the impact of PD in the presence of a co-morbid factor (hypertension) on sensitivity to stroke in terms of ischaemic lesion growth and functional outcome (Study 1). In addition, in order to examine a potential mechanism induced by PD alone: increased brain inflammation, the extent of microglia activation was measured in a cohort of SHRs that were subjected to PD but not MCAO (Study 2).

5.2 Methods

5.2.1 Animals

Spontaneously hypertensive rats (SHR) were obtained from Envigo (UK) and housed in Veterinary Research Facility (VRF) at the University of Glasgow. Experiments were carried out under license from the UK Home Office and were subject to the Animals (Scientific Procedures) Act, 1986. The report was carried out in accordance with the ARRIVE guidelines (http://www.nc3rs.org.uk/arrive). All rats had *ad libitum* access to water and standard rat chow.

5.2.2 Impact of PD on Sensitivity to Stroke (Study 1)

A total of 40 male adult SHR rats age 10-12 weeks were entered into the study. Rats were kept under a standard 12:12 light/dark cycle (lights on at 0700, lights off at 1900) for two weeks prior to allocation into one of two experimental groups. Rats were grouped housed (3 rats per cage) throughout the duration of study. Timeline of the experimental procedure for Study 1 is illustrated in Figure 5.1.

5.2.2.1 Sample Size Calculation and Blinding

To calculate the number of animals required in each group a sample size calculation was based on infarct volume data in SHR rats obtained from our pilot study optimising the MCAO occlusion time (Chapter 4). The sample size calculation was based on a formula described in Chapter 3.2.2, and an 80% power and 95% significance level. The number of animals required per group was calculated to be 16 allowing a 40% change in lesion volume to be detected. Based on this, the number of rats per group entered into the study was decided to be 20, which allows for a minimum of 34% change in lesion volume (see Table 5.1). Randomisation of rats to groups was not possible due to the limited number of stroke surgeries that could be carried out at the end of the 9-week protocol. All animals were allocated to control and PD groups in equal numbers. Batches of 3 rats were entered into the 9-week protocol as previously described in

Chapter 2.9, with the total number of 20 animals per group. Therefore, the surgeon was not blinded to the experimental groups. However, all measurements of lesion volume were carried out in a blinded manner. Each rat was given a numbered code which was only broken on the completion of all data analysis.

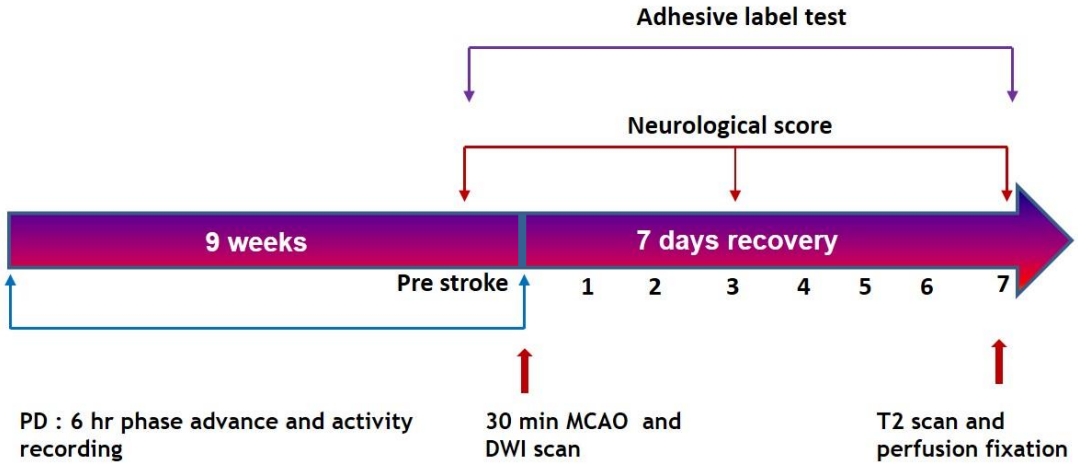

Figure 5.1 Timeline of the experimental procedure for Study 1.

T_2 Infarct Volume Mean 161.2 ± 62.93mm^3	
Effect size	**n**
10	241
20	61
30	28
34	20
40	16
50	11

Table 5.1 Power calculation using T_2 infarct volume following 30 min MCAO from pilot study (Chapter 4), based on 80% power and 95% significance level (α=0.05).

5.2.2.2 Photoperiod Disruption Protocol

Photoperiod disruption was carried out using 6-hour phase advance protocol as previously described in Chapter 2.9. Light intensity was measured by a lux meter at the beginning of the study for the room housing the control rats (~150 lux). The light/dark cycle for the room was controlled by a digital timer that was programmed for the lights to switch on 6 hours earlier than in the previous photoperiod, every 3 days for 9 weeks. Light intensity in the room housing PD rats was maintained at ~150 lux similar to that experienced by the control animals.

Based on our sample size calculation for the SHR rats, a higher number of rats were required per experimental group. Therefore, it was decided that the PD rats should be group housed (3 rats per cage) and rather than use the light/dark box (as in the previous study of normotensive rats) the PD rats were housed in a separate room in which the lights could be programmed with a timer. Rats were entered into the PD protocol in batches of 3 per group. Due to a limited number of MCAO surgeries that can be performed within the MRI facility per day, a total of 6 rats were kept longer in either 12:12 LD or PD protocol (extended protocol; >11 weeks) before MCAO.

5.2.2.3 Activity Monitoring

Locomotor activity was monitored to demonstrate disruptions of circadian rhythms as well as to determine patterns of locomotor activity in response to LD cycle as previously described in Chapter 2.10. Activity monitoring was conducted only in the PD rats due to limited access to sufficient number of activity monitors. Activity was measured in each individual cage that housed 3 rats per cage using a passive infra-red sensor. The sensor was positioned above the cage at a distance that was optimised for detection of movement in all quadrants and for insensitivity to movements outside the cage, a piece of cardboard was placed around the individual cage.

5.2.2.4 Surgical Procedures

Induction of anaesthesia was carried out in a Perspex induction chamber with 5% isoflurane in 70:30 of nitrous oxide: oxygen mixture. Fur overlying the surgical site was shaved prior to transfer to the operating table, and skin cleaned with antiseptic prior to incision. Rats were intubated and mechanically ventilated and maintained with 1.5-2% Isoflurane, in a mixture of 70:30 nitrous oxide: oxygen. Non-responsive to toe pinch indicated adequate surgical anaesthesia. Body temperature was monitored continuously with a rectal probe and maintained at 37±0.5 ºC throughout the surgery. Transient focal cerebral ischaemia was achieved via intraluminal filament model of MCAO as described in Chapter 2. Transient focal ischaemia was induced using coated monofilament (diameter 0.35-0.37mm, length 3.0-5.0mm, Doccol). The filament was introduced via small incision on common carotid artery, and advanced along the internal carotid artery to occlude the proximal end of middle cerebral artery. DWI scan was performed at 25 minutes of MCAO, and the filament was slowly withdrawn at 30 min of MCAO and the incision point was electro-coagulated by diathermy forceps as previously described. Surgical area was cleaned with sterile saline before closure.

5.2.2.5 MRI Scanning Protocol

MRI scanning was performed as described in Chapter 2. Immediately following MCAO rats were transferred under anaesthesia to a Bruker 7T Pharmascan MRI scanner. After transferring the animal into MRI rat cradle, anaesthesia was maintained via a ventilator for acute MRI scanning during MCAO or a via face mask for final infarct scanning at day 7 (2-2.5% Isoflurane in a 70:30 mixture of nitrous oxide: oxygen). Respiration and body temperature was monitored throughout the MRI scanning protocol. A 4-channel phased array surface receiver coil was placed on the rat's head before the cradle was placed inside the scanner. The rat cradle was then secured inside the scanner and a pilot sequence was obtained to ensure the correct geometry.

Diffusion Weighted Imaging (DWI)

DWI was performed to quantify the early ischaemic lesion in 8 coronal slices within the MCA territory using the sequence described in Chapter 2.5.3. Scans were acquired immediately and this was followed by an MR angiography scan (field of view = 4cm, matrix = 256, TE = 3.8ms, TR = 15ms, 50 slices of 0.4 mm thickness) to ensure that the middle cerebral artery had been completely occluded. Scans were repeated at 25 min post MCAO, prior to reperfusion. DWI scans consisted of 8 contiguous coronal slices (1.5mm thick) and quantitative ADC maps were generated for each slice using Paravision software.

T_2 weighted Imaging at Day 7

At 7 days following transient MCAO, rats were re-anaesthetised for determination of final infarct volume by T_2 weighted imaging. Anaesthesia was maintained via face mask that delivered 2-2.5% isoflurane. The animal's head was restrained using tooth and ear bars and body temperature was maintained for the duration of the scanning protocol using a closed circuit thermal jacket. Core body temperature was monitored by a rectal thermocouple. A coronal RARE T_2 sequence (effective TE: 46.8 ms, TR: 5000 s; in plane resolution of 97 um; 16 slices of 0.75 mm thickness) was acquired at 7 days after stroke onset for final infarct volume determination.

5.2.2.6 Animal Recovery

At the end of the MRI scanning protocol the rat cradle was removed from the MRI scanner and after removing the water jacket, rectal thermocouple, the rat was disconnected from the ventilator and transferred to the operating theatre. Once in the operating theatre the rat was reconnected to the ventilator and anaesthesia was maintained with 2% isoflurane in a nitrous oxide: oxygen mixture (70:30). Rats were recovered from anaesthesia as described in Chapter 2.3.4 for 7 days.

5.2.2.7 MRI Data Analysis

ADC Lesion Volume Calculation

Using ImageJ software, ADC lesion volume as calculated by applying an ADC threshold of 0.59 x 10^{-3} mm_2/sec previously established for hypertensive rats (Reid *et al.*, 2012) to the ADC maps generated at 25 min of MCAO. Lesion volume was calculated by multiplying the total area by slice thickness (1.5mm).

T_2 Infarct Volume

ImageJ was used to separate the 16 images and the hyper-intense region that represented the infarct was manually delineated using the freehand function. Measurement of individual images gave the infarct areas in mm^2, and infarct volume was calculated by summing the 16 areas and multiplying by the slice thickness (0.75 mm). As shown in this study, reperfusion induced extensive brain swelling in hypertensive rats that was still present at day 7 post MCAO (Figure 5.13). Therefore, the infarct volume was corrected for brain swelling as previously described in Chapter 2.3.2. The percentage of tissue salvage was calculated from the difference between the acute lesion and final infarct volume divided by the final infarct volume. Following T_2-weighted imaging the animals were deeply anaesthetised by increasing the Isoflurane concentration to 5% for five minutes. Animals were then removed from the MRI scanner and killed by decapitation.

5.2.2.8 Adhesive Label test

The adhesive label test was performed in all animals before MCAO, and at day 7 post MCAO as described in detail in Chapter 2.7. The pilot study in Chapter 4 revealed that rats often exhibited lack of activity and freezing behaviour at day 1 post MCAO. This was likely due to the rats' general state of well-being at this acute time point post stroke where they would be more lethargic and unwell. Testing on day 3 also revealed no significant difference from performance on day 7 (see Chapter 4). Based on this observation, assessments were made only to determine the difference between groups at Day 7 post MCAO.

5.2.2.9 Neurological Score

An 18-point neurological score, as described in Chapter 2.6 was carried out at pre-stroke, day 3 and prior to the MRI scanning for final infarct determination at day 7 post MCAO.

5.2.2.10 Study Exclusion Criteria

Animals were excluded from the study if they have died during the surgery to induce focal cerebral ischaemia, or had a small subcortical lesion on acute DWI scan (evidenced by MCA patency by MR angiography), or have small final infarct volume (<5mm^3) at day 7.

5.2.3 The Impact of PD on Microglia Activation (Study 2)

This study used 12 male SHR rats aged 10-12 weeks old at the beginning of the study. Rats were allocated to one of two groups: PD (n=6) and naïve (n=6). Both groups were age-matched. PD rats were exposed to 6-hour phase advance and naïve rats were maintained under 12:12 LD cycle for 9 weeks. Rats were grouped house (3 rats per cage) and locomotor activity was monitored only in PD rats via cage-top infrared movement sensors (as described above). At the end of 9 weeks, rats were deeply anaesthetised using 4-5% isoflurane delivered in a mixture of oxygen and nitrous oxide (30:70) administered via a face mask. Rats were transcardially perfused with 0.9% saline containing heparin (10ml/Litre) and 4% paraformaldehyde (PFA) and the brain were processed for immunohistochemistry as described in Chapter 2.

5.2.3.1 Photoperiod Disruption Protocol and Activity Monitoring

Photoperiod disruption and locomotor activity monitoring were carried out as previously described in Chapter 2.9 and 2.10. Rats in this study were group housed (3 rats per cage) throughout the phase advance protocol and continuous activity monitoring was performed in rats subjected to PD via cage-top infra-red movement sensors.

5.2.3.2 Iba-1 Immunohistochemistry

This section of the study was performed and analysed by a masters and undergraduate student as part of their research project. Rats brain were processed in paraffin wax and cut in 5µm coronal brain slices using a microtome and sections were mounted on Poly-L-lysine-coated slides. Microglia were detected by immunohistochemistry using antibodies against Iba-1 (Wako, Catalogue No. 019-19741). Sections were deparaffinised and antigen retrieval was achieved by immersion of slides in boiling citric acid (10mM, pH 6.0) for 4 minutes in a pressure cooker. After being cooled in cold water, sections were immersed in 3% H_2O_2 for 20 minutes at room temperature then incubated in a blocking solution containing 5% normal horse serum (Vector Lab, USA) in Triton X-100 (TBX, pH 7.40) for one hour at room temperature. Polyclonal anti-Iba-1 (rabbit, catalogue number: 019 19741, Wako) (1:10,000 in 2% normal horse serum and TBX) was added to the sections and incubated overnight at 4ºC. Sections were then incubated for one hour at room temperature in secondary antibody (biotinylated horse anti-rabbit IgG (Catalogue number: BP-1400, Vector Lab, USA) 1:400 in Tris-buffer (TB, pH 7.40). To visualise the antibody binding, sections were incubated in a streptavidin-biotinylated horseradish peroxidase complex (ABC Elite kit, Vector Lab, USA) for 30 minutes at room temperature. Sections were incubated in DAB (DAB, Vector Lab, UK) for 7 minutes. Sections were dehydrated in alcohol before being cleared in Histoclear and mounted for light microscopic analysis.

5.2.3.3 Quantification of Microglia

Sections were viewed using a light microscope (Leica Biosystems, UK) attached to a CCD camera and a PC and all images were captured on the same day. The observer was blinded to experimental group. Sections were viewed using x20 objective and defined regions of interest captured using QCapture Pro 6 (QImaging, Surrey, Canada). Three pre-determined coronal brain levels; Bregma -0.40mm, -1.30mm, and -1.80mm for level 3, 4, and 5, respectively from each animal were selected from the eight coronal levels previously described by Osborne et al. 1987. From each level, three areas in the cortex (green box) from each hemisphere were selected as region of interest (ROI) (Figure 5.2). The rationale of choosing these areas was that the selected ROI are supplied by MCA. ImageJ (NIH, Bethesda, MD) was then used to subtract the light background. The observer set an optimal level of threshold which would only include the area of Iba-1 immunostaining in the measurement. The area of Iba-1 immunopositivity was presented as percentage of the ROI.

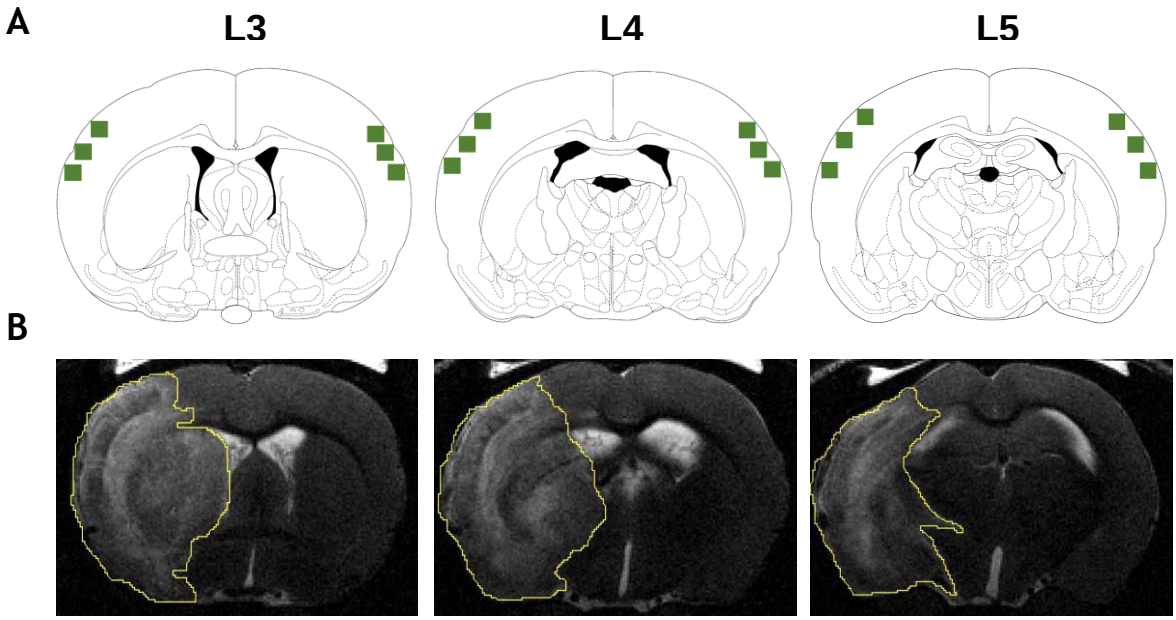

Figure 5.2 (A) Coronal sections of rat brain are at the level of Bregma -0.40mm, -1.30mm, and -1.80mm for level 3, 4, and 5, respectively (Paxinos & Watson (2006). The ROI of Iba-1 immunopositivity were selected from the area of sensorimotor cortex, as defined in green boxes. (B) The highlighted region on T_2-weighted images showing infarcted areas following MCAO. The association between MR images and the level of rat's brain is depicted in this diagram to show that the chosen ROI lie within the possible infarct areas. Images courtesy of Daniel Agriva Tamba(Tamba, 2016).

5.2.4 Statistical Analysis

The difference statistical analysis between 2 experimental groups were analysed using a Student's unpaired t-test in: Iba-1 immunopositive area, ADC lesion volume, T_2-weighted infarct volumes, Day 7 neurological score, and Day 7 adhesive label test. Changes in IS and IV from baseline to PD period, evolution of lesion volume, difference in pre-stroke and day 7 data for neurological score and adhesive label test were assessed using a paired Student's t-test. All statistical analyses were done using GraphPad Prism 6.0 (GraphPad Software, Inc., USA) and using $p< 0.05$ as the level of significance.

5.3 Results

5.3.1 Mortality and Excluded Animals

A total of 40 animals were initially entered into experimental stroke study (Study 1). Out of the 40 rats, 5 rats were excluded: 2 rats from control group and 3 rats from PD group. Out of 5 rats, 3 showed a small subcortical lesion on DWI, indicating incomplete occlusion of the middle cerebral artery as evidenced by MR angiography that eventually resulted in no infarct on T_2-weighted images. One rat was excluded due to the presence of pre-existing brain lesion on the opposite hemisphere shown on DWI scan. One rat died during the surgery to induce focal cerebral ischaemia. Included animals demonstrated complete occlusion of the left middle cerebral artery, and infarct was evident on T_2 weighted MRI on day 7 (Figure 5.3). Therefore, the final group sizes for data analysis were n=18 in the control group and n=17 in the PD group (Figure 5.4).

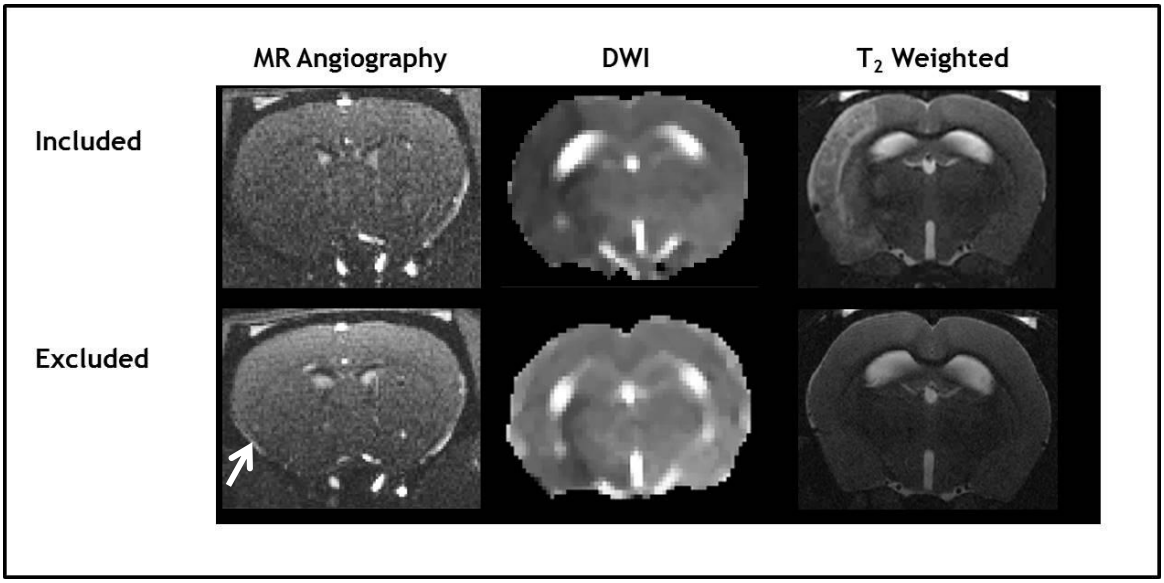

Figure 5.3 Excluded animal showed an evidence of left middle cerebral artery patency (arrow) on MR angiography during MCAO, which resulted in small acute lesion on DWI scan and no obvious infarct on T_2-weighted MRI.

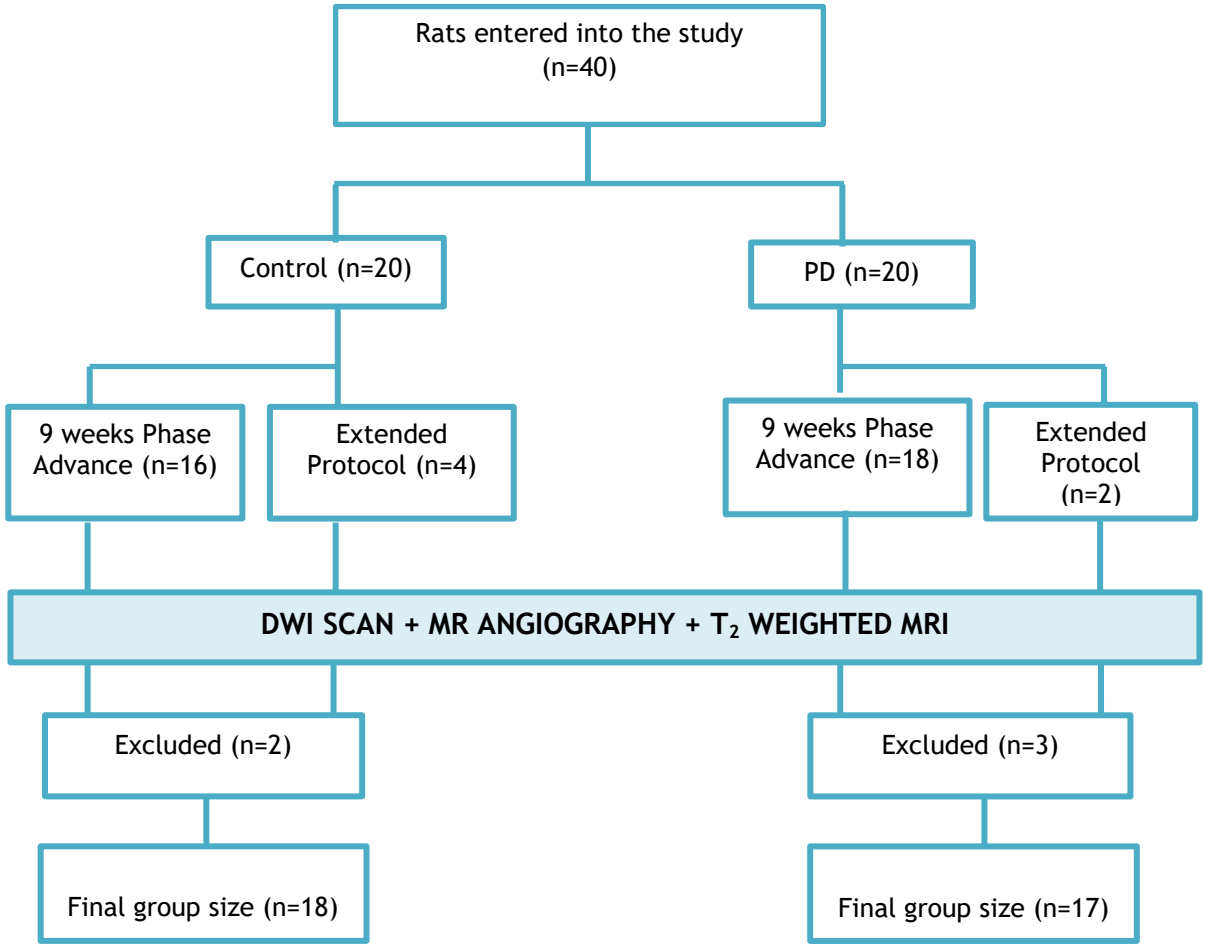

Figure 5.4 Data breakdown showing total number of animals entered into the study and the final n number for data analysis. The extended protocol refers to animals subjected to phase advance protocol for more than 11 weeks.

5.3.2 Impact of PD on Sensitivity to MCAO (Study 1)

5.3.2.1 Activity Monitoring

Photoperiod Disruption Results in Disruption in Locomotor Activity and Rhythmicity in PD Rats

Baseline activity recording was conducted over 4 days prior to commencement of PD protocol. Activity recording in the baseline 12:12 light/dark period showed rats in the LD cycle maintained robust diurnal activity rhythms; in which majority of the animal activity was confined to the dark phase. These activity patterns were disrupted on commencement of the phase advance protocol (Figure 5.5). Disruption in circadian rhythmicity during the PD period compared to the baseline period was confirmed by changes in the rhythmicity parameters; inter-daily stability (IS) and intra-daily variability (IV) between these periods.

The IS was significantly decreased in the PD period compared to baseline; 0.77 ± 0.10 and 0.25 ± 0.02 (arbitrary units), mean ± SD for baseline and PD periods respectively (paired Student's t-test, $P<0.0001$). Variability within days was increased by PD as indicated by significant increases in the IV compared to the baseline period; (0.45 ± 0.08 and 0.78 ± 0.08 (arbitrary units, mean ± SD for baseline and PD periods respectively (Figure 5.6B, paired Student's t-test, $P= 0.0002$).

The mean effect of PD on the rhythmicity of all animals is illustrated in Figure 5.6A which shows that both IS and IV deviated from baseline values when PD commenced, and that baseline values were not recovered. Therefore, locomotor activity rhythmicity remained profoundly disrupted for the duration of the PD intervention.

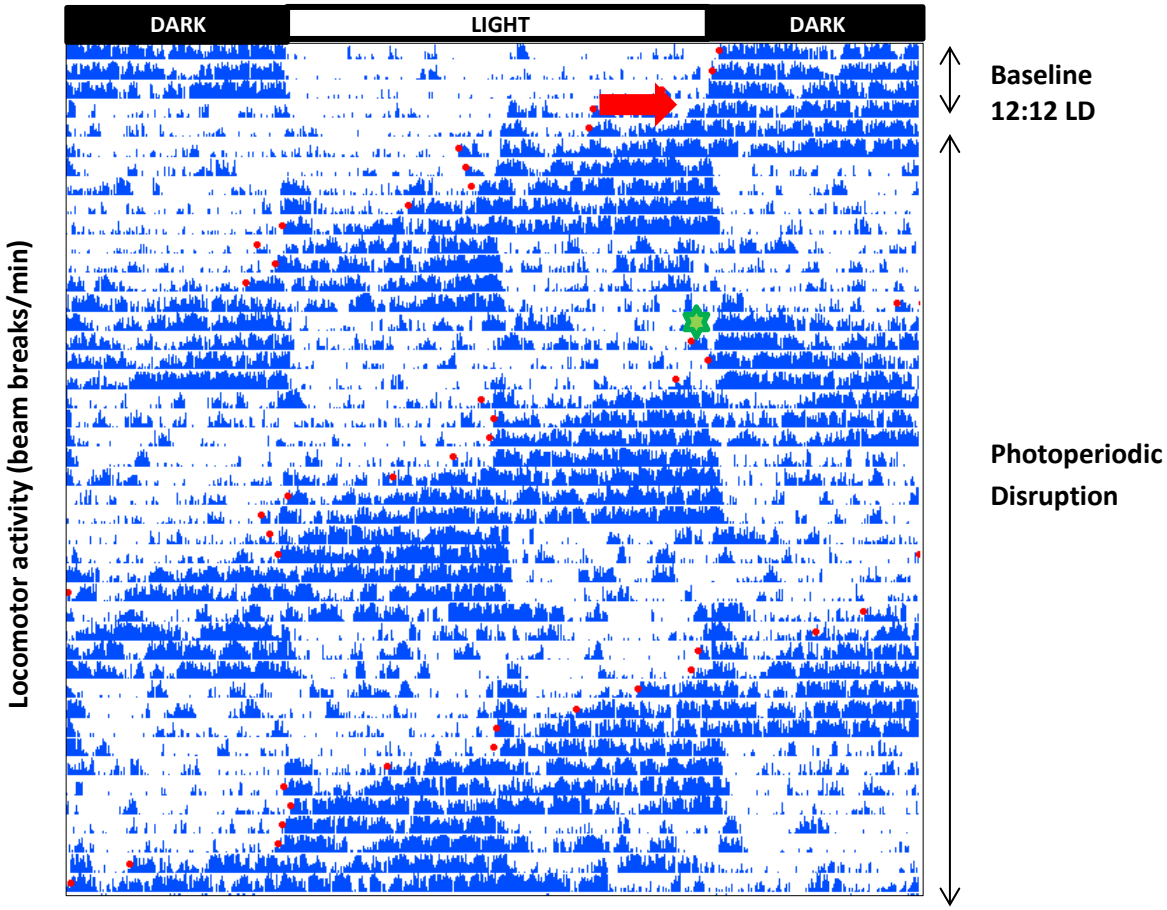

Figure 5.5 Impact of LD and 6-hour phase advances on diurnal rhythms of locomotor activity in PD rats. Double-plotted actogram from representative animal displayed the typical circadian rhythm in locomotor activity (high activity during the dark phase and low activity in the light phase), that was disrupted in the PD period. Each line represents the days of recording and blue shading representing the locomotor activity. Values on the x-axis denotes the time of the day. Red dots represent the onset of locomotor activity. Dark and clear bars indicate the dark and light phase respectively. Arrow indicates the onset of the phase advance protocol. Star indicates the day animals reached re-entrainment to the new LD cycle.

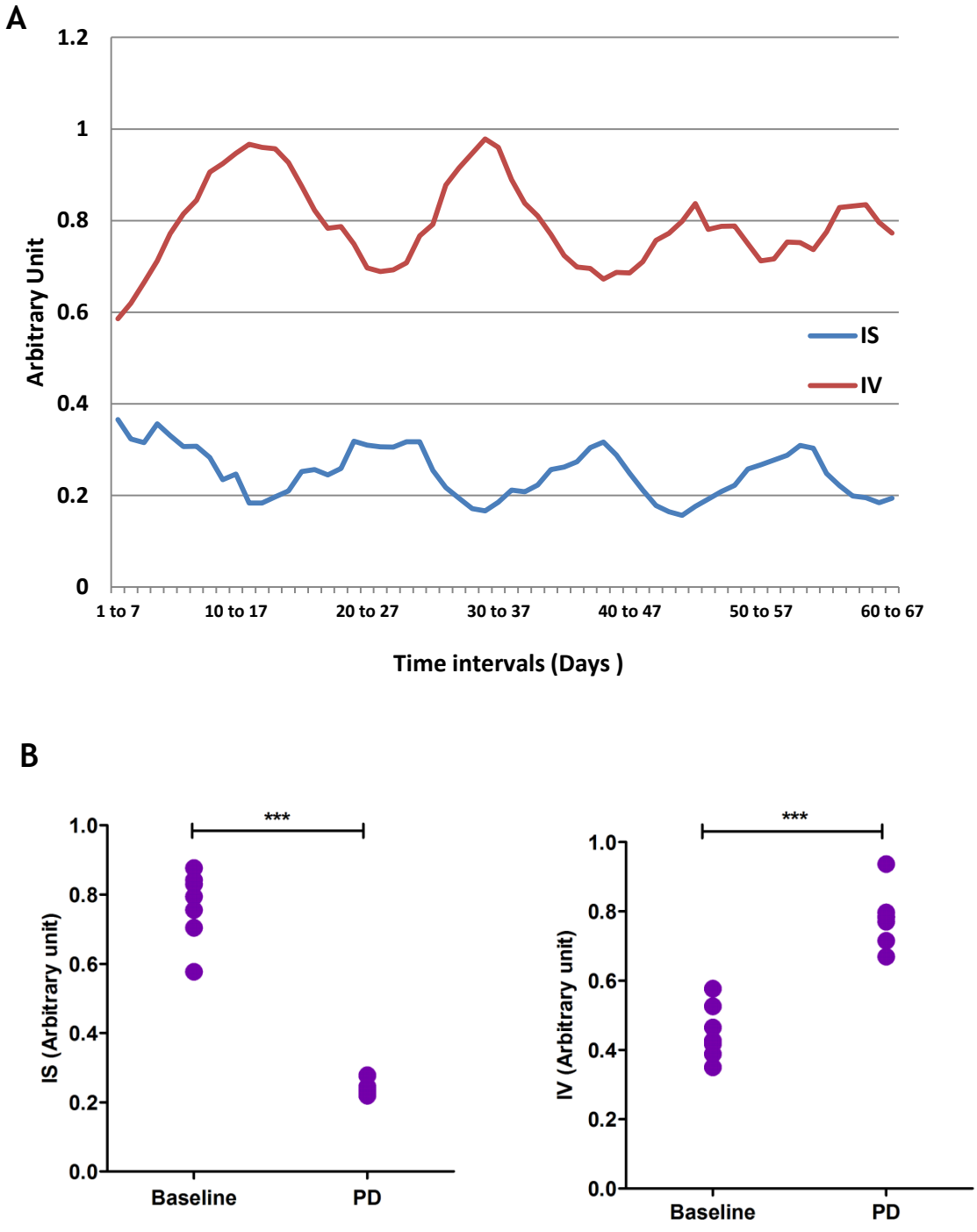

Figure 5.6 (A) The mean effect of PD on the rhythmicity of all animals. Both IS and IV deviated from baseline values when PD commenced, and baseline values were not recovered. (B) Changes in IS and IV from baseline to PD period. The IS was significantly decreased in the PD period compared to baseline (Student's paired t-test, $P<0.0001$, $n=17$). Variability within days was increased by PD as indicated by significant increases in the IV compared to the baseline period (Student's paired t-test, $P= 0.0002$, $n=17$).

5.3.2.2 ADC Lesion Volume at 25 min After MCAO

Mean ADC-derived lesion volume was not significantly different at 25 min of MCAO in control and PD groups (Control: 288.4 ± 35.87 mm^3 and PD: 280.6 ± 52.90 mm^3, P= 0.6104, Student's unpaired t-test, Figure 5.8A). ADC maps for both groups demonstrated a widespread ADC-derived lesion involving cortical and sub-cortical regions across all 8 coronal slices. A similar pattern was observed in the T_2 infarct areas at day 7 with apparent reduction in lesion volume rostro-caudally in both groups (Figure 5.10).

5.3.2.3 Final Infarct Volume

At 7 days post MCAO, ipsilateral swelling and contralateral compression was still evident on T2 MRI images in both experimental groups. Hemisphere volumes were measured in both groups (control; 652.5 ± 25.64 mm3 vs 709.1±42.12mm3 & PD: 668.2 ± 36.38 mm3 vs 723.1±52.43mm3 for the contralateral and ipsilateral hemisphere respectively, as shown in Figure 5.7).

In view of this, the correction for oedema was applied for the calculation of final infarct volume at day 7. At day 7, there was no significant difference in oedema corrected final infarct volume between experimental groups (191.0±70mm^3 vs 172.3±74mm^3, P=0.44, infarct volume of PD and control respectively, Figure 5.8B). Reperfusion resulted in significant tissue salvage when assessing the reduction in lesion volume from 30 min to day 7 within groups (33 ± 25% vs 37 ± 27%, control vs PD respectively, paired Student's t-test, P<0.0001, Figure 5.9) however this was not significantly different between groups (P=0.62, unpaired Student's t-test, Figure 5.10 and 5.11).

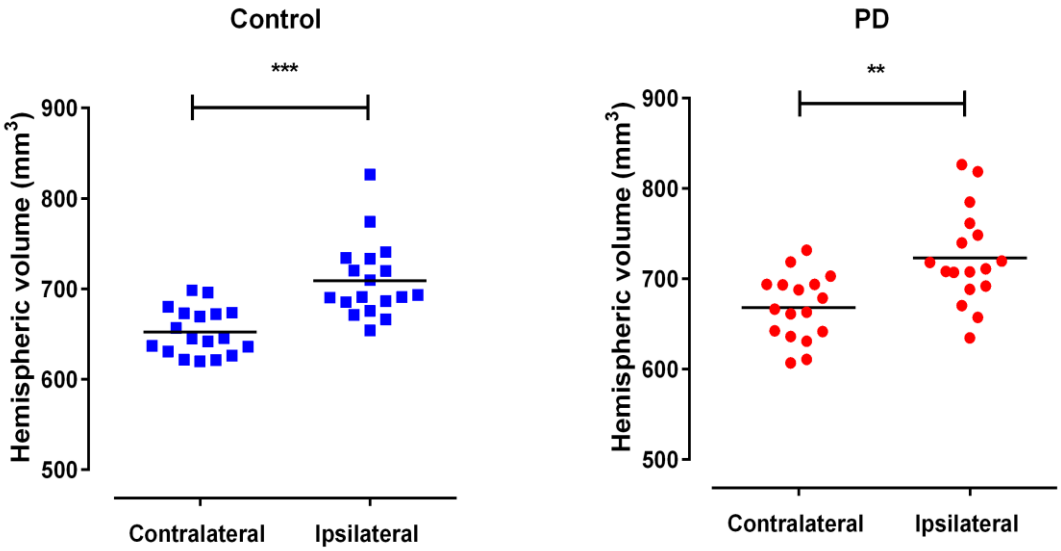

Figure 5.7 Volume of each hemisphere at day 7 after MCAO. Reperfusion in SHR rats following 30 mins MCAO induced significant increase in volume of ipsilateral hemisphere in both groups. (Control vs PD, ***P< 0.0001 vs**P=0.0012, Student's unpaired t-test, n=17-18). Data points indicate individual rat and horizontal bar represents the mean.

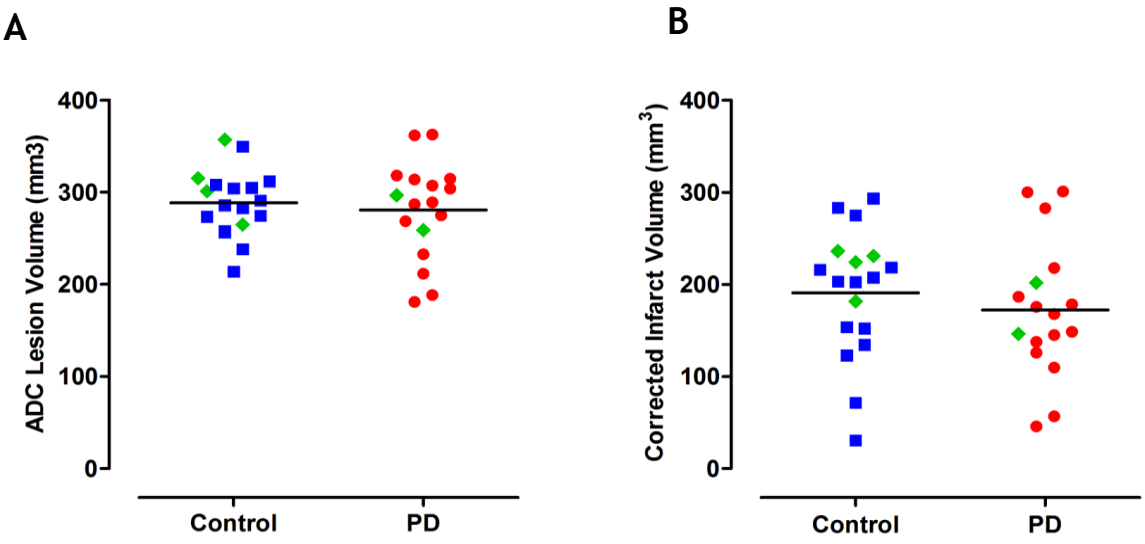

Figure 5.8 (A) Scatter plot representing the ADC lesion volume at 25 min of MCAO and (B) infarct volume (corrected for swelling) at day 7 for all animals that completed 9-week phase advance protocol. Data points indicate individual rats and horizontal bar represents the mean. Green data points represent animals from the extended protocol (>11 weeks). Since the data from animals in the extended protocol was not significantly different from the established protocol, the data were pooled together for analysis. The difference in ADC lesion volume and final infarct volume between the two groups were not statistically significant (unpaired Student's t-test P=0.6 and 0.4 respectively, n=17-18).

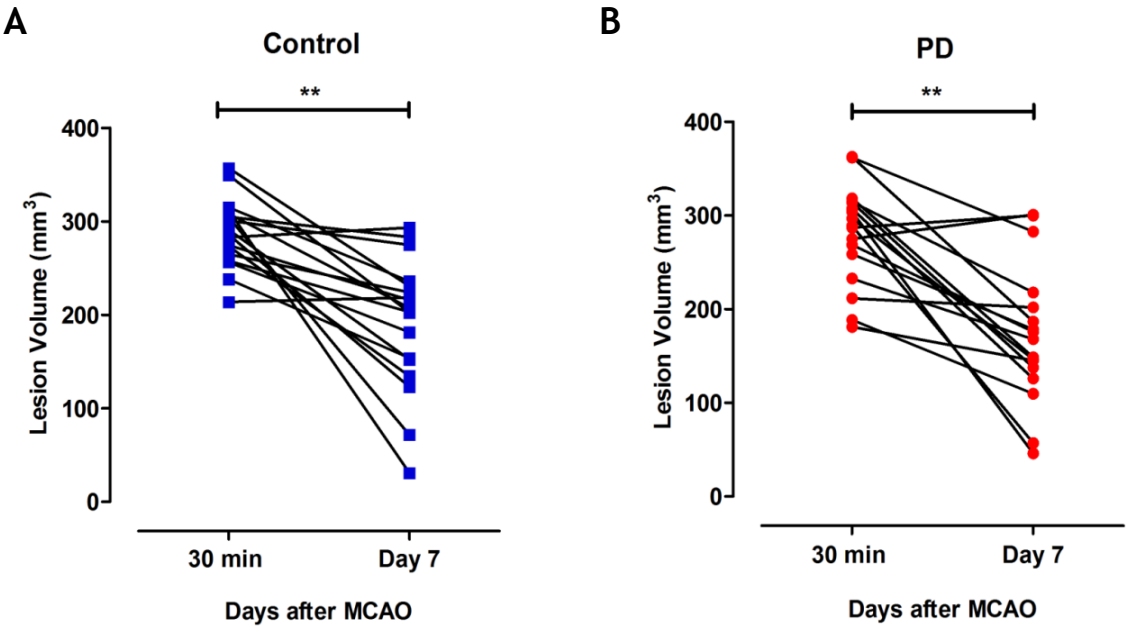

Figure 5.9 Evolution of lesion volume from 30 min of MCAO to day 7 in Control (**A**) and PD group (**B**). Reperfusion induced significant tissue salvage in both control and PD rats (paired Student's t-test, **P<0.0001, n=17-18). Data points indicate individual rat.

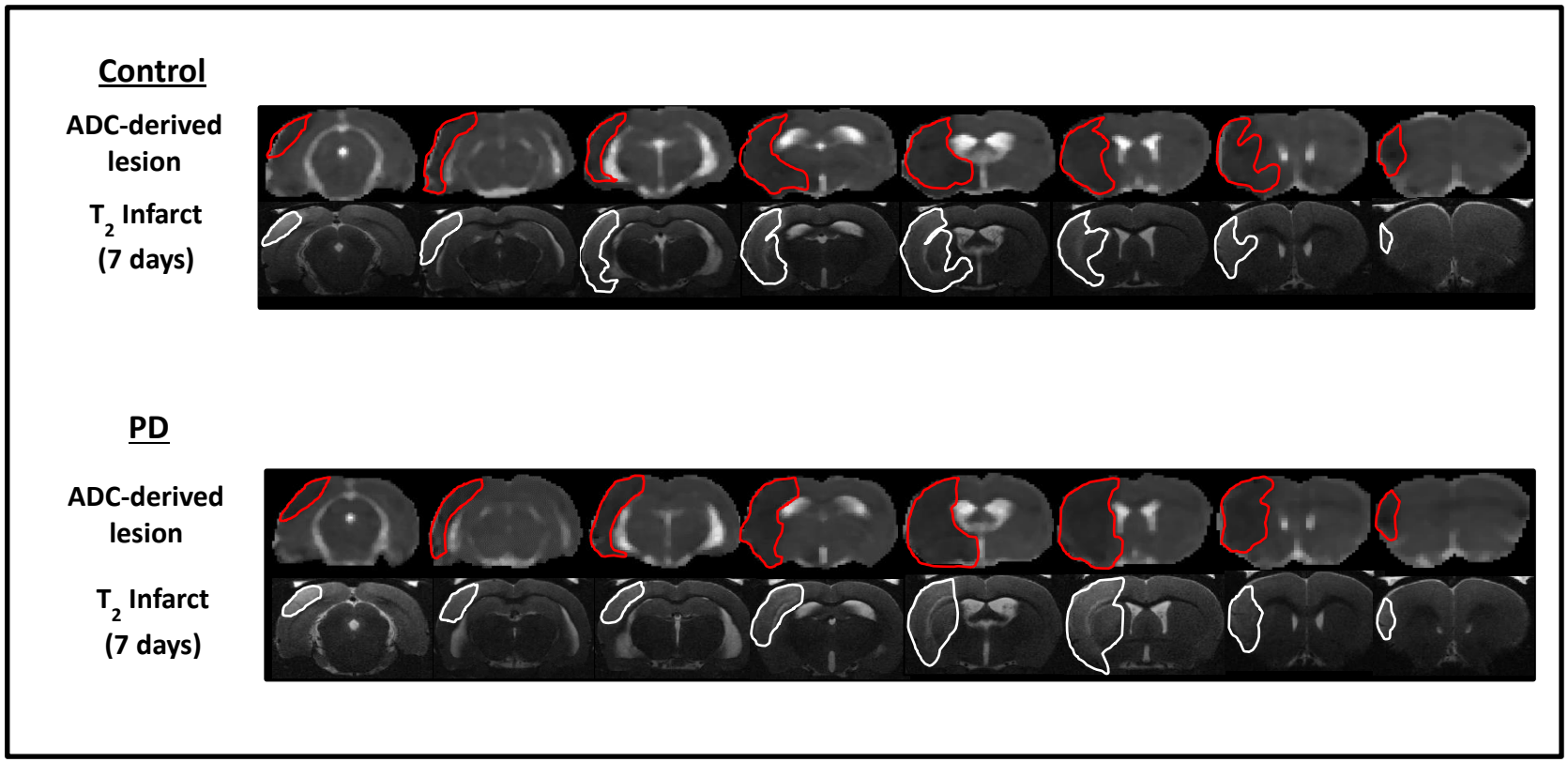

Figure 5.10 Caudal to rostral distribution of ADC-derived lesion and 8 coronal slices of final T_2 infarct from the same animal (median rat). The region highlighted in red depicts the ADC-derived lesion at 25 min post MCAO, and area highlighted in white indicates the infarct at 7 days.

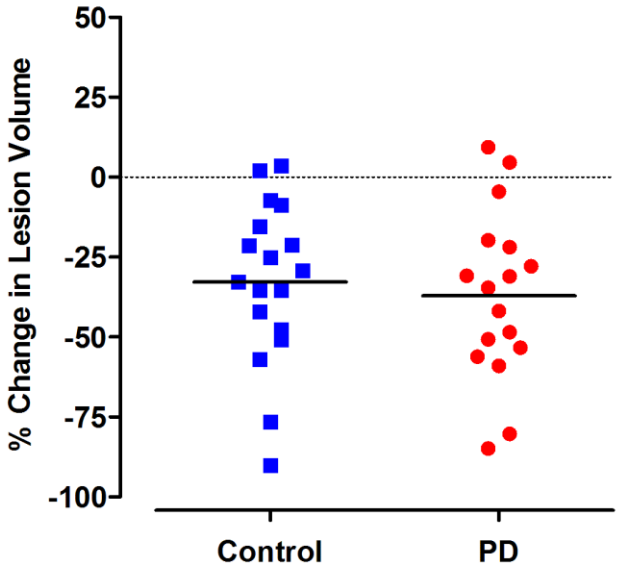

Figure 5.11 % change in lesion volume from 30 min to day 7 after MCAO; unpaired Student's t-test, P=0.64, n=17-18. Data points indicate individual rat and the horizontal bar represents the mean.

5.3.2.4 Neurological Score

Functional outcome at day 7 post MCAO was assessed by an 18-point neurological score. Prior to surgery, all animals demonstrated maximum scoring of 18 which indicates no obvious neurological deficits. Neurological score was significantly reduced on day 3 for both experimental groups which is expected at this time point due to a combination of rats being unwell at this acute time point and the neurological deficit. Neurological deficits improved from day 3 to day 7 however it was still significantly reduced compared to baseline. Repeated measures one-way ANOVA revealed a significant effect of day on score ($P<0.0001$, Figure 5.12A). Post-test comparisons using the Dunnet test indicated that neurological score was significantly reduced at day 3 post MCAO compared to the pre-stroke (day 0) in both groups (Control and PD; $P<0.0001$). The score at day 7 was higher than the initial deficit on day 3, thereby indicating a degree of recovery. However, the improvement in neurological score between control and PD groups assessed at day 7 was not statistically significant (Control vs PD: median score=14 vs 14, $P=0.65$, Mann-Whitney test). Using the non-parametric Spearman's correlation, an r^2 value of -0.33 demonstrates that there is an inverse weak relationship between infarct volume and neurological score, whereby as infarct volume decreases, neurological score increases. The correlation between infarct volume and neurological score at day 7 was however, not significantly correlated with final infarct volume measured at the same time point ($P>0.05$, Figure 5.12B).

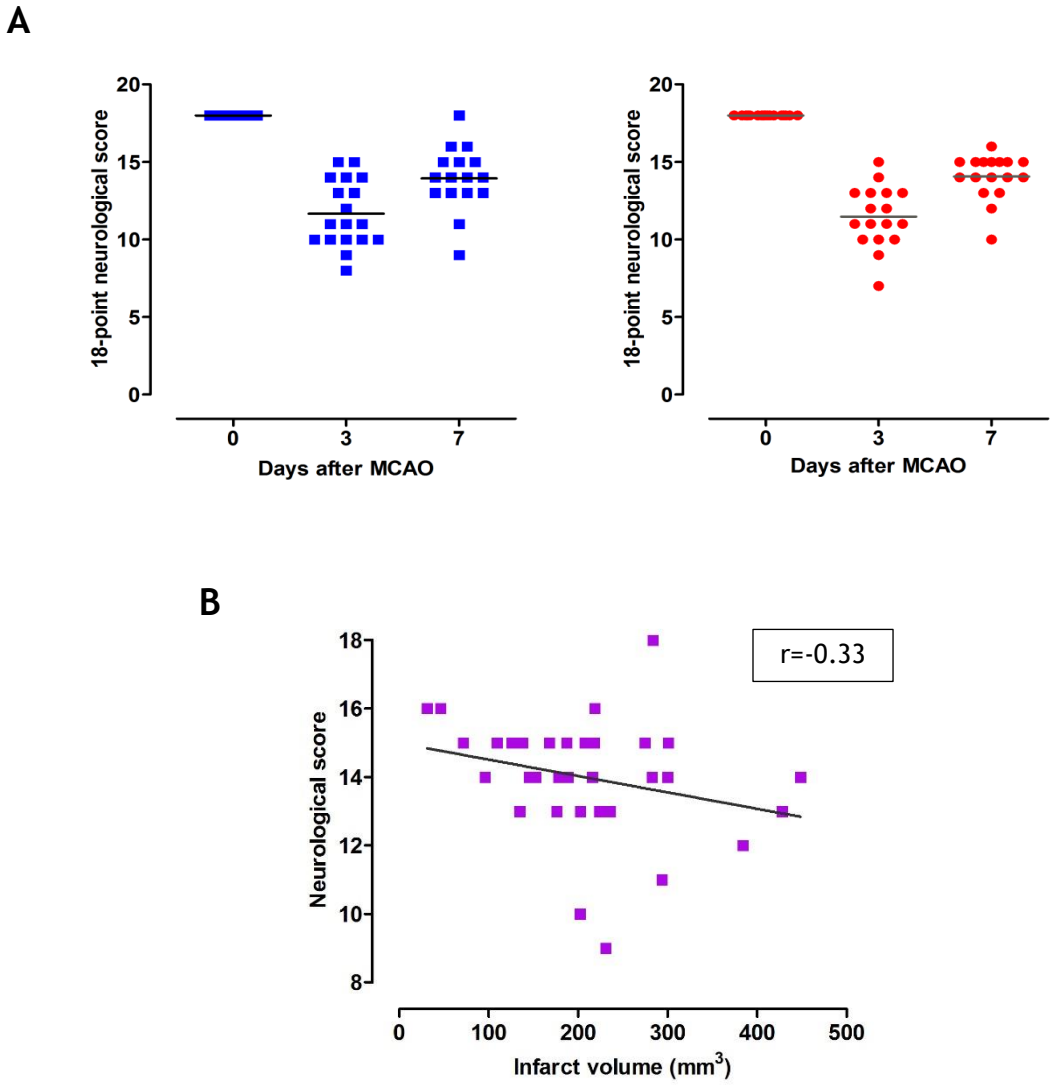

Figure 5.12 Assessment of functional outcome using 18-point neurological scoring system. (A) Rats were assessed at pre-stroke (day 0), day 3, and day 7 post MCAO. A score of 3 indicates severe neurological impairment and maximum score of 18 indicates no observable deficit. Data points indicate individual rat and the horizontal line denotes the median score. The neurological score between groups at day 7 was not statistically significant (Mann-Whitney test, P=0.65, n=17-18). (B) An inverse weak correlation was found between final infarct volume at 7 days post-MCAO and neurological score at the same time point for all rats. The correlation was not statistically significant. Spearman's non-parametric correlation, r=-0.33, P>0.05, n=35.

5.3.2.5 Adhesive Label Test

Transient MCAO for 30 min resulted in a significant increase in both time to contact and to remove when assessed at day 7 post MCAO. Both control and PD rats exhibited a significant increase in the time to contact at day 7 post MCAO compared to their pre-stroke performance (Control: 88.33±47.35s vs -1.32±12.43s, PD: 79.78±44.13s vs -2.15±11.7s, paired Student's t-test, $P<0.0001$). Similarly, removal time for both groups at day 7 rats was severely affected (Control: 85.23±43.92s vs 3.29±17.37s, PD: 81.12±48.68s vs -2.46±11.97, Student's paired t-test, $P<0.0001$). This observation indicates a bias for contacting and removing stimuli from the unaffected paw that persisted for 7 days in both groups (Figure 5.13). Using unpaired Student's t-test, the difference in contacting and removal time for both groups at day 7 were not statistically significant (difference in contact time: Control vs PD, $P=0.58$, difference in removal time: Control vs PD, $P= 0.79$).

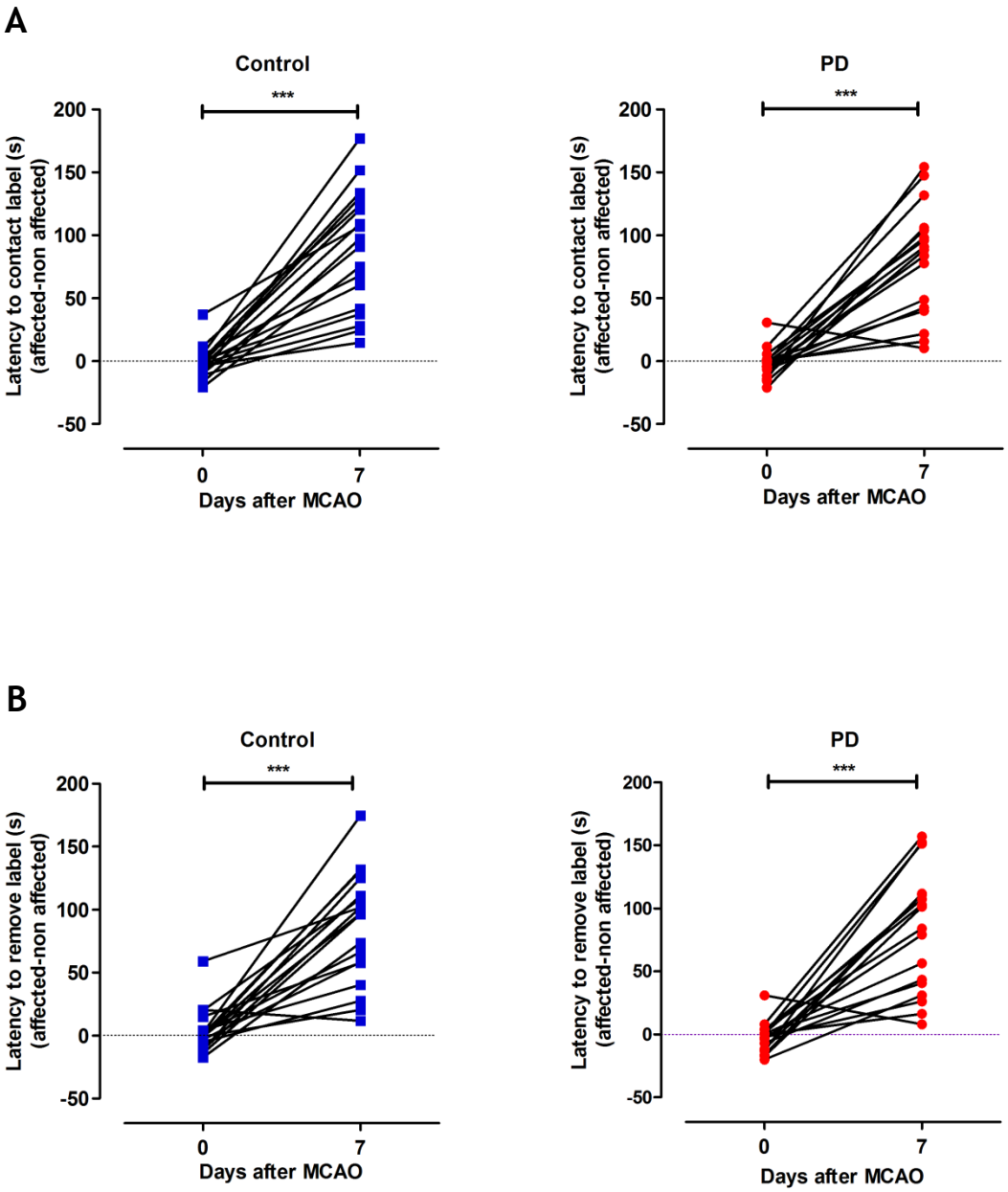

Figure 5.13 Contact and removal difference times at baseline and at 7 days post MCAO. The mean contact and removal difference time was significantly increased at 7 post MCAO compared to day 0 (pre-stroke) in both groups (Student's paired t-test, ***P<0.0001, n=17-18). The mean difference contact and removal times at day 7 is highly variable, with some animals showed a degree of recovery (A and B). The dotted horizontal line indicates zero, which denotes symmetrical limb contact (and removal) latencies. Data points indicated individual rats. 5.3.3 The impact of PD on Microglia Activation (Study 2).

5.3.3.1 Activity Monitoring

Photoperiod Disruption Results in Disruption in Locomotor Activity and Rhythmicity in PD Rats

In this study, the locomotor activity was monitored in rats exposed to PD protocol only. The total number of animal in PD group was 6 and were grouped housed (n=3/cages). Therefore, only two sets of locomotor activity data were collected at the end of the 9-week PD protocol. Due to the limited nature of the activity data obtained from this study, quantitative analysis was not performed and a double plotted actogram from a representative rat is shown of illustrative purposes only (Figure 5.14).

5.3.3.2 The Expression of Microglial Marker in naïve and PD rats

Both naive and PD rats demonstrated Iba-1 immunopositivity. Representative slides from both groups show microglia with typical morphology stained with the Iba-1 antibody (Figure 5.15A and 5.15B). Iba-1 immunostaining was not observed in the negative control slide (no primary antibody; Figure 5.15C). Figure 5.15D represents the % of Iba-1 immunopositivity in one ROI, and the mean % of ROI in individual animals are presented in Figure 5.15E. Unpaired t-test revealed no significant effect of PD on the % of Iba-1 immunopositivity (naïve: 4.8±1.3; PD: 4.7±1.6, Student's unpaired t-test, P= 0.63, Figure 5.15D). Similarly, there was no different between naïve and PD groups in the mean of % ROI in individual animals (naïve: 4.8±0.8, PD: 4.7±0.5, Student's unpaired t-test P=0.842, Figure 5.15E).

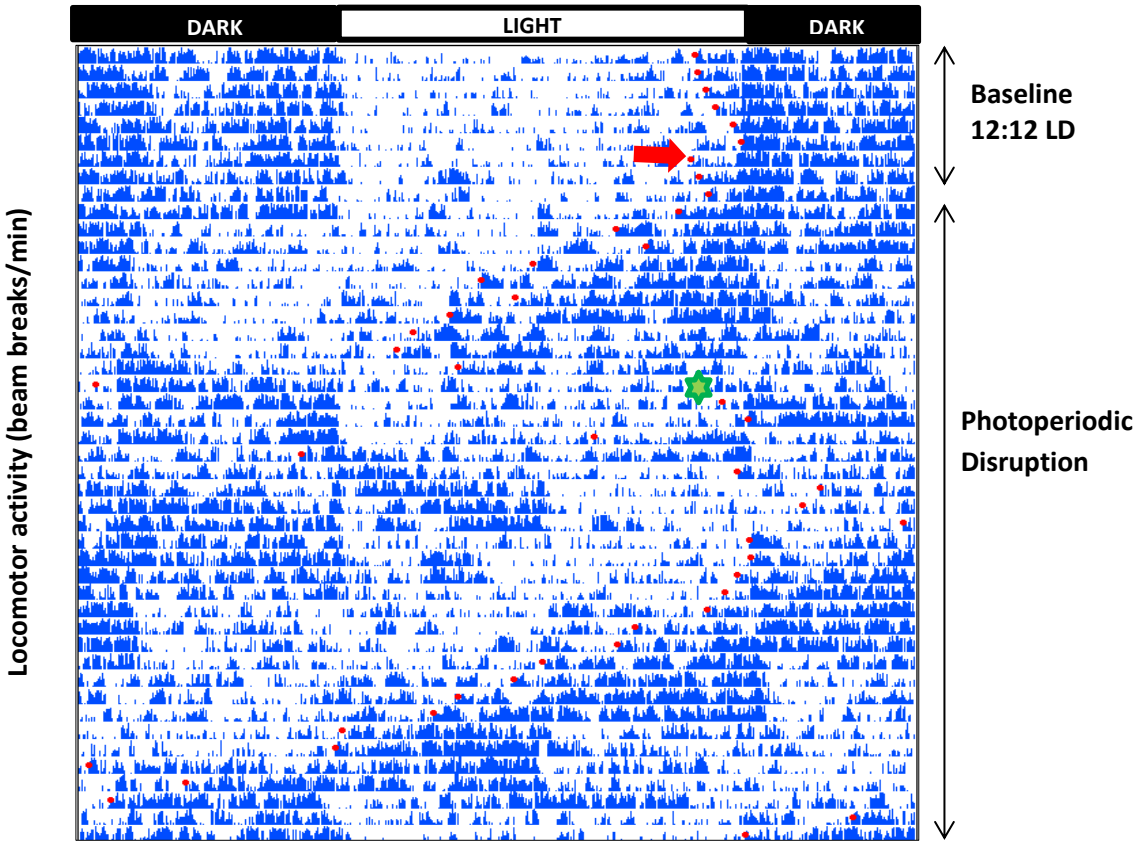

Figure 5.14 Double-plotted actogram from representative animal displayed the typical circadian rhythm in locomotor activity at baseline (high activity during the dark phase and low activity in the light phase), that was disrupted in the PD period. Each line represents the days of recording and blue shading representing the locomotor activity. Values on the x-axis denotes the time of the day. Red dots represent the onset of locomotor activity. Dark and clear bars indicate the dark and light phase respectively. Arrow and star indicate the onset of the phase advance protocol and the day animals reached re-entrainment to the new LD cycle, respectively.

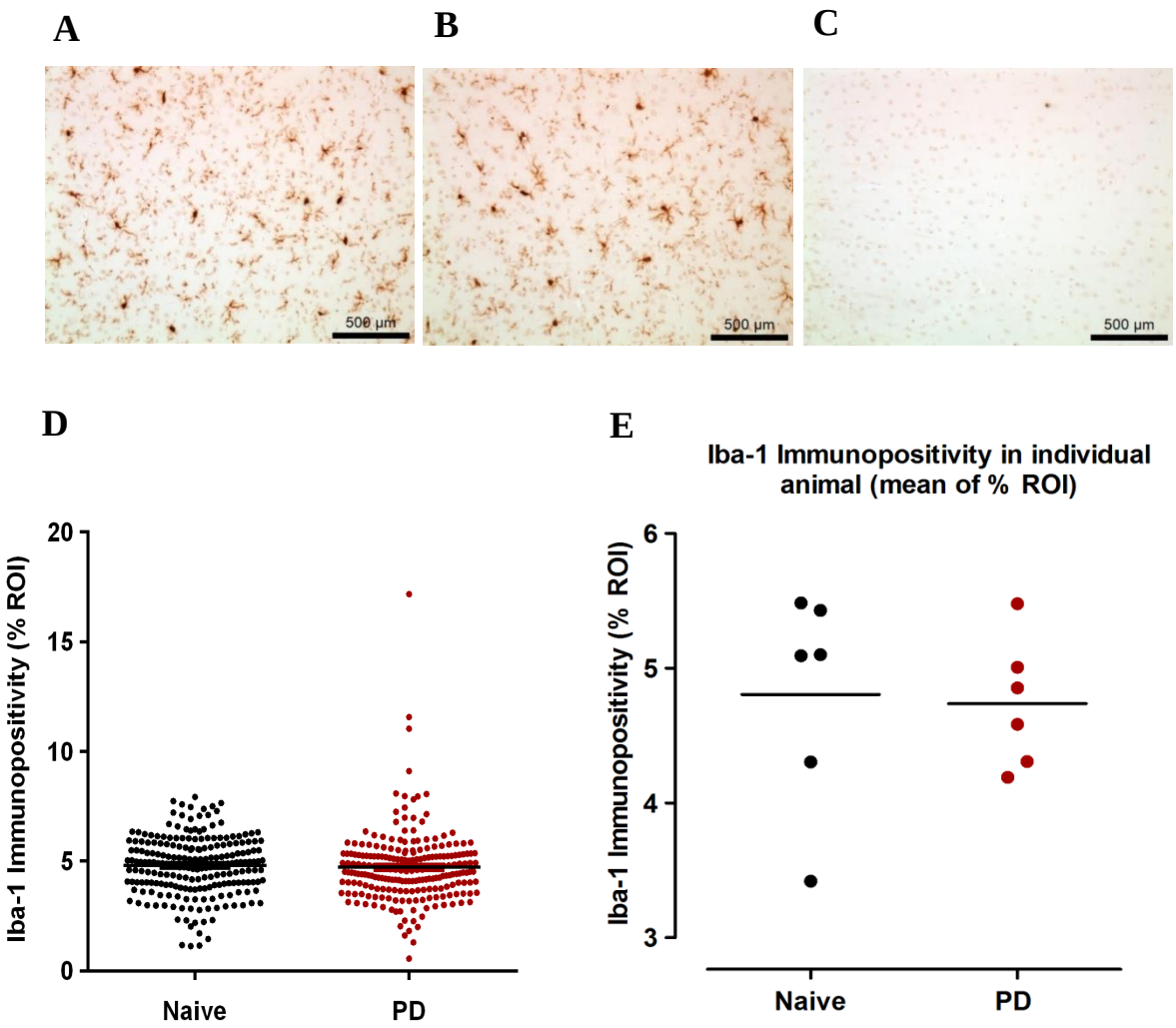

Figure 5.15 Iba-1 immunopositivity in naive and PD group. (A) and (B) Iba-1 immunopositivity was observed in both Naive and PD group. The thickness of each brain slice was 5µm. (C) No Iba-1 immunopositivity observed in negative control slide. (D) Each data point indicates percentage of Iba-1 immunopositivity in one ROI which shows comparable results; Student's unpaired t-test, P= 0.63. (E) Mean of % ROI as expressed in individual animal was also not significantly different between groups; Student's unpaired t-test, P=0.842, n=6.

5.4 Discussion

Circadian disruption is associated with metabolic and physiological changes such as diabetes and hypertension that have potential to adversely modify the ischaemic penumbra, hence increased sensitivity to stroke. Impact of circadian disruption on cardiovascular functions and tolerance to injury raised the possibility of associated cerebrovascular pathology. In the present study, we aimed to determine the impact of PD in the presence of pre-existing hypertension. Transient ischaemia was chosen as this model allows us to study the impact of PD on ischaemic injury following ischaemia-reperfusion as well as on lesion evolution.

5.4.1 PD Did Not Influence Lesion Evolution Following Focal Cerebral Ischaemia (Study 1)

The data shown that PD had no effect on lesion evolution in hypertensive rats. In the present study, we determined the acute lesion volume during MCAO (immediately prior to reperfusion) in both experimental groups and then in the same rats measured the final infarct volume at day 7 following reperfusions. This allowed us to calculate the extent of tissue salvage induced by reperfusion and therefore assess whether PD influences the ability of reperfusion to recover brain tissue. We demonstrated that in SHR rats exposed to normal light/dark cycle, reperfusion when initiated 30 minutes following MCAO resulted in a reduction in lesion volume of 33%. This confirms that early reperfusion in the presence of hypertension can salvage brain tissue. The presence of hypertension has been previously shown to exacerbate damage following cerebral ischaemia (D Duverger and MacKenzie, 1988). In SHR that underwent 9-week phase advance to induce circadian disruption we demonstrated that reperfusion at 30 minutes resulted in a similar extent of tissue salvage; 37% compared to the control. Similarly, no differences in final infarct volume were observed between the two groups.

This is in contrast to a recently published study by Earnest and colleagues (Earnest *et al.*, 2016), which demonstrated that PD significantly enhanced the severity of focal cerebral ischaemia in Sprague-Dawley rats. With regards to our

study, MCA was transiently occluded by intraluminal filament. Vessel occlusion was confirmed by an acute MR angiography scan and reperfusion was established at an earlier time point (30 min). In the study by Earnest et al., transient focal ischaemia was achieved via injection of a vasoconstrictor peptide, endothelin-1 (ET-1) onto the MCA in which rats were also subjected to a stereotaxic surgery. Moreover, no specific measurement was taken by Earnest and colleagues to confirm the exact time of reperfusion. Endothelin-1 is known to induce severe, sustained, but ultimately reversible occlusion of cerebral vessels *in vivo* (Macrae *et al.*, 1993). In view of this, the methods of inducing transient MCAO as well as the nature of reperfusion (gradual versus rapid), may account for the discrepancies of results between the two studies.

Pre-existing hypertension is one of the important factors that influence the rate of lesion growth (McCabe *et al.*, 2009), hence increasing stroke severity. In this case, increased vascular resistance secondary to arterial remodelling and hypertrophy, impair cerebral vasodilation such that compensatory mechanism to ischaemic insult is compromised. Moreover, extensive evidence implicates inflammation in stroke susceptibility and poor outcome (Murray *et al.*, 2014). Stroke-sensitive rat strains such as the SHR and SHRSP have previously been shown to display an elevated response to inflammatory stimuli (Sirén *et al.*, 1992). Our study was carried out in a highly pertinent stroke model, spontaneously hypertensive rats. It is apparent that hypertension may exacerbate the infarct volume (Hom *et al.*, 2007; Möller *et al.*, 2015). Consequently, adding another damaging factor such as circadian disruption may increase the possibility of 'ceiling effect' such that damage is already elevated at baseline. Therefore, an increase resulting from additional pathophysiology will be arduous to be noticed.

Lack of effect of PD may suggest that SHRs might have a level of resistance towards the phase advance protocol. The circadian system in the SHR has been characterised in a study by (Sládek *et al.*, 2012). According to their study, the analysis of the SHR circadian clock at molecular level revealed that the clock genes expression from central clock SCN was phase advanced relative to 12:12 LD cycle, which means that SHRs exhibited a phase advance rhythm compared to that of a normotensive strain Wistar rats. For instance, under

normal 12:12 LD cycle, SHR exhibited an early onset of locomotor activity, which started just before the light went off. Moreover, the output rhythm from the SCN in SHR was dampened that leads to impaired peripheral clock genes expression in the liver and heart (Cui *et al.*, 2011). These observations also suggest that deficiencies in circadian timing are responsible for metabolic and cardiovascular phenotype in SHRs. Therefore, lesser impact of PD on SHRs might be due to pre-existing 'disrupted' rhythm.

No significant differences in neurological score were seen between the control and PD groups at day 7 post MCAO. This suggests that PD does not worsen neurological scores in this study. This data was in agreement with infarct volume at day 7 in PD group which was comparable with the control group. Even though the correlation was not significant, the inverse correlation between neurological score and infarct volume shows that neurological function is improved in rats with smaller infarct volumes, as compared to rats with larger infarcts which are more severely functionally impaired. The extent of forelimb asymmetry evaluated by adhesive label test was also not affected by PD.

5.4.2 PD Has No Impact on Microglial Activation in Non-Stroke SHR Brains (Study 2)

Our data demonstrated that PD for 9 weeks did not alter activated microglial numbers in the brain. To date, no studies have investigated the impact of photoperiod disruption protocol on microglia response in the rat brain. However, there are several other studies employing different experimental shift work models which have linked circadian disruption with immune system alterations. Forced shift work in Wistar rats leads to enhanced TNF-α and IL-6 production by hepatic Kuppfer cells after LPS stimulation in comparison to control rats (Guerrero-Vargas *et al.*, 2015). Additionally, mice exposed to circadian desynchronization by experimental jet-lag resulted in uncoordinated inflammatory responses to LPS challenge that led to increased mortality. Dysregulation of immune system was evident by upregulation of several key immune factors in serum of shifted mice, including IL-6, IL-1β, IL-12, IL-13 and decreased in anti-inflammatory mediator IL-10 (Castanon-Cervantes *et al.*, 2010).

The impact of circadian disruption on microglia response has previously been documented in a mouse model using a dim light at night (5 lux) protocol. This study demonstrated an enhanced expression of microglial markers Iba-1 in the arcuate nucleus after chronic exposure to dim light at night (Wyse et al., 2016). This finding is in agreement with other study utilizing similar dim light paradigm, indicating enhanced microglial cytokines gene expression after LPS challenge (Fonken *et al.*, 2013).

There are a number of experimental factors that could explain the discrepancies between our results and findings from the previous study in mouse that have demonstrated increased microglia (Fonken *et al.*, 2013). One potential explanation is related to differences in the protocols used to induce circadian disruption where the mouse studies have used a model of dim light at night whereas we used a phase advance protocol. As discussed in detail in chapter 4, the differences in the protocols used could partly account for the heterogeneity of the study results. Apart from light/dark protocols, another difference was the light intensity in which 5lux of night time light exposure was used in the mouse studies, compared with 150lux in the present study. Indeed, the intensity of the light signal has been shown to have different consequences on circadian rhythm. Dose dependent stimulatory effect of light has been elicited in another study such that subjects exposed to higher light intensity (800 lux) developed larger increase in heart rate (Scheer *et al.*, 1999). Additionally, higher mean blood glucose level was observed in diabetic prone rats exposed to constant darkness protocol as compared to 6-hour phase advance protocol for 10 weeks (Gale *et al.*, 2011).

It is also evident that microglia activation was enhanced only after an episode of immune challenge (i.e. intraperitoneal injection with LPS). Fonken and colleagues found that there was no difference in microglia cytokine expression in mice exposed to dim light at night and control mice which did not receive immune challenge (Fonken *et al.*, 2013). This finding suggests an important interaction between immune challenge and circadian disruption in which the impact of circadian disruption is apparent in the presence of inflammatory challenge (i.e. LPS). Master circadian clock in SCN conveys timing

information to the immune system and coordinate immune function via anticipatory state for optimal immune response (Buijs *et al.*, 2008). Following circadian disruption, the critical state of anticipation and readiness to immune challenge is impaired, therefore in this case has increased vulnerability and severity to infection (Logan and Sarkar, 2012).

5.4.3 Summary

We demonstrated that stroke outcome was not exacerbated in SHR's that had undergone photoperiod disruption when compared to SHR's maintained under normal light/dark cycles. Similarly, PD did not induce any significant changes in microglia activation in the brains of SHR's. Poor collaterals and pre-existing hypertension in SHR may explained to lesser effect of PD on lesion evolution, as there may have been less penumbral tissue available for PD to exert its detrimental effect. Even though PD rats exhibited significant disruption in behavioural rhythm, it was unclear if circadian desynchrony was established with this protocol. It is suggested for future study to include gene expression profile and circadian biomarker. Moreover, early chronotype in SHR might account for the lack of effect of PD on this strain due to pre-existing disrupted rhythm. It was therefore concluded that PD in context of major stroke co-morbidity/risk factor does not exacerbate ischaemic damage and that this fits with the lack of effect of PD on microglial activation.

Chapter 6-General Discussion

6.1 Introduction

Over the past 20 years, large epidemiological studies associate shift work with the development of a major stroke risk factors such as hypertension, diabetes and obesity (Karlsson, 2001; Morikawa *et al.*, 2005). The mechanism underlying the impact shift work on health has been attributed to desynchronization between external changes in the environmental with the internal circadian system (Rüger and Scheer, 2009). Stroke risk factors associated with PD such as hypertension and hyperglycaemia have been shown to increase sensitivity to stroke in human and animal studies (McCabe *et al.*, 2009; Muir *et al.*, 2011; Tarr *et al.*, 2013) . However, little is known about the impact of PD on sensitivity to stroke and stroke outcome.

Studies performed in this thesis presented one of the most relevant models that are being used to mimic human shift work; by shifting the light/dark cycle (Opperhuizen et al. 2015). However, the result in this thesis demonstrates that PD did not increase stroke sensitivity in young, normotensive animals and did not interact with major stroke risk factor; hypertension to impact on lesion evolution following focal cerebral ischaemia. The findings from this thesis will be discussed in terms of study limitations and some of the future strategies with regards to animal models of shift work.

6.2 Study Limitations

One of the primary aims in this thesis is to determine the impact of disruption in the light/dark cycle on stroke outcome. In this study, photoperiod disruption was induced by 6-hour phase advance the light input every 3 days. A limitation of this approach is that it does not model all of the features of human shift work. Since the working schedules profoundly interfere with activity, sleep, timing of food and feeding pattern, available animal studies have been focused on the four most relevant models that are being used to mimic human shift work: altered timing of (1) food intake, (2) activity, (3) sleep, or (4) light exposure. These daily rhythms are strongly interconnected such that disturbance of one aspect impacts on the others (Opperhuizen *et al.*, 2015).

Photoperiod disruption protocol as employed in this thesis, is only one aspect of modelling shift work in animal studies and may not truly represents human shift work. The predominant theory underlying health consequences of shift work stresses on the concept of desynchronization which can occur at different levels; from changes in behaviour (activity, feeding and sleep pattern) to altered gene expression and hormone secretion (Salgado-Delgado *et al.*, 2013). One potential caveat concerning the present experiment is that no measure of circadian desynchronization was provided or assessed in the PD and control rats. Despite changes in locomotor activity pattern following PD protocol, it is yet to be determined if PD has resulted in desynchronization at organ and molecular level. Therefore, it is suggested in the future study to confirm that circadian desynchronization is manifested by PD protocol by assessing the metabolic gene expression at peripheral organs, disruption in physiological rhythms of blood glucose, blood pressure, body temperature and circadian biomarkers. In addition, these additional parameters will allow us to draw comparisons with regards to outcome measures with different types of manipulations used in shift work studies.

Despite the known primary event leading to stroke that is the disruption in cerebral blood flow, pre-clinical stroke research is still struggling with translational issues (Dirnagl *et al.*, 2013). To date, the exact mechanisms underpinning cardiometabolic disturbances among shift workers are poorly understood (Vyas *et al.*, 2012) making modelling shift work in animals a very challenging exercise. It is reasonable to postulate that shifting the light/dark cycle may not be the primary event leading to cardiometabolic disturbance among shift workers. Experimental studies employing feeding at rest phase in rodents appears to have more detrimental effect on metabolism (Ribas-Latre and Eckel-Mahan, 2016). In this case, food acts as a ‘stronger’ *zeitgeber* for peripheral clock (Damiola, 2000) and several studies supported the ideas that timing of food intake have an important impact on metabolism (Arble et al. 2009)(Garaulet *et al.*, 2013)(Hibi *et al.*, 2013). Moreover, shifting the time of food intake is of relevance to human shift work as changed dietary habits is one of the characteristics in shift workers (Lowden *et al.*, 2010).

6.3 Future Strategies for Animal Shift Work Studies

To date, there are no standardised protocols established for modelling shift work in animals. The difference in the protocols across laboratories may partly account for the heterogeneity of the results (Gale et al, 2011)(Tsai *et al.*, 2005). A review on animal models of shift work have identified various protocols with none of the protocols being replicated by other research groups. Furthermore, there appears to be no standardized procedures for assessing circadian parameters such as clock gene expression in peripheral organs, activity rhythm, hormones, body temperature, sleep disturbances and metabolic parameters making it difficult to compare results between models (Opperhuizen *et al., 2015)*. The inconsistencies of pre-clinical data concerning shift work will compromise the strength and quality of the studies and therefore they need of critical re-evaluation. The pre-clinical groups working on shift work studies should therefore work within networks and agree on standardize protocols for inducing circadian disruption in animal models, and come up with recommended guidelines in order to improve quality and reproducibility of animal model of shift work. Standardization would reduce the heterogeneity between studies for both methods and outcome parameters and provide high quality study to inform the process of translation.

Using animal models by manipulating only one aspect of shift work allowed us to focus on studying the impact of one particular aspect of shift work (i.e. shifting the light) on health. However, given the complexity and interconnection of all aspects of human shift work, future studies in animal models could address some of these issues by incorporating more than one aspects of human shift work. For instance, a protocol employing shifting the light/dark cycle and restricted feeding during active phase provide more accurate representation of the human shift work (Arble *et al.,* 2010). In principle, using diurnal rodent models (i.e. the Nile rat) would be a clinically relevant model to study shift work, as day-active animals are more similar to human and therefore of better choice when it comes to circadian studies (Opperhuizen *et al.,* 2015). Future research should also include more animal studies incorporating the effects of interventions to alleviate the negative impact of shift work. For example, feeding during the rest phase has been shown

to induce obesity and internal desynchrony in a rat model of night work which was restored by restricting food intake to activity phase in the same model (Salgado-Delgado *et al.*, 2010). Data on the impact of interventions could be useful for proposing new occupational health and safety guidelines to counter health risks among shift workers.

6.4 Conclusion

Population-based studies on detrimental effect of shift work are mainly associational and the pathophysiology underlying this association is poorly understood. The primary aim of the available animal models of shift work is to uncover the links between circadian disruption and cardiometabolic diseases. Due to complexity of human shift work, mimicking all aspect of human shift work in one animal model is a key challenge in this area. The findings reported in this thesis demonstrated that PD does not exacerbate ischaemic damage by increasing the severity of the ischaemic insult in both normotensive and hypertensive animals. The results further suggest that shifting the light/dark cycle may not be the primary event leading to cardiometabolic disturbances. Future experimental shift work studies should incorporate standardized guidelines and protocols in the study design and use animal models that better mirror human shift work population.

List of References

Adibhatla, R. M. and Hatcher, J. F. (2010) 'Lipid oxidation and peroxidation in CNS health and disease: from molecular mechanisms to therapeutic opportunities.', *Antioxidants & redox signaling*, 12(1), pp. 125–169. doi: 10.1089/ars.2009.2668.

Alibhai, F. J., Tsimakouridze, E. V., Chinnappareddy, N., Wright, D. C., Billia, F., O'Sullivan, M. L., Pyle, W. G., Sole, M. J. and Martino, T. A. (2014) 'Short-Term Disruption of Diurnal Rhythms After Murine Myocardial Infarction Adversely Affects Long-Term Myocardial Structure and Function', *Circulation Research*, 114(11), pp. 1713–1722. doi: 10.1161/CIRCRESAHA.114.302995.

Allaman-Pillet, N., Roduit, R., Oberson, A., Abdelli, S., Ruiz, J., Beckmann, J. S., Schorderet, D. F. and Bonny, C. (2004) 'Circadian regulation of islet genes involved in insulin production and secretion', *Molecular and Cellular Endocrinology*, 226(1–2), pp. 59–66. doi: 10.1016/j.mce.2004.06.001.

Allen, C. L. and Bayraktutan, U. (2008) 'Risk factors for ischaemic stroke.', *International journal of stroke : official journal of the International Stroke Society*, 3(2), pp. 105–16. doi: 10.1111/j.1747-4949.2008.00187.x.

Amenta, F., Di Tullio, M. A. and Tomassoni, D. (2003) 'Arterial hypertension and brain damage--evidence from animal models (review).', *Clinical and experimental hypertension (New York, N.Y. : 1993)*, 25(6), pp. 359–80. doi: doi:10.1081/CEH-120023545.

Andersen, K. K., Olsen, T. S., Dehlendorff, C. and Kammersgaard, L. P. (2009) 'Hemorrhagic and Ischemic Strokes Compared', *Stroke*, 40(6).

Anea, C. B., Zhang, M., Stepp, D. W., Simkins, G. B., Reed, G., Fulton, D. J. and Rudic, R. D. (2009) 'Vascular disease in mice with a dysfunctional circadian clock.', *Circulation*, 119(11), pp. 1510–7. doi: 10.1161/CIRCULATIONAHA.108.827477.

Ankarcrona, M., Dypbukt, J. M., Bonfoco, E., Zhivotovsky, B., Orrenius, S., Lipton, S. A. and Nicotera, P. (1995) 'Glutamate-induced neuronal death: A succession of necrosis or apoptosis depending on mitochondrial function', *Neuron*, 15(4), pp. 961–973. doi: 10.1016/0896-6273(95)90186-8.

Arble, D. M., Bass, J., Laposky, A. D., Vitaterna, M. H. and Turek, F. W. (2009) 'Circadian Timing of Food Intake Contributes to Weight Gain', *Obesity*, 17(11), pp. 2100–2102. doi: 10.1038/oby.2009.264.

Arble, D. M. D., Ramsey, K. K. M., Bass, J. and Turek, F. F. W. (2010) 'Circadian disruption and metabolic disease: Findings from animal models', *Best Practice & Research Clinical Endocrinology & Metabolism*, 24(5), pp. 785–800. doi: 10.1016/j.beem.2010.08.003.

Arboix, A. and Alió, J. (2010) 'Cardioembolic Stroke: Clinical Features, Specific Cardiac Disorders and Prognosis', *Current Cardiology Reviews*, 6, pp. 150–161. doi: 10.2174/157340310791658730.

Aspey, B. S., Taylor, F. L., Terruli, M. and Harrison, M. J. G. (2000) 'Temporary middle cerebral artery occlusion in the rat: consistent protocol for a model of stroke and reperfusion', *Neuropathology and Applied Neurobiology*. Blackwell Science Ltd, 26(3), pp. 232–242. doi: 10.1046/j.1365-2990.2000.00221.x.

Baird, T. A., Parsons, M. W., Barber, P. A., Butcher, K. S., Desmond, P. M., Tress, B. M., Colman, P. G., Jerums, G., Chambers, B. R. and Davis, S. M. (2002) 'The influence of diabetes mellitus and hyperglycaemia on stroke incidence and outcome.', *Journal of clinical neuroscience : official journal of the Neurosurgical Society of Australasia*, 9(6), pp. 618–626. doi: 10.1054/jocn.2002.1081.

Baird, T. A., Parsons, M. W., Phanh, T., Butcher, K. S., Desmond, P. M., Tress, B. M., Colman, P. G., Chambers, B. R. and Davis, S. M. (2003) 'Persistent poststroke hyperglycemia is independently associated with infarct expansion and worse clinical outcome', *Stroke*, 34(9), pp. 2208–2214. doi: 10.1161/01.STR.0000085087.41330.FF.

Bartol-Munier, I., Gourmelen, S., Pevet, P. and Challet, E. (2006) 'Combined effects of high-fat feeding and circadian desynchronization.', *International journal of obesity (2005)*. Nature Publishing Group, 30(1), pp. 60–7. doi: 10.1038/sj.ijo.0803048.

Bass, J. and Takahashi, J. S. (2010) 'Circadian integration of metabolism and energetics.', *Science (New York, N.Y.)*, 330(6009), pp. 1349–54. doi: 10.1126/science.1195027.

Beevers, G., Lip, G. Y. and O'Brien, E. (2001) 'ABC of hypertension: The pathophysiology of hypertension.', *BMJ (Clinical research ed.)*. BMJ Group, 322(7291), pp. 912–6.

Belayev, L., Alonso, O. F., Busto, R., Zhao, W. and Ginsberg, M. D. (1996) 'Middle Cerebral Artery Occlusion in the Rat by Intraluminal Suture', *Stroke*, 27(9).

Benakis, C., Garcia-Bonilla, L., Iadecola, C. and Anrather, J. (2014) 'The role of microglia and myeloid immune cells in acute cerebral ischemia.', *Frontiers in cellular neuroscience*. Frontiers, 8, p. 461. doi: 10.3389/fncel.2014.00461.

Biessels, G. J., van der Heide, L. P., Kamal, A., Bleys, R. L. A. . and Gispen, W. H. (2002) 'Ageing and diabetes: implications for brain function', *European Journal of Pharmacology*, 441(1–2), pp. 1–14. doi: 10.1016/S0014-2999(02)01486-3.

Biessels, G. J., Van der Heide, L. P., Kamal, A., Bleys, R. L. A. W. and Gispen, W. H. (2002) 'Ageing and diabetes: Implications for brain function', *European Journal of Pharmacology*, pp. 1–14. doi: 10.1016/S0014-2999(02)01486-3.

Bogousslavsky, J., Van Melle, G. and Regli, F. (1988) 'The Lausanne Stroke Registry: analysis of 1,000 consecutive patients with first stroke.', *Stroke*, 19(9).

Brennan, A. M., Won Suh, S., Joon Won, S., Narasimhan, P., Kauppinen, T. M., Lee, H., Edling, Y., Chan, P. H. and Swanson, R. A. (2009) 'NADPH oxidase is the primary source of superoxide induced by NMDA receptor activation', *Nature Neuroscience*. Nature Publishing Group, 12(7), pp. 857–863. doi: 10.1038/nn.2334.

Browning, J. L., Heizer, M. L., Widmayer, M. A. and Baskin, D. S. (1997) 'Effects of halothane, alpha-chloralose, and pCO2 on injury volume and CSF beta-endorphin levels in focal cerebral ischemia', *Molecular & Chemical Neuropathology*, 31(1), pp. 29–42.

Buijs, F. N., Cazarez, F., Basualdo, M. C., Scheer, F. A. J. L., Perusqu??a, M., Centurion, D. and Buijs, R. M. (2014) 'The suprachiasmatic nucleus is part of a neural feedback circuit adapting blood pressure response', *Neuroscience*, 266, pp. 197–207. doi: 10.1016/j.neuroscience.2014.02.018.

Buijs, R. M., La Fleur, S. E., Wortel, J., Van Heyningen, C., Zuiddam, L., Mettenleiter, T. C., Kalsbeek, A., Nagai, K. and Niijima, A. (2003) 'The suprachiasmatic nucleus balances sympathetic and parasympathetic output to peripheral organs through separate preautonomic neurons', *Journal of Comparative Neurology*. Wiley Subscription

Services, Inc., A Wiley Company, 464(1), pp. 36–48. doi: 10.1002/cne.10765.

Buijs, R. M. and Kalsbeek, A. (2001) 'Hypothalamic integration of central and peripheral clocks.', *Nature reviews. Neuroscience*, 2(7), pp. 521–526. doi: 10.1038/35081582.

Buijs, R. M., Van der Vliet, J., Garidou, M. L., Huitinga, I. and Escobar, C. (2008) 'Spleen vagal denervation inhibits the production of antibodies to circulating antigens', *PLoS ONE*, 3(9). doi: 10.1371/journal.pone.0003152.

Burrows, F., Haley, M. J., Scott, E., Coutts, G., Lawrence, C. B., Allan, S. M. and Schiessl, I. (2016) 'Systemic inflammation affects reperfusion following transient cerebral ischaemia.', *Experimental neurology*, 277, pp. 252–60. doi: 10.1016/j.expneurol.2016.01.013.

Carmichael, S. T. (2005) 'Rodent models of focal stroke: Size, mechanism, and purpose', *NeuroRX*. Springer-Verlag, 2(3), pp. 396–409. doi: 10.1602/neurorx.2.3.396.

Cascio, C. S., Shinsako, J. and Dallman, M. F. (1987) 'The suprachiasmatic nuclei stimulate evening ACTH secretion in the rat', *Brain Research*, 423(1–2), pp. 173–178. doi: 10.1016/0006-8993(87)90837-7.

Castanon-Cervantes, O., Wu, M., Ehlen, J. C., Paul, K., Gamble, K. L., Johnson, R. L., Besing, R. C., Menaker, M., Gewirtz, A. T. and Davidson, A. J. (2010) 'Dysregulation of inflammatory responses by chronic circadian disruption.', *Journal of immunology (Baltimore, Md. : 1950)*. American Association of Immunologists, 185(10), pp. 5796–805. doi: 10.4049/jimmunol.1001026.

Choi, D. W. and Rothman, S. M. (1990) 'The role of glutamate neurotoxicity in hypoxic-ischemic neuronal death.', *Annual review of neuroscience*, 13, pp. 171–182. doi: 10.1146/annurev.neuro.13.1.171.

Coyle, P. and Heistad, D. D. (1987) 'Blood flow through cerebral collateral vessels one month after middle cerebral artery occlusion', *Stroke*, 18(0039–2499 (Print)), pp. 407–411. doi: 10.1161/01.STR.18.2.407.

Coyle, P. and Jokelainen, P. T. (1983) 'Differential outcome to middle cerebral artery occlusion in spontaneously hypertensive stroke-prone rats (SHRSP) and Wistar Kyoto (WKY) rats', *Stroke*, 14(4), pp. 605–611. doi: 10.1161/01.STR.14.4.605.

Cui, H., Kohsaka, A., Waki, H., Bhuiyan, M. E. R., Gouraud, S. S. and Maeda, M. (2011) 'Metabolic cycles are linked to the cardiovascular diurnal rhythm in rats with essential hypertension', *PLoS ONE*, 6(2). doi: 10.1371/journal.pone.0017339.

Curtis, A. M., Cheng, Y., Kapoor, S., Reilly, D., Price, T. S. and Fitzgerald, G. A. (2007) 'Circadian variation of blood pressure and the vascular response to asynchronous stress', *Proceedings of the National Academy of Sciences of the United States of America*, 104(9), pp. 3450–3455. doi: 10.1073/pnas.0611680104.

Dahlöf, B. (2007) 'Prevention of stroke in patients with hypertension.', *The American journal of cardiology*, 100(3A), p. 17J–24J. doi: 10.1016/j.amjcard.2007.05.010.

Damiola, F. (2000a) 'Restricted feeding uncouples circadian oscillators in peripheral tissues from the central pacemaker in the suprachiasmatic nucleus', *Genes & Development*, 14(23), pp. 2950–2961. doi: 10.1101/gad.183500.

Damiola, F. (2000b) 'Restricted feeding uncouples circadian oscillators in peripheral tissues from the central pacemaker in the suprachiasmatic nucleus', *Genes & Development*, 14(23), pp. 2950–2961. doi: 10.1101/gad.183500.

Danaei, G., Singh, G. M., Paciorek, C. J., Lin, J. K., Cowan, M. J., Finucane, M. M.,

Farzadfar, F., Stevens, G. A., Riley, L. M., Lu, Y., Rao, M. and Ezzati, M. (2013) 'The Global Cardiovascular Risk Transition: Associations of Four Metabolic Risk Factors with National Income, Urbanization, and Western Diet in 1980 and 2008', *Circulation*. NIH Public Access, 127(14), pp. 1493–1502. doi: 10.1161/CIRCULATIONAHA.113.001470.

Dandona, P., Aljada, A. and Bandyopadhyay, A. (2004) 'Inflammation: The link between insulin resistance, obesity and diabetes', *Trends in Immunology*, pp. 4–7. doi: 10.1016/j.it.2003.10.013.

Davidson, A. J., Sellix, M. T., Daniel, J., Yamazaki, S., Menaker, M. and Block, G. D. (2006) 'Chronic jet-lag increases mortality in aged mice.', *Current biology : CB*, 16(21), pp. R914-6. doi: 10.1016/j.cub.2006.09.058.

Deibel, S. H., Hong, N. S., Himmler, S. M. and McDonald, R. J. (2014) 'The effects of chronic photoperiod shifting on the physiology of female Long-Evans rats', *Brain Research Bulletin*. Elsevier Inc., 103, pp. 72–81.

Dirnagl, U., Hakim, A., Macleod, M., Fisher, M., Howells, D., Alan, S. M., Steinberg, G., Planas, A., Boltze, J., Savitz, S., Iadecola, C. and Meairs, S. (2013) 'A concerted appeal for international cooperation in preclinical stroke research.', *Stroke; a journal of cerebral circulation*, 44(6), pp. 1754–60. doi: 10.1161/STROKEAHA.113.000734.

Dirnagl, U., Iadecola, C. and Moskowitz, M. A. (1999) 'Pathobiology of ischaemic stroke: an integrated view', *Trends in Neurosciences*, 22(9), pp. 391–397. doi: 10.1016/S0166-2236(99)01401-0.

Donnan, G. A., Baron, J., Davis, S. and Sharp, F. R. (2007) *The Ischaemic Penumbra*. New York, NY: Informa Healthcare.

Durgan, D. J., Hotze, M. A., Tomlin, T. M., Egbejimi, O., Graveleau, C., Abel, E. D., Shaw, C. A., Bray, M. S., Hardin, P. E. and Young, M. E. (2005) 'The intrinsic circadian clock within the cardiomyocyte', *American Journal of Physiology - Heart and Circulatory Physiology*, 289(4).

Durgan, D. J., Tsai, J.-Y. Y., Grenett, M. H., Pat, B. M., Ratcliffe, W. F., Villegas-Montoya, C., Garvey, M. E., Nagendran, J., Dyck, J. R. B., Bray, M. S., Gamble, K. L., Gimble, J. M., Young, M. E. and Phil, D. (2011) 'Evidence suggesting that the cardiomyocyte circadian clock modulates responsiveness of the heart to hypertrophic stimuli in mice', *Chronobiol.Int.*, 28(1525–6073 (Electronic)), pp. 187–203. doi: 10.3109/07420528.2010.550406.

Duverger, D. and MacKenzie, E. T. (1988) 'The Quantification of Cerebral Infarction following Focal Ischemia in the Rat: Influence of Strain, Arterial Pressure, Blood Glucose Concentration, and Age', *Journal of Cerebral Blood Flow & Metabolism*. SAGE PublicationsSage UK: London, England, 8(4), pp. 449–461. doi: 10.1038/jcbfm.1988.86.

Duverger, D. and MacKenzie, E. T. (1988) 'The quantification of cerebral infarction following focal ischemia in the rat: influence of strain, arterial pressure, blood glucose concentration, and age.', *Journal of cerebral blood flow and metabolism : official journal of the International Society of Cerebral Blood Flow and Metabolism*, 8, pp. 449–461. doi: 10.1038/jcbfm.1988.86.

Earnest, D. J., Neuendorff, N., Coffman, J., Selvamani, A. and Sohrabji, F. (2016) 'Sex Differences in the Impact of Shift Work Schedules on Pathological Outcomes in an Animal Model of Ischemic Stroke', *Endocrinology*, 157(7), pp. 2836–2843. doi: 10.1210/en.2016-1130.

Eckel-Mahan, K. and Sassone-Corsi, P. (2013) 'Metabolism and the circadian clock converge.', *Physiological reviews*, 93(1), pp. 107–35. doi: 10.1152/physrev.00016.2012.

Eckle, T., Hartmann, K., Bonney, S., Reithel, S., Mittelbronn, M., Walker, L. A., Lowes, B. D., Han, J., Borchers, C. H., Buttrick, P. M., Kominsky, D. J., Colgan, S. P. and Eltzschig, H. K. (2012) 'Adora2b-elicited Per2 stabilization promotes a HIF-dependent metabolic switch crucial for myocardial adaptation to ischemia', *Nature Medicine*. Nature Research, 18(5), pp. 774–782. doi: 10.1038/nm.2728.

Evans, A., Brown, W., Kenyon, C., Maxted, K. and Smith, D. (1994) 'Improved system for measuring systolic blood pressure in the conscious rat', *Medical & biological engineering & computing*. Springer, 32(1), pp. 101–102.

Feigin, V. L., Forouzanfar, M. H., Krishnamurthi, R., Mensah, G. A., Connor, M., Bennett, D. A., Moran, A. E., Sacco, R. L., Anderson, L., Truelsen, T., O'Donnell, M., Venketasubramanian, N., Barker-Collo, S., Lawes, C. M. M., Wang, W., Shinohara, Y., Witt, E., Ezzati, M., Naghavi, M. and Murray, C. (2014) 'Global and regional burden of stroke during 1990-2010: findings from the Global Burden of Disease Study 2010.', *Lancet (London, England)*, 383(9913), pp. 245–54.

Feigin, V. L., Mensah, G. A., Norrving, B., Murray, C. J. L. and Roth, G. A. (2015) 'Atlas of the Global Burden of Stroke (1990-2013): The GBD 2013 Study', *Neuroepidemiology*. Karger Publishers, 45(3), pp. 230–236. doi: 10.1159/000441106.

Feng, M., Whitesall, S., Zhang, Y., Beibel, M., D'Alecy, L. and DiPetrillo, K. (2008) 'Validation of volume-pressure recording tail-cuff blood pressure measurements.', *American journal of hypertension*, 21(12), pp. 1288–91. doi: 10.1038/ajh.2008.301.

La Fleur, S. E., Kalsbeek, A., Wortel, J. and Buijs, R. M. (1999) 'A suprachiasmatic nucleus generated rhythm in basal glucose concentrations', *Journal of Neuroendocrinology*, 11(8), pp. 643–652. doi: 10.1046/j.1365-2826.1999.00373.x.

la Fleur, S., Kalsbeek, A., Wortel, J., Fekkes, M. L. and Buijs, R. M. (2001) 'A Daily Rhythm in Glucose Tolerance', *Diabetes*, 50(6).

Fonken, L. K., Frank, M. G., Kitt, M. M., Barrientos, R. M., Watkins, L. R. and Maier, S. F. (2015) 'Microglia inflammatory responses are controlled by an intrinsic circadian clock.', *Brain, behavior, and immunity*, 45, pp. 171–9. doi: 10.1016/j.bbi.2014.11.009.

Fonken, L. K., Lieberman, R. A., Weil, Z. M. and Nelson, R. J. (2013) 'Dim light at night exaggerates weight gain and inflammation associated with a high-fat diet in male mice.', *Endocrinology*. Endocrine Society Chevy Chase, MD, 154(10), pp. 3817–25. doi: 10.1210/en.2013-1121.

Fonken, L. K., Weil, Z. M. and Nelson, R. J. (2013) 'Mice exposed to dim light at night exaggerate inflammatory responses to lipopolysaccharide', *Brain, Behavior, and Immunity*. Elsevier Inc., 34, pp. 159–163. doi: 10.1016/j.bbi.2013.08.011.

Fox, G., Gallacher, D., Shevde, S., Loftus, J. and Swayne, G. (1993) 'Anatomic variation of the middle cerebral artery in the Sprague-Dawley rat.', *Stroke*, 24(12).

Furukawa, K., Fu, W., Li, Y., Witke, W., Kwiatkowski, D. J. and Mattson, M. P. (1997) 'The actin-severing protein gelsolin modulates calcium channel and NMDA receptor activities and vulnerability to excitotoxicity in hippocampal neurons', *The Journal of Neuroscience*, 17(21), pp. 8178–8186.

Gale, J. E., Cox, H. I., Qian, J., Block, G. D., Colwell, C. S. and Matveyenko, A. V (2011) 'Disruption of Circadian Rhythms Accelerates Development of Diabetes through Pancreatic Beta-Cell Loss and Dysfunction', *Journal of biological rhythms*, 26(5), pp. 423–433.

Garaulet, M., Gómez-Abellán, P., Alburquerque-Béjar, J. J., Lee, Y.-C., Ordovás, J. M. and Scheer, F. A. J. L. (2013) 'Timing of food intake predicts weight loss effectiveness.', *International journal of obesity (2005)*, 37(4), pp. 604–11. doi: 10.1038/ijo.2012.229.

Garcia, J. H., Wagner, S., Liu, K. F. and Hu, X. J. (1995) 'Neurological deficit and extent of neuronal necrosis attributable to middle cerebral artery occlusion in rats. Statistical validation.', *Stroke; a journal of cerebral circulation*, 26, p. 627–634; discussion 635. doi: 10.1161/01.STR.26.4.627.

Gavin, J. R., Alberti, K. G. M. M., Davidson, M. B., DeFronzo, R. a, Drash, a, Gabbe, S. G., Genuth, S., Harris, M. I., Kahn, R., Keen, H., Knowler, W. C., Lebovitz, H., Maclaren, N. K., Palmer, J. P., Raskin, P., Rizza, R. a and Stern, M. P. (1997) 'Report of the Expert Committee on the Diagnosis and Classification of Diabetes Mellitus', *Diabetes Care*, 20(7), pp. 1183–1197. doi: 10.2337/diacare.26.2007.S5.

Gerriets, T., Stolz, E., Walberer, M., Müller, C., Kluge, a., Bachmann, a., Fisher, M., Kaps, M. and Bachmann, G. (2004) 'Noninvasive Quantification of Brain Edema and the Space-Occupying Effect in Rat Stroke Models Using Magnetic Resonance Imaging', *Stroke*, 35(2), pp. 566–571. doi: 10.1161/01.STR.0000113692.38574.57.

Gibson, E. M., Wang, C., Tjho, S., Khattar, N. and Kriegsfeld, L. J. (2010) 'Experimental "jet lag" inhibits adult neurogenesis and produces long-term cognitive deficits in female hamsters.', *PloS one*. Public Library of Science, 5(12), p. e15267. doi: 10.1371/journal.pone.0015267.

Gill, R., Andiné, P., Hillered, L., Persson, L. and Hagberg, H. (1992) 'The effect of MK-801 on cortical spreading depression in the penumbral zone following focal ischaemia in the rat.', *Journal of cerebral blood flow and metabolism*, 12(3), pp. 371–9. doi: 10.1038/jcbfm.1992.54.

Go, A. S. (2009) 'The ACTIVE Pursuit of Stroke Prevention in Patients with Atrial Fibrillation', *New England Journal of Medicine*, 360(20), pp. 2127–2129. doi: 10.1056/NEJMe0902676.

Go, A. S., Mozaffarian, D., Roger, V. L., Benjamin, E. J., Berry, J. D., Blaha, M. J., Dai, S., Ford, E. S., Fox, C. S., Franco, S., Fullerton, H. J., Gillespie, C., Hailpern, S. M., Heit, J. A., Howard, V. J., Huffman, M. D., Judd, S. E., Kissela, B. M., Kittner, S. J., Lackland, D. T., Lichtman, J. H., Lisabeth, L. D., Mackey, R. H., Magid, D. J., Marcus, G. M., Marelli, A., Matchar, D. B., McGuire, D. K., Mohler, E. R., Moy, C. S., Mussolino, M. E., Neumar, R. W., Nichol, G., Pandey, D. K., Paynter, N. P., Reeves, M. J., Sorlie, P. D., Stein, J., Towfighi, A., Turan, T. N., Virani, S. S., Wong, N. D., Woo, D., Turner, M. B. and American Heart Association Statistics Committee and Stroke Statistics Subcommittee (2014) 'Heart disease and stroke statistics--2014 update: a report from the American Heart Association.', *Circulation*, 129(3), pp. e28–e292. doi: 10.1161/01.cir.0000441139.02102.80.

Goldstein, L. B., Adams, R., Alberts, M. J., Appel, L. J., Brass, L. M., Bushnell, C. D., Culebras, A., DeGraba, T. J., Gorelick, P. B., Guyton, J. R., Hart, R. G., Howard, G., Kelly-Hayes, M., Nixon, J. V. I., Sacco, R. L., American Heart Association and American Stroke Association Stroke Council (2006) *Primary prevention of ischemic stroke: a guideline from the American Heart Association/American Stroke Association Stroke Council: cosponsored by the Atherosclerotic Peripheral Vascular Disease Interdisciplinary Working Group; Cardiovascular Nursing Counc*, *Circulation*. doi: 10.1161/01.STR.0000223048.70103.F1.

Gönenç, A., Hacışevki, A., Tavil, Y., Çengel, A. and Torun, M. (2013) 'Oxidative stress in patients with essential hypertension: a comparison of dippers and non-dippers.',

European journal of internal medicine, 24(2), pp. 139–44. doi: 10.1016/j.ejim.2012.08.016.

Grabowski, M., Mattsson, B., Nordborg, C. and Johansson, B. B. (1993) 'Brain capillary density and cerebral blood flow after occlusion of the middle cerebral artery in normotensive Wistar-Kyoto rats and spontaneously hypertensive rats', *J Hypertens*, 11(12), pp. 1363–1368.

Guerrero-Vargas, N. N., Guzmán-Ruiz, M., Fuentes, R., García, J., Salgado-Delgado, R., Basualdo, M. del C., Escobar, C., Markus, R. P. and Buijs, R. M. (2015) 'Shift Work in Rats Results in Increased Inflammatory Response after Lipopolysaccharide Administration: A Role for Food Consumption.', *Journal of biological rhythms*, 30(4), pp. 318–30. doi: 10.1177/0748730415586482.

Günther, A., Küppers-Tiedt, L., Schneider, P.-M., Kunert, I., Berrouschot, J., Schneider, D. and Rossner, S. (2005) 'Reduced infarct volume and differential effects on glial cell activation after hyperbaric oxygen treatment in rat permanent focal cerebral ischaemia.', *The European journal of neuroscience*, 21(11), pp. 3189–94. doi: 10.1111/j.1460-9568.2005.04151.x.

Hachinski, V., Donnan, G. A., Gorelick, P. B., Hacke, W., Cramer, S. C., Kaste, M., Fisher, M., Brainin, M., Buchan, A. M., Lo, E. H., Skolnick, B. E., Furie, K. L., Hankey, G. J., Kivipelto, M., Morris, J., Rothwell, P. M., Sacco, R. L., Smith, S. C., Wang, Y., Bryer, A., Ford, G. A., Iadecola, C., Martins, S. C. O., Saver, J., Skvortsova, V., Bayley, M., Bednar, M. M., Duncan, P., Enney, L., Finklestein, S., Jones, T. A., Kalra, L., Kleim, J., Nitkin, R., Teasell, R., Weiller, C., Desai, B., Goldberg, M. P., Heiss, W. D., Saarelma, O., Schwamm, L. H., Shinohara, Y., Trivedi, B., Wahlgren, N., Wong, L. K., Hakim, A., Norrving, B., Prudhomme, S., Bornstein, N. M., Davis, S. M., Goldstein, L. B., Leys, D. and Tuomilehto, J. (2010) 'Stroke: Working toward a prioritized world agenda', *International Journal of Stroke*, pp. 238–256. doi: 10.1111/j.1747-4949.2010.00442.x.

Hacke, W., Kaste, M., Bluhmki, E., Brozman, M., Dávalos, A., Guidetti, D., Larrue, V., Lees, K. R., Medeghri, Z., Machnig, T., Schneider, D., von Kummer, R., Wahlgren, N. and Toni, D. (2008) 'Thrombolysis with Alteplase 3 to 4.5 Hours after Acute Ischemic Stroke', *New England Journal of Medicine*. Massachusetts Medical Society , 359(13), pp. 1317–1329. doi: 10.1056/NEJMoa0804656.

Hankey, G. J. (2006) 'Potential new risk factors for ischemic stroke: what is their potential?', *Stroke*, 37(8), pp. 2181–8. doi: 10.1161/01.STR.0000229883.72010.e4.

Hansson, G. K. and Libby, P. (2006) 'The immune response in atherosclerosis: a double-edged sword', *Nature Reviews Immunology*, 6(7), pp. 508–519. doi: 10.1038/nri1882.

Hastings, M. H., Reddy, A. B. and Maywood, E. S. (2003) 'A clockwork web: circadian timing in brain and periphery, in health and disease', *Nature Reviews Neuroscience*, 4(8), pp. 649–661. doi: 10.1038/nrn1177.

HATFIELD, R. H., MENDELOW, A. D., PERRY, R. H., ALVAREZS, L. M. and MODHA, P. (1991) 'Triphenyltetrazolium chloride (TTC) as a marker for ischaemic changes in rat brain following permanent middle cerebral artery occlusion', *Neuropathology and Applied Neurobiology*. Blackwell Publishing Ltd, 17(1), pp. 61–67. doi: 10.1111/j.1365-2990.1991.tb00694.x.

Heiss, W.-D. (2000) 'Ischemic Penumbra: Evidence From Functional Imaging in Man', *Journal of Cerebral Blood Flow & Metabolism*. SAGE PublicationsSage UK: London, England, 20(9), pp. 1276–1293. doi: 10.1097/00004647-200009000-00002.

Heiss, W.-D. (2012) 'The ischemic penumbra: how does tissue injury evolve?', *Annals of the New York Academy of Sciences*, 1268, pp. 26–34. doi: 10.1111/j.1749-

6632.2012.06668.x.

Hibi, M., Masumoto, A., Naito, Y., Kiuchi, K., Yoshimoto, Y., Matsumoto, M., Katashima, M., Oka, J. and Ikemoto, S. (2013) 'Nighttime snacking reduces whole body fat oxidation and increases LDL cholesterol in healthy young women', *AMERICAN JOURNAL OF PHYSIOLOGY-REGULATORY INTEGRATIVE AND COMPARATIVE PHYSIOLOGY*, 304(2), pp. R94–R101. doi: 10.1152/ajpregu.00115.2012.

Hom, S., Fleegal, M. A., Egleton, R. D., Campos, C. R., Hawkins, B. T. and Davis, T. P. (2007) 'Comparative changes in the blood-brain barrier and cerebral infarction of SHR and WKY rats.', *American journal of physiology. Regulatory, integrative and comparative physiology*, 292(5), pp. R1881-92. doi: 10.1152/ajpregu.00761.2005.

Hossmann, K. A. and Heiss, W.-D. (2014) 'Neuropathology and pathophysiology of stroke', *Neuropathology and pathophysiology ofstroke. Textbook of Stroke Medicine*, p. 1.

Howells, D. W., Porritt, M. J., Rewell, S. S. J., O'Collins, V., Sena, E. S., van der Worp, H. B., Traystman, R. J. and Macleod, M. R. (2010) 'Different strokes for different folks: the rich diversity of animal models of focal cerebral ischemia.', *Journal of cerebral blood flow and metabolism : official journal of the International Society of Cerebral Blood Flow and Metabolism*, 30(8), pp. 1412–1431. doi: 10.1038/jcbfm.2010.66.

Iadecola, C. (1997) 'Bright and dark sides of nitric oxide in ischemic brain injury.', *Trends in neurosciences*, 20(3), pp. 132–139. doi: S0166-2236(96)10074-6 [pii].

Iadecola, C. and Anrather, J. (2011) 'The immunology of stroke: from mechanisms to translation.', *Nature medicine*. Nature Publishing Group, 17(7), pp. 796–808. doi: 10.1038/nm.2399.

Iadecola, C., Cho, S., Feuerstein, G. Z. and Hallenbeck, J. (2004) 'Cerebral Ischemia and Inflammation', in *Stroke: Pathophysiology, Diagnosis, and Management*, pp. 883–893. doi: 10.1016/B0-44-306600-0/50052-3.

Iadecola, C. and Davisson, R. L. (2008) 'Hypertension and cerebrovascular dysfunction.', *Cell metabolism*, 7(6), pp. 476–84. doi: 10.1016/j.cmet.2008.03.010.

Johnson, R. N., Metcalf, P. A. and Baker, J. R. (1983) 'Fructosamine: A new approach to the estimation of serum glycosylprotein. An index of diabetic control', *Clinica Chimica Acta*, 127(1), pp. 87–95. doi: 10.1016/0009-8981(83)90078-5.

Jung, S., Gilgen, M., Slotboom, J., El-Koussy, M., Zubler, C., Kiefer, C., Luedi, R., Mono, M.-L., Heldner, M. R., Weck, A., Mordasini, P., Schroth, G., Mattle, H. P., Arnold, M., Gralla, J. and Fischer, U. (2013) 'Factors that determine penumbral tissue loss in acute ischaemic stroke', *Brain*. Oxford University Press, 136(12), pp. 3554–3560. doi: 10.1093/brain/awt246.

Karlsson, B. (2001) 'Is there an association between shift work and having a metabolic syndrome? Results from a population based study of 27 485 people', *Occupational and Environmental Medicine*, 58(11), pp. 747–752. doi: 10.1136/oem.58.11.747.

Kawai, N., Keep, R. F. and Betz, A. L. (1997) 'Hyperglycemia and the Vascular Effects of Cerebral Ischemia', *Stroke*, 28(1).

Kerr, S., Brosnan, M. J., McIntyre, M., Reid, J. L., Dominiczak, A. F. and Hamilton, C. A. (1999) 'Superoxide Anion Production Is Increased in a Model of Genetic Hypertension', *Hypertension*, 33(6).

Kishi, T., Hirooka, Y., Kimura, Y., Ito, K., Shimokawa, H. and Takeshita, A. (2004) 'Increased Reactive Oxygen Species in Rostral Ventrolateral Medulla Contribute to

Neural Mechanisms of Hypertension in Stroke-Prone Spontaneously Hypertensive Rats', *Circulation*, 109(19).

Kishi, T. and Sunagawa, K. (2011) 'Experimental "jet lag" causes sympathoexcitation via oxidative stress through AT 1 receptor in the brainstem', *Proceedings of the Annual International Conference of the IEEE Engineering in Medicine and Biology Society, EMBS*, pp. 1969–1972. doi: 10.1109/IEMBS.2011.6090555.

Kissela, B. M., Khoury, J., Kleindorfer, D., Woo, D., Schneider, A., Alwell, K., Miller, R., Ewing, I., Moomaw, C. J., Szaflarski, J. P., Gebel, J., Shukla, R. and Broderick, J. P. (2005) 'Epidemiology of Ischemic Stroke in Patients With Diabetes: The Greater Cincinnati/Northern Kentucky Stroke Study', *Diabetes Care*, 28(2), pp. 355–359. doi: 10.2337/diacare.28.2.355.

Koizumi, J., Yoshida, Y., Nakazawa, T. and Ooneda, G. (1986) 'Experimental studies of ischemic brain edema', *Nosotchu*. 一般社団法人 日本脳卒中学会, 8(1), pp. 1–8. doi: 10.3995/jstroke.8.1.

Kriz, J. and Lalancette-Hébert, M. (2009) 'Inflammation, plasticity and real-time imaging after cerebral ischemia', *Acta Neuropathologica*. Springer-Verlag, 117(5), pp. 497–509. doi: 10.1007/s00401-009-0496-1.

Ku Mohd Noor, K. M., Wyse, C., Roy, L. A., Biello, S. M., McCabe, C. and Dewar, D. (2016) 'Chronic photoperiod disruption does not increase vulnerability to focal cerebral ischemia in young normotensive rats', *Journal of Cerebral Blood Flow & Metabolism*. SAGE Publications, p. 0271678X16671316. doi: 10.1177/0271678X16671316.

Kurose, T., Hyo, T., Seino, Y. and Yabe, D. (2014) 'The role of chronobiology and circadian rhythms in type 2 diabetes mellitus: implications for management of diabetes', *ChronoPhysiology and Therapy*. Dove Press, Volume 4, p. 41. doi: 10.2147/CPT.S44804.

Lalancette-Hébert, M., Swarup, V., Beaulieu, J. M., Bohacek, I., Abdelhamid, E., Weng, Y. C., Sato, S. and Kriz, J. (2012) 'Galectin-3 is required for resident microglia activation and proliferation in response to ischemic injury.', *The Journal of neuroscience : the official journal of the Society for Neuroscience*, 32(30), pp. 10383–95. doi: 10.1523/JNEUROSCI.1498-12.2012.

Lammie, G. A. (2002) 'Hypertensive cerebral small vessel disease and stroke', *Brain Pathology*, 12(3), pp. 358–370. doi: 10.1111/j.1750-3639.2002.tb00450.x.

Lee, R. M. K. W. (1995) 'Morphology of cerebral arteries', *Pharmacology & Therapeutics*, 66(1), pp. 149–173. doi: 10.1016/0163-7258(94)00071-A.

Lee, S., Shafe, A. C. E. and Cowie, M. R. (2011) 'UK stroke incidence, mortality and cardiovascular risk management 1999-2008: time-trend analysis from the General Practice Research Database.', *BMJ open*. British Medical Journal Publishing Group, 1(2), p. e000269. doi: 10.1136/bmjopen-2011-000269.

Lefta, M., Campbell, K. S., Feng, H. Z., Jin, J. P. and Esser, K. A. (2012) 'Development of dilated cardiomyopathy in Bmal1-deficient mice', *Am J Physiol Heart Circ Physiol*, 303(4), pp. H475-85. doi: 10.1152/ajpheart.00238.2012.

Letourneur, A., Roussel, S., Toutain, J., Bernaudin, M. and Touzani, O. (2011) 'Impact of genetic and renovascular chronic arterial hypertension on the acute spatiotemporal evolution of the ischemic penumbra: a sequential study with MRI in the rat.', *Journal of cerebral blood flow and metabolism : official journal of the International Society of Cerebral Blood Flow and Metabolism*, 31(2), pp. 504–13. doi: 10.1038/jcbfm.2010.118.

Li, F., Omae, T. and Fisher, M. (1999) 'Spontaneous Hyperthermia and its Mechanism in the Intraluminal Suture Middle Cerebral Artery Occlusion Model of Rats', *Stroke*, 30(11).

Liu, S., Zhen, G., Meloni, B. P., Campbell, K. and Winn, H. R. (2009) 'RODENT STROKE MODEL GUIDELINES FOR PRECLINICAL STROKE TRIALS (1ST EDITION).', *Journal of experimental stroke & translational medicine*. NIH Public Access, 2(2), pp. 2–27. doi: 10.6030/1939-067X-2.2.2.

Lo, E. H., Dalkara, T. and Moskowitz, M. A. (2003) 'Mechanisms, challenges and opportunities in stroke.', *Nature Reviews Neuroscience*, 4(5), pp. 399–415. doi: 10.1038/nrn1106.

Logan, R. W. and Sarkar, D. K. (2012) 'Circadian nature of immune function', *Molecular and Cellular Endocrinology*, pp. 82–90. doi: 10.1016/j.mce.2011.06.039.

Longa, E. Z., Weinstein, P. R., Carlson, S. and Cummins, R. (1989) 'Reversible middle cerebral artery occlusion without craniectomy in rats.', *Stroke*, 20(1).

Lowden, A., Moreno, C., Holmbäck, U., Lennernäs, M. and Tucker, P. (2010) 'Eating and shift work - effects on habits, metabolism and performance.', *Scandinavian journal of work, environment & health*, 36(2), pp. 150–62.

Luitse, M. J. A., Biessels, G. J., Rutten, G. E. H. M. and Kappelle, L. J. (2012) 'Diabetes, hyperglycaemia, and acute ischaemic stroke.', *The Lancet. Neurology*, 11(3), pp. 261–71. doi: 10.1016/S1474-4422(12)70005-4.

MacDougall, N. J. J. and Muir, K. W. (2011) 'Hyperglycaemia and infarct size in animal models of middle cerebral artery occlusion: systematic review and meta-analysis.', *Journal of cerebral blood flow and metabolism : official journal of the International Society of Cerebral Blood Flow and Metabolism*, 31(3), pp. 807–18. doi: 10.1038/jcbfm.2010.210.

Macrae, I. M. (2011) 'Preclinical stroke research--advantages and disadvantages of the most common rodent models of focal ischaemia.', *British journal of pharmacology*, 164(4), pp. 1062–78. doi: 10.1111/j.1476-5381.2011.01398.x.

MacRae, I. M. (1992) 'New models of focal cerebral ischaemia', *British Journal of Clinical Pharmacology*, 34(4), pp. 302–308. doi: 10.1111/j.1365-2125.1992.tb05634.x.

Macrae, I. M., Robinson, M. J., Graham, D. I., Reid, J. L. and McCulloch, J. (1993) 'Endothelin-1-induced reductions in cerebral blood flow: dose dependency, time course, and neuropathological consequences.', *Journal of cerebral blood flow and metabolism*, 13(2), pp. 276–284. doi: 10.1038/jcbfm.1993.34.

Marcheva, B., Ramsey, K. M., Buhr, E. D., Kobayashi, Y., Su, H., Ko, C. H., Ivanova, G., Omura, C., Mo, S., Vitaterna, M. H., Lopez, J. P., Philipson, L. H., Bradfield, C. a, Crosby, S. D., JeBailey, L., Wang, X., Takahashi, J. S. and Bass, J. (2010) 'Disruption of the clock components CLOCK and BMAL1 leads to hypoinsulinaemia and diabetes.', *Nature*. Nature Publishing Group, 466(7306), pp. 627–31. doi: 10.1038/nature09253.

Marks, L., Carswell, H. V, Peters, E. E., Graham, D. I., Patterson, J., Dominiczak, a F. and Macrae, I. M. (2001) 'Characterization of the microglial response to cerebral ischemia in the stroke-prone spontaneously hypertensive rat.', *Hypertension*, 38(1), pp. 116–122. doi: 10.1161/01.HYP.38.1.116.

Marsh, E. E., Biller, J., Adams, H. P., Marler, J. R., Hulbert, J. R., Love, B. B. and Gordon, D. L. (1990) 'Circadian variation in onset of acute ischemic stroke.', *Archives of neurology*, 47(11), pp. 1178–1180. doi: 10.1001/archneur.1990.00530110032012.

Martino, T. A., Tata, N., Belsham, D. D., Chalmers, J., Straume, M., Lee, P., Pribiag, H., Khaper, N., Liu, P. P., Dawood, F., Backx, P. H., Ralph, M. R. and Sole, M. J. (2007) 'Disturbed diurnal rhythm alters gene expression and exacerbates cardiovascular disease with rescue by resynchronization.', *Hypertension (Dallas, Tex. : 1979)*, 49(5), pp. 1104–13. doi: 10.1161/HYPERTENSIONAHA.106.083568.

Martino, T. A. and Young, M. E. (2015) 'Influence of the cardiomyocyte circadian clock on cardiac physiology and pathophysiology.', *Journal of biological rhythms*, 30(3), pp. 183–205. doi: 10.1177/0748730415575246.

Martino, T. a, Oudit, G. Y., Herzenberg, A. M., Tata, N., Koletar, M. M., Kabir, G. M., Belsham, D. D., Backx, P. H., Ralph, M. R. and Sole, M. J. (2008) 'Circadian rhythm disorganization produces profound cardiovascular and renal disease in hamsters.', *American journal of physiology. Regulatory, integrative and comparative physiology*, 294(5), pp. R1675-83. doi: 10.1152/ajpregu.00829.2007.

McCabe, C., Gallagher, L., Gsell, W., Graham, D., Dominiczak, A. F. and MacRae, I. M. (2009) 'Differences in the evolution of the ischemic penumbra in stroke-prone spontaneously hypertensive and wistar-kyoto rats', *Stroke*, 40(12), pp. 3864–3868. doi: 10.1161/STROKEAHA.109.559021.

McColl, B. W., Allan, S. M. and Rothwell, N. J. (2009) 'Systemic infection, inflammation and acute ischemic stroke.', *Neuroscience*, 158(3), pp. 1049–61. doi: 10.1016/j.neuroscience.2008.08.019.

McColl, B. W., Rose, N., Robson, F. H., Rothwell, N. J. and Lawrence, C. B. (2010) 'Increased Brain Microvascular MMP-9 and Incidence of Haemorrhagic Transformation in Obese Mice after Experimental Stroke', *Journal of Cerebral Blood Flow & Metabolism*. SAGE PublicationsSage UK: London, England, 30(2), pp. 267–272. doi: 10.1038/jcbfm.2009.217.

McColl, B. W., Rothwell, N. J. and Allan, S. M. (2007) 'Systemic inflammatory stimulus potentiates the acute phase and CXC chemokine responses to experimental stroke and exacerbates brain damage via interleukin-1- and neutrophil-dependent mechanisms.', *The Journal of neuroscience : the official journal of the Society for Neuroscience*, 27(16), pp. 4403–12. doi: 10.1523/JNEUROSCI.5376-06.2007.

Metz, G. A. S. (2010) 'Rodent Models of Stroke'. Edited by U. Dirnagl. Totowa, NJ: Humana Press (Neuromethods), 47, pp. 199–212. doi: 10.1007/978-1-60761-750-1.

Mighiu, A. S. and Heximer, S. P. (2012) 'Controlling Parasympathetic Regulation of Heart Rate: A Gatekeeper Role for RGS Proteins in the Sinoatrial Node', *Frontiers in Physiology*. Frontiers, 3, p. 204. doi: 10.3389/fphys.2012.00204.

Minami, M., Togashi, H., Koike, Y., Saito, H., Nakamura, N. and Yasuda, H. (1985) 'Changes in ambulation and drinking behavior related to stroke in stroke-prone spontaneously hypertensive rats.', *Stroke; a journal of cerebral circulation*, 16(1), pp. 44–8.

Mitchell, A. B., Cole, J. W., McArdle, P. F., Cheng, Y.-C., Ryan, K. A., Sparks, M. J., Mitchell, B. D. and Kittner, S. J. (2015) 'Obesity increases risk of ischemic stroke in young adults.', *Stroke; a journal of cerebral circulation*, 46(6), pp. 1690–2. doi: 10.1161/STROKEAHA.115.008940.

Modo, M., Stroemer, R. ., Tang, E., Veizovic, T., Sowniski, P. and Hodges, H. (2000) 'Neurological sequelae and long-term behavioural assessment of rats with transient middle cerebral artery occlusion', *Journal of Neuroscience Methods*, 104(1), pp. 99–109. doi: 10.1016/S0165-0270(00)00329-0.

Molcan, L., Teplan, M., Vesela, a and Zeman, M. (2013) 'The long-term effects of phase advance shifts of photoperiod on cardiovascular parameters as measured by radiotelemetry in rats.', *Physiological measurement*, 34(12), pp. 1623–32. doi: 10.1088/0967-3334/34/12/1623.

Möller, K., Pösel, C., Kranz, A., Schulz, I., Scheibe, J., Didwischus, N., Boltze, J., Weise, G. and Wagner, D.-C. (2015) 'Arterial Hypertension Aggravates Innate Immune Responses after Experimental Stroke.', *Frontiers in cellular neuroscience*. Frontiers, 9, p. 461. doi: 10.3389/fncel.2015.00461.

Moore, R. Y. (1996) 'Chapter 8 Entrainment pathways and the functional organization of the circadian system', *Progress in Brain Research*, 111, pp. 103–119. doi: 10.1016/S0079-6123(08)60403-3.

Morikawa, Y., Nakagawa, H., Miura, K., Soyama, Y., Ishizaki, M., Kido, T., Naruse, Y., Suwazono, Y. and Nogawa, K. (2005) 'Shift work and the risk of diabetes mellitus among Japanese male factory workers.', *Scandinavian journal of work, environment & health*, 31(3), pp. 179–83. doi: 10.5271/sjweh.867.

Moskowitz, M. a., Lo, E. H. and Iadecola, C. (2010) 'The science of stroke: Mechanisms in search of treatments', *Neuron*, 67(2), pp. 181–198. doi: 10.1016/j.neuron.2010.07.002.

Muir, K. W. (2013) 'Stroke', *Medicine*, 41(3), pp. 169–174. doi: 10.1016/j.mpmed.2012.12.005.

Muir, K. W. (2016) 'Stroke in 2015: the year of endovascular treatment.', *The Lancet. Neurology*. Elsevier, 15(1), pp. 2–3. doi: 10.1016/S1474-4422(15)00337-3.

Muir, K. W., McCormick, M., Baird, T. and Ali, M. (2011) 'Prevalence, Predictors and Prognosis of Post-Stroke Hyperglycaemia in Acute Stroke Trials: Individual Patient Data Pooled Analysis from the Virtual International Stroke Trials Archive (VISTA).', *Cerebrovascular diseases extra*. Karger Publishers, 1(1), pp. 17–27. doi: 10.1159/000324319.

Muir, K. W., Tyrrell, P., Sattar, N. and Warburton, E. (2007) 'Inflammation and ischaemic stroke', *Curr Opin Neurol*, 20(3), pp. 334–342. doi: 10.1097/WCO.0b013e32813ba151.

Mulvany, M. J., Hansen, O. K. and Aalkjaer, C. (1978) 'Direct evidence that the greater contractility of resistance vessels in spontaneously hypertensive rats is associated with a narrowed lumen, a thickened media, and an increased number of smooth muscle cell layers.', *Circulation research*, 43(6), pp. 854–64.

Murray, K. N., Buggey, H. F., Denes, A. and Allan, S. M. (2013) 'Systemic immune activation shapes stroke outcome.', *Molecular and cellular neurosciences*, 53, pp. 14–25. doi: 10.1016/j.mcn.2012.09.004.

Murray, K. N., Girard, S., Holmes, W. M., Parkes, L. M., Williams, S. R., Parry-Jones, A. R. and Allan, S. M. (2014) 'Systemic inflammation impairs tissue reperfusion through endothelin-dependent mechanisms in cerebral ischemia.', *Stroke; a journal of cerebral circulation*, 45(11), pp. 3412–9. doi: 10.1161/STROKEAHA.114.006613.

Murtagh, B. and Smalling, R. W. (2006) 'Cardioembolic stroke', *Current Atherosclerosis Reports*, pp. 310–316. doi: 10.1007/s11883-006-0009-9.

Musiek, E. S., Lim, M. M., Yang, G., Bauer, A. Q., Qi, L., Lee, Y., Roh, J. H., Ortiz-Gonzalez, X., Dearborn, J. T., Culver, J. P., Herzog, E. D., Hogenesch, J. B., Wozniak, D. F., Dikranian, K., Giasson, B. I., Weaver, D. R., Holtzman, D. M. and Fitzgerald, G. A.

(2013) ‘Circadian clock proteins regulate neuronal redox homeostasis and neurodegeneration.’, *The Journal of clinical investigation*, 123(12), pp. 5389–400. doi: 10.1172/JCI70317.

Nagoshi, E., Saini, C., Bauer, C., Laroche, T., Naef, F. and Schibler, U. (2004) ‘Circadian Gene Expression in Individual Fibroblasts’, *Cell*, 119, pp. 693–705. doi: 10.1016/j.cell.2004.11.015.

Nishimura, Y., Ito, T. and Saavedra, J. M. (2000) ‘Angiotensin II AT(1) blockade normalizes cerebrovascular autoregulation and reduces cerebral ischemia in spontaneously hypertensive rats.’, *Stroke; a journal of cerebral circulation*, 31(10), pp. 2478–2486. doi: 10.1161/01.STR.31.10.2478.

Nonaka, H., Emoto, N., Ikeda, K., Fukuya, H., Rohman, M. S., Raharjo, S. B., Yagita, K., Okamura, H. and Yokoyama, M. (2001) ‘Angiotensin II induces circadian gene expression of clock genes in cultured vascular smooth muscle cells.’, *Circulation*, 104(15), pp. 1746–8.

Noor, R., Wang, C. X. and Shuaib, A. (2003) *Effects of hyperthermia on infarct volume in focal embolic model of cerebral ischemia in rats*, *Neuroscience Letters*. doi: 10.1016/S0304-3940(03)00802-4.

O’Collins, V. E., Donnan, G. A., Macleod, M. R. and Howells, D. W. (2013) *Animal Models for the Study of Human Disease*, *Animal Models for the Study of Human Disease*. Elsevier. doi: 10.1016/B978-0-12-415894-8.00023-3.

Ogata, J., Yamanishi, H. and Ishibashi-Ueda, H. (2011) ‘Review: Role of cerebral vessels in ischaemic injury of the brain’, *Neuropathology and Applied Neurobiology*, 37(1), pp. 40–55. doi: 10.1111/j.1365-2990.2010.01141.x.

Opperhuizen, A.-L., van Kerkhof, L. W. M., Proper, K. I., Rodenburg, W. and Kalsbeek, A. (2015) ‘Rodent models to study the metabolic effects of shiftwork in humans.’, *Frontiers in pharmacology*. Frontiers, 6, p. 50. doi: 10.3389/fphar.2015.00050.

Osborne, K. a, Shigeno, T., Balarsky, a M., Ford, I., McCulloch, J., Teasdale, G. M. and Graham, D. I. (1987) ‘Quantitative assessment of early brain damage in a rat model of focal cerebral ischaemia.’, *Journal of neurology, neurosurgery, and psychiatry*, 50(4), pp. 402–410. doi: 10.1136/jnnp.50.4.402.

Palmer, a. J., Bulpitt, C. J., Fletcher, a. E., Beevers, D. G., Coles, E. C., Ledingham, J. G., O’Riordan, P. W., Petrie, J. C., Rajagopalan, B. E. and Webster, J. (1992) ‘Relation between blood pressure and stroke mortality’, *Hypertension*, 20(5), pp. 601–605. doi: 10.1161/01.HYP.20.5.601.

Patel, A. R., Ritzel, R., McCullough, L. D. and Liu, F. (2013) ‘Microglia and ischemic stroke: a double-edged sword.’, *International journal of physiology, pathophysiology and pharmacology*, 5(2), pp. 73–90.

Patton, D. F. and Mistlberger, R. E. (2013) ‘Circadian adaptations to meal timing: neuroendocrine mechanisms.’, *Frontiers in neuroscience*. Frontiers, 7, p. 185. doi: 10.3389/fnins.2013.00185.

Pekovic-Vaughan, V., Gibbs, J., Yoshitane, H., Yang, N., Pathiranage, D., Guo, B., Sagami, A., Taguchi, K., Bechtold, D., Loudon, A., Yamamoto, M., Chan, J., van der Horst, G. T. J., Fukada, Y. and Meng, Q.-J. (2014) ‘The circadian clock regulates rhythmic activation of the NRF2/glutathione-mediated antioxidant defense pathway to modulate pulmonary fibrosis.’, *Genes & development*. Cold Spring Harbor Laboratory Press, 28(6), pp. 548–60. doi: 10.1101/gad.237081.113.

Penev, P. D., Kolker, D. E., Zee, P. C. and Turek, F. W. (1998) 'Chronic circadian desynchronization decreases the survival of animals with cardiomyopathic heart disease', *Am J Physiol Heart Circ Physiol*, 275(6), pp. H2334-2337.

Phillips, D. J., Savenkova, M. I. and Karatsoreos, I. N. (2015) 'Environmental disruption of the circadian clock leads to altered sleep and immune responses in mouse.', *Brain, behavior, and immunity*, 47, pp. 14–23. doi: 10.1016/j.bbi.2014.12.008.

Phillips, S. J. and Whisnant, J. P. (1992) 'Hypertension and the brain. The National High Blood Pressure Education Program.', *Archives of internal medicine*, 152(5), pp. 938–945. doi: 10.1001/archinte.152.5.938.

Popp, A., Jaenisch, N., Witte, O. W. and Frahm, C. (2009) 'Identification of ischemic regions in a rat model of stroke.', *PloS one*. Public Library of Science, 4(3), p. e4764. doi: 10.1371/journal.pone.0004764.

Reid, E., Graham, D., Lopez-Gonzalez, M. R., Holmes, W. M., Macrae, I. M. and McCabe, C. (2012) 'Penumbra detection using PWI/DWI mismatch MRI in a rat stroke model with and without comorbidity: comparison of methods.', *Journal of cerebral blood flow and metabolism : official journal of the International Society of Cerebral Blood Flow and Metabolism*, 32(9), pp. 1765–77. doi: 10.1038/jcbfm.2012.69.

Ribas-Latre, A. and Eckel-Mahan, K. (2016) 'Interdependence of nutrient metabolism and the circadian clock system: Importance for metabolic health.', *Molecular metabolism*. Elsevier, 5(3), pp. 133–52. doi: 10.1016/j.molmet.2015.12.006.

Ribo, M., Molina, C., Montaner, J., Rubiera, M., Delgado-Mederos, R., Arenillas, J. F., Quintana, M. and Alvarez-Sabín, J. (2005) 'Acute hyperglycemia state is associated with lower tPA-induced recanalization rates in stroke patients', *Stroke*, 36(8), pp. 1705–1709. doi: 10.1161/01.STR.0000173161.05453.90.9f.

Richards, J., Diaz, A. N. and Gumz, M. L. (2014) 'Clock genes in hypertension: novel insights from rodent models.', *Blood pressure monitoring*, 19(5), pp. 249–54. doi: 10.1097/MBP.0000000000000060.

Rodríguez-Yáñez, M. and Castillo, J. (2008) 'Role of inflammatory markers in brain ischemia.', *Current opinion in neurology*, 21(3), pp. 353–7. doi: 10.1097/WCO.0b013e3282ffafbf.

Rose, L., Bakal, D. A., Fung, T. S., Farn, P. and Weaver, L. E. (1994) 'Tactile extinction and functional status after stroke. A preliminary investigation.', *Stroke*, 25(10).

Roy, L. A. (2015) *Hyperglycaemia in Acute Ischaemic Stroke: Brain Imaging Studies in a Rodent Model of Stroke. PhD thesis*. University of Glasgow. doi: glathesis:2015-7191.

Rüger, M. and Scheer, F. A. J. L. (2009) 'Effects of circadian disruption on the cardiometabolic system.', *Reviews in endocrine & metabolic disorders*, 10(4), pp. 245–60. doi: 10.1007/s11154-009-9122-8.

Saha, J. K., Xia, J., Grondin, J. M., Engle, S. K. and Jakubowski, J. a (2005) 'Acute hyperglycemia induced by ketamine/xylazine anesthesia in rats: mechanisms and implications for preclinical models.', *Experimental biology and medicine (Maywood, N.J.)*, 230(10), pp. 777–784. doi: 230/10/777 [pii].

Saka, Ö., Mcguire, A. and Wolfe, C. (2009) 'Cost of stroke in the United Kingdom', *Age and Ageing*, 38(1), pp. 27–32. doi: 10.1093/ageing/afn281.

Salgado-Delgado, R., Angeles-Castellanos, M., Saderi, N., Buijs, R. M. and Escobar, C. (2010) 'Food intake during the normal activity phase prevents obesity and circadian desynchrony in a rat model of night work.', *Endocrinology*, 151(3), pp. 1019–29. doi:

10.1210/en.2009-0864.

Salgado-Delgado, R. C., Saderi, N., Basualdo, M. D. C., Guerrero-Vargas, N. N., Escobar, C. and Buijs, R. M. (2013) 'Shift work or food intake during the rest phase promotes metabolic disruption and desynchrony of liver genes in male rats.', *PloS one*, 8(4), p. e60052. doi: 10.1371/journal.pone.0060052.

Salgado-Delgado, R., Nadia, S., Angeles-Castellanos, M., Buijs, R. M. and Escobar, C. (2010) 'In a rat model of night work, activity during the normal resting phase produces desynchrony in the hypothalamus.', *Journal of biological rhythms*, 25(6), pp. 421–31. doi: 10.1177/0748730410383403.

Saper, C. B., Scammell, T. E. and Lu, J. (2005) 'Hypothalamic regulation of sleep and circadian rhythms.', *Nature*, 437(7063), pp. 1257–1263. doi: 10.1038/nature04284.

Saposnik, G., Gladstone, D., Raptis, R., Zhou, L. and Hart, R. G. (2013) 'Atrial fibrillation in ischemic stroke: Predicting response to thrombolysis and clinical outcomes', *Stroke*, 44(1), pp. 99–104. doi: 10.1161/STROKEAHA.112.676551.

Sarwar, N., Gao, P., Seshasai, S. R., Gobin, R., Kaptoge, S., Di Angelantonio, E., Ingelsson, E., Lawlor, D. A., Selvin, E., Stampfer, M., Stehouwer, C. D., Lewington, S., Pennells, L., Thompson, A., Sattar, N., White, I. R., Ray, K. K. and Danesh, J. (2010) 'Diabetes mellitus, fasting blood glucose concentration, and risk of vascular disease: a collaborative meta-analysis of 102 prospective studies 2', *Lancet*, 375(1474–547X (Electronic)), pp. 2215–2222. doi: 10.1016/S0140-6736(10)60484-9.

Schallert, T., Fleming, S. M., Leasure, J. L., Tillerson, J. L. and Bland, S. T. (2000) 'CNS plasticity and assessment of forelimb sensorimotor outcome in unilateral rat models of stroke, cortical ablation, parkinsonism and spinal cord injury.', *Neuropharmacology*, 39(5), pp. 777–87.

Schallert, T. and Whishaw, I. Q. (1984) 'Bilateral Cutaneous Stimulation of the Somatosensory System in Hemidecorticate Rats', *Behavioral Neuroacience Copyright*, 98(3), pp. 518–540. doi: 10.1037//0735-7044.98.3.518.

Scheer, F. A., van Doornen, L. J. and Buijs, R. M. (1999) 'Light and diurnal cycle affect human heart rate: possible role for the circadian pacemaker.', *Journal of biological rhythms*, 14(3), pp. 202–12.

Scheer, F. A., Hilton, M. F., Mantzoros, C. S. and Shea, S. a (2009) 'Adverse metabolic and cardiovascular consequences of circadian misalignment.', *Proceedings of the National Academy of Sciences of the United States of America*, 106(11), pp. 4453–8. doi: 10.1073/pnas.0808180106.

Scheer, F. A., Kalsbeek, A. and Buijs, R. M. (2003) 'Cardiovascular control by the suprachiasmatic nucleus: neural and neuroendocrine mechanisms in human and rat.', *Biological chemistry*, 384(5), pp. 697–709. doi: 10.1515/BC.2003.078.

Scheiermann, C., Kunisaki, Y. and Frenette, P. S. (2013) 'Circadian control of the immune system.', *Nature reviews. Immunology*. NIH Public Access, 13(3), pp. 190–8. doi: 10.1038/nri3386.

Schmid-Elsaesser, R., Zausinger, S., Hungerhuber, E., Baethmann, A., Reulen, H.-J. and Garcia, J. H. (1998) 'A Critical Reevaluation of the Intraluminal Thread Model of Focal Cerebral Ischemia : Evidence of Inadvertent Premature Reperfusion and Subarachnoid Hemorrhage in Rats by Laser-Doppler Flowmetry Editorial Comment: Evidence of Inadvertent Premature Reper', *Stroke*, 29(10), pp. 2162–2170. doi: 10.1161/01.STR.29.10.2162.

Scorrano, F., Carrasco, J., Pastor-Ciurana, J., Belda, X., Rami-Bastante, A., Bacci, M. L. and Armario, A. (2015) 'Validation of the long-term assessment of hypothalamic-pituitary-adrenal activity in rats using hair corticosterone as a biomarker.', *FASEB journal : official publication of the Federation of American Societies for Experimental Biology*. Federation of American Societies for Experimental Biology, 29(3), pp. 859–67. doi: 10.1096/fj.14-254474.

Shelton, F. de N. A. P., Volpe, B. T. and Reding, M. (2001) 'Motor Impairment as a Predictor of Functional Recovery and Guide to Rehabilitation Treatment After Stroke', *Neurorehabilitation and Neural Repair*. Sage PublicationsSage CA: Thousand Oaks, CA, 15(3), pp. 229–237. doi: 10.1177/154596830101500311.

Shimamura, N., Matchett, G., Tsubokawa, T., Ohkuma, H. and Zhang, J. (2006) 'Comparison of silicon-coated nylon suture to plain nylon suture in the rat middle cerebral artery occlusion model', *Journal of Neuroscience Methods*, 156(1–2), pp. 161–165. doi: 10.1016/j.jneumeth.2006.02.017.

Shimamura, T., Nakajima, M., Iwasaki, T., Hayasaki, Y., Yonetani, Y. and Iwaki, K. (1999) 'Analysis of circadian blood pressure rhythm and target-organ damage in stroke-prone spontaneously hypertensive rats.', *Journal of hypertension*, 17(2), pp. 211–20.

Shuaib, A., Butcher, K., Mohammad, A. A., Saqqur, M. and Liebeskind, D. S. (2011) 'Collateral blood vessels in acute ischaemic stroke: A potential therapeutic target', *The Lancet Neurology*, pp. 909–921. doi: 10.1016/S1474-4422(11)70195-8.

Simard, J. M., Kent, T. A., Chen, M., Tarasov, K. V. and Gerzanich, V. (2007) 'Brain oedema in focal ischaemia: molecular pathophysiology and theoretical implications', *Lancet Neurology*, pp. 258–268. doi: 10.1016/S1474-4422(07)70055-8.

Sirén, A. L., Heldman, E., Doron, D., Lysko, P. G., Yue, T. L., Liu, Y., Feuerstein, G. and Hallenbeck, J. M. (1992) 'Release of proinflammatory and prothrombotic mediators in the brain and peripheral circulation in spontaneously hypertensive and normotensive Wistar-Kyoto rats.', *Stroke*, 23(11).

Sládek, M., Polidarová, L., Nováková, M., Parkanová, D. and Sumová, A. (2012) 'Early chronotype and tissue-specific alterations of circadian clock function in spontaneously hypertensive rats.', *PloS one*, 7(10), p. e46951. doi: 10.1371/journal.pone.0046951.

Stroemer, P., Patel, S., Hope, A., Oliveira, C., Pollock, K. and Sinden, J. (2009) 'The Neural Stem Cell Line CTX0E03 Promotes Behavioral Recovery and Endogenous Neurogenesis After Experimental Stroke in a Dose-Dependent Fashion', *Neurorehabilitation and Neural Repair*, 23(9), pp. 895–909. doi: 10.1177/1545968309335978.

Stroke.org.uk (2016) 'State of The Nation Stroke statistics-January 2016', *Stroke Association Resource Sheet*, (January), pp. 1–13. doi: 10.1080/07393149508429756.

Stroke Association (2014) *Research Spend in the UK: Comparing stroke, cancer, coronary heart disease and dementia*.

Strong, A. J., Smith, S. E., Whittington, D. J., Meldrum, B. S., Parsons, A. A., Krupinski, J., Hunter, A. J. and Patel, S. (2000) 'Factors Influencing the Frequency of Fluorescence Transients as Markers of Peri-Infarct Depolarizations in Focal Cerebral Ischemia', *Stroke*, 31(1).

Suessenbacher, A., Potocnik, M., Drler, J., Fluckinger, G., Wanitschek, M., Pachinger, O., Frick, M. and Alber, H. F. (2011) 'Comparison of peripheral endothelial function in shift versus nonshift workers', *American Journal of Cardiology*, 107(6), pp. 945–948. doi: 10.1016/j.amjcard.2010.10.077.

Suzuki, H., Swei, A., Zweifach, B. W. and Schmid-Schönbein, G. W. (1995) 'In Vivo Evidence for Microvascular Oxidative Stress in Spontaneously Hypertensive Rats', *Hypertension*, 25(5).

Swanson, R. A., Morton, M. T., Tsao-Wu, G., Savalos, R. A., Davidson, C. and Sharp, F. R. (1990) 'A semiautomated method for measuring brain infarct volume', *Journal of Cerebral Blood Flow & Metabolism*, 10(2), pp. 290–293. doi: 10.1038/jcbfm.1990.47.

Swerdel, J. N., Rhoads, G. G., Cheng, J. Q., Cosgrove, N. M., Moreyra, A. E., Kostis, J. B. and Kostis, W. J. (2016) 'Ischemic Stroke Rate Increases in Young Adults: Evidence for a Generational Effect?', *Journal of the American Heart Association*, 5(12). doi: 10.1161/JAHA.116.004245.

Tamura, A., Graham, D. I., McCulloch, J. and Teasdale, G. M. (1981) 'Focal Cerebral Ischaemia in the Rat: 1. Description of Technique and Early Neuropathological Consequences Following Middle Cerebral Artery Occlusion', *Journal of Cerebral Blood Flow & Metabolism*. SAGE Publications, 1(1), pp. 53–60. doi: 10.1038/jcbfm.1981.6.

Tarr, D., Graham, D., Roy, L. A., Holmes, W. M., McCabe, C., Mhairi Macrae, I., Muir, K. W. and Dewar, D. (2013) 'Hyperglycemia accelerates apparent diffusion coefficient-defined lesion growth after focal cerebral ischemia in rats with and without features of metabolic syndrome.', *Journal of cerebral blood flow and metabolism : official journal of the International Society of Cerebral Blood Flow and Metabolism*. Nature Publishing Group, 33(10), pp. 1556–1563. doi: 10.1038/jcbfm.2013.107.

Touzani, O., Roussel, S. and MacKenzie, E. T. (2001) 'The ischaemic penumbra.', *Current opinion in neurology*, 14, pp. 83–88. doi: 10.1097/00019052-200102000-00013.

Truelsen, T., Begg, S. and Mathers, C. (2001) 'The global burden of cerebrovascular disease'.

Truelsen, T., Piechowski-Jóźwiak, B., Bonita, R., Mathers, C., Bogousslavsky, J. and Boysen, G. (2006) 'Stroke incidence and prevalence in Europe: a review of available data.', *European journal of neurology*, 13(6), pp. 581–98. doi: 10.1111/j.1468-1331.2006.01138.x.

Tsai, L.-L., Tsai, Y.-C., Hwang, K., Huang, Y.-W. and Tzeng, J.-E. (2005) 'Repeated light-dark shifts speed up body weight gain in male F344 rats.', *American journal of physiology. Endocrinology and metabolism*, 289(2), pp. E212–E217. doi: 10.1152/ajpendo.00603.2004.

Tureyen, K., Bowen, K., Liang, J., Dempsey, R. J. and Vemuganti, R. (2011) 'Exacerbated brain damage, edema and inflammation in type-2 diabetic mice subjected to focal ischemia.', *Journal of neurochemistry*, 116(4), pp. 499–507. doi: 10.1111/j.1471-4159.2010.07127.x.

Turin, T. C., Kita, Y., Rumana, N., Nakamura, Y., Takashima, N., Ichikawa, M., Sugihara, H., Morita, Y., Hirose, K., Okayama, A., Miura, K. and Ueshima, H. (2012) 'Is there any circadian variation consequence on acute case fatality of stroke? Takashima Stroke Registry, Japan (1990-2003)', *Acta Neurologica Scandinavica*, 125(3), pp. 206–212. doi: 10.1111/j.1600-0404.2011.01522.x.

Vanassche, T., Lauw, M. N., Eikelboom, J. W., Healey, J. S., Hart, R. G., Alings, M., Avezum, A., Díaz, R., Hohnloser, S. H., Lewis, B. S., Shestakovska, O., Wang, J. and Connolly, S. J. (2015) 'Risk of ischaemic stroke according to pattern of atrial fibrillation: Analysis of 6563 aspirin-treated patients in active-a and averroes', *European Heart Journal*, 36(5), pp. 281–287. doi: 10.1093/eurheartj/ehu307.

Vithian, K. and Hurel, S. (2010) 'Microvascular complications: pathophysiology and management.', *Clinical medicine (London, England)*. Royal College of Physicians, 10(5), pp. 505–9. doi: 10.7861/CLINMEDICINE.10-5-505.

Vosko, A. M., Colwell, C. S. and Avidan, A. Y. (2010) 'Jet lag syndrome: Circadian organization, pathophysiology, and management strategies', *Nature and Science of Sleep*, 2, pp. 187–198. doi: 10.2147/NSS.S6683.

Vyas, M. V, Garg, A. X., Iansavichus, A. V, Costella, J., Donner, A., Laugsand, L. E., Janszky, I., Mrkobrada, M., Parraga, G. and Hackam, D. G. (2012) 'Shift work and vascular events: systematic review and meta-analysis.', *BMJ (Clinical research ed.)*. BMJ Group, 345(July), p. e4800. doi: 10.1136/bmj.e4800.

Wiebking, N., Maronde, E. and Rami, A. (2013) 'Increased neuronal injury in clock gene Per-1 deficient-mice after cerebral ischemia.', *Current neurovascular research*, 10(2), pp. 112–25.

Wilking, M., Ndiaye, M., Mukhtar, H. and Ahmad, N. (2013) 'Circadian rhythm connections to oxidative stress: implications for human health.', *Antioxidants & redox signaling*, 19(2), pp. 192–208. doi: 10.1089/ars.2012.4889.

Wyse, C. A., Selman, C., Page, M. M., Coogan, A. N. and Hazlerigg, D. G. (2011) 'Circadian desynchrony and metabolic dysfunction; did light pollution make us fat?', *Medical hypotheses*, 77(6), pp. 1139–44. doi: 10.1016/j.mehy.2011.09.023.

Wyse, C. a, Biello, S. M. and Gill, J. M. R. (2014) 'The bright-nights and dim-days of the urban photoperiod: implications for circadian rhythmicity, metabolism and obesity.', *Annals of medicine*, 46(5), pp. 253–63. doi: 10.3109/07853890.2014.913422.

Yamamoto, H., Nagai, K. and Nakagawa, H. (1987) 'Role of SCN in daily rhythms of plasma glucose, FFA, insulin and glucagon.', *Chronobiology international*, 4(4), pp. 483–91. doi: 10.3109/07420528709078539.

Yamori, Y., Horie, R., Handa, H., Sato, M. and Fukase, M. (1976) 'Pathogenetic similarity of strokes in stroke-prone spontaneously hypertensive rats and humans.', *Stroke*, 7(1).

Yao, H. and Nabika, T. (2012) 'Standards and pitfalls of focal ischemia models in spontaneously hypertensive rats: with a systematic review of recent articles.', *Journal of translational medicine*, 10(1), p. 139. doi: 10.1186/1479-5876-10-139.

Yoo, S.-H., Yamazaki, S., Lowrey, P. L., Shimomura, K., Ko, C. H., Buhr, E. D., Siepka ţ, S. M., Hong, H.-K., Jun Oh, W., Joon Yoo, O., Menaker, M. and Takahashi, J. S. (2003) 'PERIOD2::LUCIFERASE real-time reporting of circadian dynamics reveals persistent circadian oscillations in mouse peripheral tissues'.

Young, M. E. (2006) 'The circadian clock within the heart: potential influence on myocardial gene expression, metabolism, and function.', *American journal of physiology. Heart and circulatory physiology*, 290(1), pp. H1–H16. doi: 10.1152/ajpheart.00582.2005.

Young, M. E. and Bray, M. S. (2007) 'Potential role for peripheral circadian clock dyssynchrony in the pathogenesis of cardiovascular dysfunction.', *Sleep medicine*, 8(6), pp. 656–67. doi: 10.1016/j.sleep.2006.12.010.

Zausinger, S., Baethmann, A. and Schmid-Elsaesser, R. (2002) 'Anesthetic methods in rats determine outcome after experimental focal cerebral ischemia: Mechanical ventilation is required to obtain controlled experimental conditions', *Brain Research Protocols*, 9(2), pp. 112–121. doi: 10.1016/S1385-299X(02)00138-1.

Zhang, H., Prabhakar, P., Sealock, R. and Faber, J. E. (2010) 'Wide Genetic Variation in the Native Pial Collateral Circulation is a Major Determinant of Variation in Severity of Stroke', *Journal of Cerebral Blood Flow & Metabolism*. SAGE PublicationsSage UK: London, England, 30(5), pp. 923–934. doi: 10.1038/jcbfm.2010.10.

Zhang, N., Komine-Kobayashi, M., Tanaka, R., Liu, M., Mizuno, Y. and Urabe, T. (2005) 'Edaravone Reduces Early Accumulation of Oxidative Products and Sequential Inflammatory Responses After Transient Focal Ischemia in Mice Brain', *Stroke*, 36(10), pp. 2220–2225. doi: 10.1161/01.STR.0000182241.07096.06.